# TISSUE TRANSGLUTAMINASE AND ITS ROLE IN HUMAN CANCER PROGRESSION

A Dissertation

Presented to the Faculty of the Graduate School

of Cornell University

In Partial Fulfillment of the Requirements for the Degree of

Doctor of Philosophy

by

Bo Li

August 2011

# TISSUE TRANSGLUTAMINASE AND ITS ROLE IN HUMAN CANCER PROGRESSION

Bo Li, Ph. D.

Cornell University 2011

Tissue transglutaminase (tTG) is a protein-crosslinking enzyme whose expression is up-regulated in several human cancers. Here I show that tTG is a key participant in a novel EGFR/Src-signaling pathway and a potential target for inhibiting EGFR-promoted tumor progression. Specifically, EGF up-regulates tTG expression in human breast cancer cells, and knock-downs of tTG expression or the treatment of breast cancer cells with a tTG-specific inhibitor, blocks EGF-stimulated anchorage-independent growth. The combined actions of Ras and Cdc42, lead to the activation of PI 3-kinase and NFκB, mediating the EGF-dependent up-regulation of tTG in breast cancer cells. Moreover, overexpression of wild-type tTG in these cancer cells, but not its enzymatically-defective counterpart, fully mimics the actions of EGF. Surprisingly, the tTG-promoted growth of breast cancer cells is dependent on its ability to activate Src, as an outcome of a complex formed between tTG and the breast cancer marker and intermediate filament protein keratin-19.

Microvesicles (MVs) derived from human cancer cells are receiving a good deal of attention because of their ability to participate in the transfer of signaling proteins between cancer cells and to contribute to their invasive activity. Here I show that MVs may play another important role in promoting oncogenesis, as MVs shed by

two different human cancer cells, MDAMB231 breast cancer cells and U87 glioblastoma cells, are capable of conferring transformed characteristics onto normal cells. I further show that tTG crosslinks fibronectin in MVs derived from cancer cells and that the ensuing MV-mediated transfer of both crosslinked-fibronectin and tTG to recipient cells function cooperatively to induce their transformation. This new role for MVs in cancer progression led to my investigating the signaling pathways that induce MV formation in cancer cells. These efforts resulted in the identification of a RhoA-ROCK-LIMK signaling pathway that plays a critical role in directing the biogenesis of MVs in cancer cells.

## BIOGRAPHICAL SKETCH

Bo Li was born and raised in Qingdao, a beautiful city on the eastern coast of China. During his childhood, his whole family lived in the vicinity of Qingdao Ocean University, due to the fact that his father worked there as a marine biologist. Occasionally Bo was brought to the laboratory where his father was doing research, and he was deeply attracted by the various biology and chemistry experiments that were performed there. Holding this strong curiosity towards science, he finished his secondary school in Qingdao and went to Peking University to pursue further education. He chose Chemistry as his major and became interested in working on biological questions using his Chemistry knowledge and background. This was the primary reason that he decided to join Dr. Luhua Lai's group, whose major research interests were the predication and modeling of protein structures, as well as the computed-aided drug design. Bo worked in her lab for three years as an undergraduate student and research assistant, on the project focusing on designing small-molecule inhibitors against Human Leukocyte Antigen-Death Receptor 4, an immuno-receptor linked to the progression of rheumatoid arthritis. After graduation from Peking University, he was fortunate enough to be accepted by the Chemistry department of Cornell University, and then became a Ph.D. student in Dr. Richard Cerione's group. There he switched his research focus from theoretical drug design to cell biology, doing research related to the function of a particular enzyme called tissue transglutaminase，and also one type of unconventional secretory structures called microvesicles, which carry tissue transglutaminase as their cargo. Although the life as

a bio-researcher was not easy, he did enjoy every minute spent in the Cerione group, due to the consistent excitation of working on cutting-edge questions, as well as the family-like atmosphere always existed in this crowd. After graduation, he plans to start his postdoctoral training in the laboratory of Dr. M. Celeste Simon at the University of Pennsylvania, where he will study the mechanism of hypoxia, which is a physiological response frequently occurs in the process of tumor development.

## ACKNOWLEDGMENTS

I am deeply grateful to my parents, who encouraged and supported me all the way through my life. They not only helped me recognize my genuine interest towards science, but also showed me how to pursue it progressively as a career goal. Their love and encouragement have always been my driving force to overcome any difficulties.

Looking back at the past six years at Cornell, I would like to express my great appreciation to my research advisor Dr. Richard Cerione, who created an incredible nice atmosphere in our group. He also consistently provided both mental support and scientific inspiration to everyone in this laboratory. I felt really lucky to become his student. I would also like to thank Dr. Marc Antonyak, who taught me hand by hand all the cell biology assays that I used in my thesis research, and also took a lot of efforts to train me to think as a scientific researcher. His friendship and brotherhood are the most cherishable gifts that I gained here.

Many thanks to my thesis committee member Dr. Brain Crane, Dr. Barbara Baird and also Dr. Maurine Linder for their full support of my research and recommendations.

I am very grateful for the friendship, advice and favor from the Cerione group members, including Jenny Guo, Jianbin Wang, Qiyu Feng, Jingwen Zhang, Lindsey Boroughs, Sunando Datta, Joe Druso, Joy Lin, Thi Ly, Makoto Endo, Shawn Milano, Sungsoo Yoo, Sandra Dias, Sekar Ramachandran, Jon Erickson, Yeyun Zhou, and also my collaborators Kirsten Bryant, David Holowka, Le Cheng and Alexander Nikitin. Without their help my research goal would be impossible to achieve.

Finally, I would like to thank Ariel Yang, my fiancée, for all her love and emotional support. I am always feeling fortunate to have her as part of my life.

## TABLE OF CONTENTS

# CHAPTER 1

## Overview

*Introduction*

Tissue transglutaminase, or tTG, is a $Ca^{2+}$-dependent acyltransferase that catalyzes the formation of new amide bonds between the γ-carboxamide of glutamine and the ε-amino group of lysine or another primary amine (i.e. transamidation) (1, 2). This protein crosslinking capability has been implicated in a wide range of cellular processes including neuronal growth and regeneration, bone development, wound healing, angiogenesis, cellular differentiation, and apoptosis (3-20). Interestingly, there is a growing appreciation of the roles played by tTG in the growth, survival, and migration of cancer cells, and it has been suggested that loss of the normal regulation of tTG may have significant consequences for the development of the malignant state (21-25).

To better understand the multifaceted functions of tTG, we began by considering its structural features. What makes this protein particularly interesting from a structure-function perspective is the fact that it is not only capable of acyl-transferase activity, but that it also exhibits GTP-binding and GTP-hydrolytic activity (26) and that there is a reciprocal relationship between its "G-protein-like functions" and its ability to catalyze protein crosslinking reactions (27). Indeed, the three-dimensional structures for guanine nucleotide-bound tTG, and for tTG that has its transamidation active site accessible and capable of binding substrates, are

dramatically different (28, 29). This likely explains some of the marked differences in the cellular effects caused by GTP-binding-defective tTG mutants versus mutants that are defective for transamidation activity (4, 23, 30-34).

With this structure-function perspective as a back drop, we will then describe some of the initial lines of study that have implicated tTG in cell survival, and then show how these findings have led to a growing appreciation that tTG has interesting and important roles in cancer cell biology. In particular, previous work from our laboratory suggested that tTG helps ensure that cells remain viable during their differentiation (19, 20). This is a potentially important function because factors that normally cause cell-cycle arrest and differentiation can also trigger apoptotic programs and so it is necessary that these factors induce the expression and activation of additional gene products that can provide protection against apoptotic stresses (35). tTG appears to be one such protein, so that when cells receive signals triggering growth-arrest, the up-regulation of tTG expression occurs in order to help to tip the balance toward differentiation rather than cell death (19). From these initial results, we then went on to discover that the ability of tTG to confer a survival response in cells extends beyond those conditions leading to cellular differentiation and in fact contributes to the ability of mitogenic stimuli such as EGF to provide a survival advantage to human breast cancer cells (36-38). Moreover, we went on to find that tTG also plays roles in stimulating the ability of human breast cancer cells to grow in the absence of a substratum (i.e. anchorage-independent growth) (39) and that it plays an important role in the EGF-stimulated migration and invasive activity of cancer cells (40). These various studies will be elaborated upon further in the sections below.

*Catalytic mechanism of tTG*

tTG catalyzes the transamidation reaction between two substrates, a glutamine-containing protein substrate 1 and a lysine-containing protein substrate 2 or a polyamine, through the cooperation of a protease-like catalytic triad Cys277, His335 and Asp358 (41). Similar to the cysteine protease family (42), the catalytic process is comprised of two steps: the transient acylation of Cys277 by its nucleophilic attack on the glutamine side-chain of substrate 1 to form an acyl-thiolate intermediate, and the subsequent deacylation of Cys277 by the nucleophilic attack from the amino group of substrate 2, leading to the release of cross-linked products from the catalytic site (1, 43, 44). Specifically, as the first step, His335 attacks Cys277 to create a thiolate–imidazolium ion pair, with the help of Asp358 to counterbalance the positive change on His335 through its carboxylate group formed under conditions of physiological pH (44). The glutamine side-chain of substrate 1 approaches the vicinity of Cys277 and is attacked by the thiolate ion, resulting in the formation of an acyl-thiolate intermediate, accompanied by the release of an ammonia molecule (1, 43, 45). Because of the high-energy consumption required to produce the tetrahedral adduct, the formation of an acyl-thiolate intermediate is the rate-limiting step of the transamidation reaction (2). The amino group of the second substrate then generates the amide ion by its interaction with the nearby His335 and Asp358 through the same mechanism as in the first step, and then participates in a nucleophilic attack on the acyl-thiolate intermediate (1, 43). The formation of the tetrahedral adduct in this step involves a

**Figure 1.1 Mechanism of tTG-catalyzed transamidation reaction.** First, a thiolate anion is formed at the side chain of Cys277, which then attacks the glutamine group of substrate 1. Release of ammonia occurs after the proton donation from His335, which creates an acyl-thiolate intermediate. Next, the lysine side chain of substrate 2 approaches the catalytic site and undergoes a nucleophilic attack upon the intermediate, leading to the formation of a tetrahedral adduct and the subsequent release of the cross-linked product. As a result, substrates 1 and 2 are covalently linked to each other through a newly-formed peptide bond.

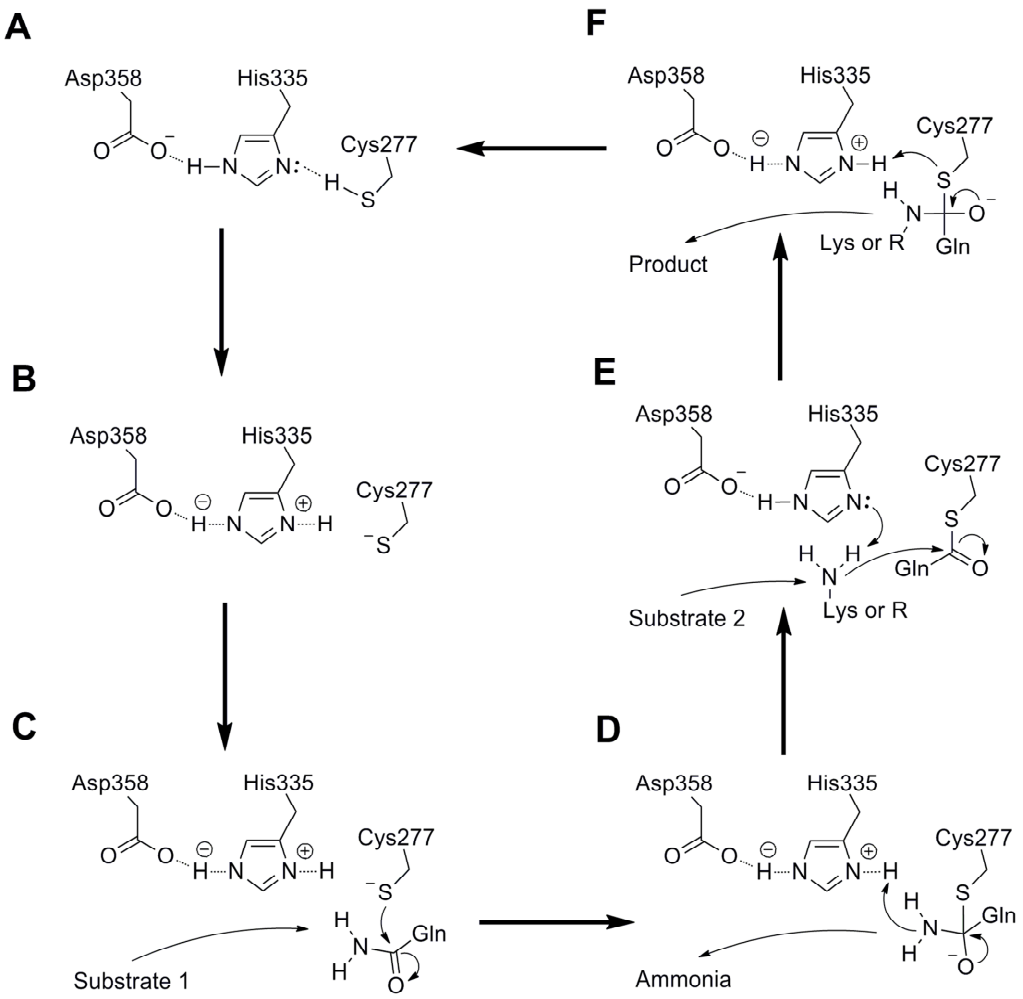
A
Asp358
His335
Cys277
B
Asp358
His335
Cys277
C
Asp358
His335
Cys277
Substrate 1
Gln
D
Asp358
His335
Cys277
Ammonia
Gln
E
Asp358
His335
Cys277
Substrate 2
Lys or R
Gln
F
Asp358
His335
Cys277
Product
Lys or R
Gln

low-energy barrier, therefore the specificity of the attacking amino group is not high (45). It either comes from a protein-bound lysine residue or a small polyamine compound (2). Finally, the break-down of the tetrahedral adduct leads to the release of the cross-linked product, while restoring the catalytic triad and completing the transamidation reaction (44, 45). The detailed mechanism is illustrated in Figure 1.1.

*A comparison between the active and inactive conformation of tTG*

Although the catalytic mechanism of tTG was clarified several years ago, how the non-core residues cooperate to facilitate and regulate the transamidation activity has been less clear. Efforts to address this issue led to the sequence alignment between tTG and Human factor XIIIA, a hetero-tetrameric transglutaminase-family member implicated in blood coagulation (46). The X-ray crystal structure of the human recombinant, dimeric fXIIIA2 was determined in 1994 (47), and sequence homology between XIIIA and tTG predicted that tTG probably folded into four sequential domains: an N-terminal β-sandwich domain, the central catalytic core domain, and two β-barrel domains at the C-terminal end of this protein (48). This result was confirmed by the first tTG structure that was solved in 2002 at 2.8 Å resolution, which showed that tTG was folded as a "closed" or inactive conformation (28). In this structure, the carboxylic group of Asp358 formed a hydrogen bond with the imidazole ring of His335, and the hydroxyl group of Cys277 was positioned close to His335, waiting to generate the thiolate–imidazolium ion pair through the resonant cooperation of the catalytic triad. This structure was thought to be catalytically inactive because of the inaccessibility of its catalytic core to the outer environment (28). The proposed

**Figure 1.2 The structural superimposing and comparison of inactive tTG to active tTG.** The overall structure of inactive tTG (PDB ID: 1KV3) is shown in dark grey color and the overall structure of active tTG (PDB ID: 2Q3Z) is shown in light grey color. Both of them have a β-sandwich domain, a catalytic core domain and two β-barrel domains arranged from the N-terminal end to the C-terminal end. The N-terminal β-sandwich domains of these two structures are superimposed, highlighting the conformational change at the C-terminal end. The arrow indicates the 120° swing angle of the C-terminal β-barrel domains when tTG changes from its inactive conformation to its active conformation.

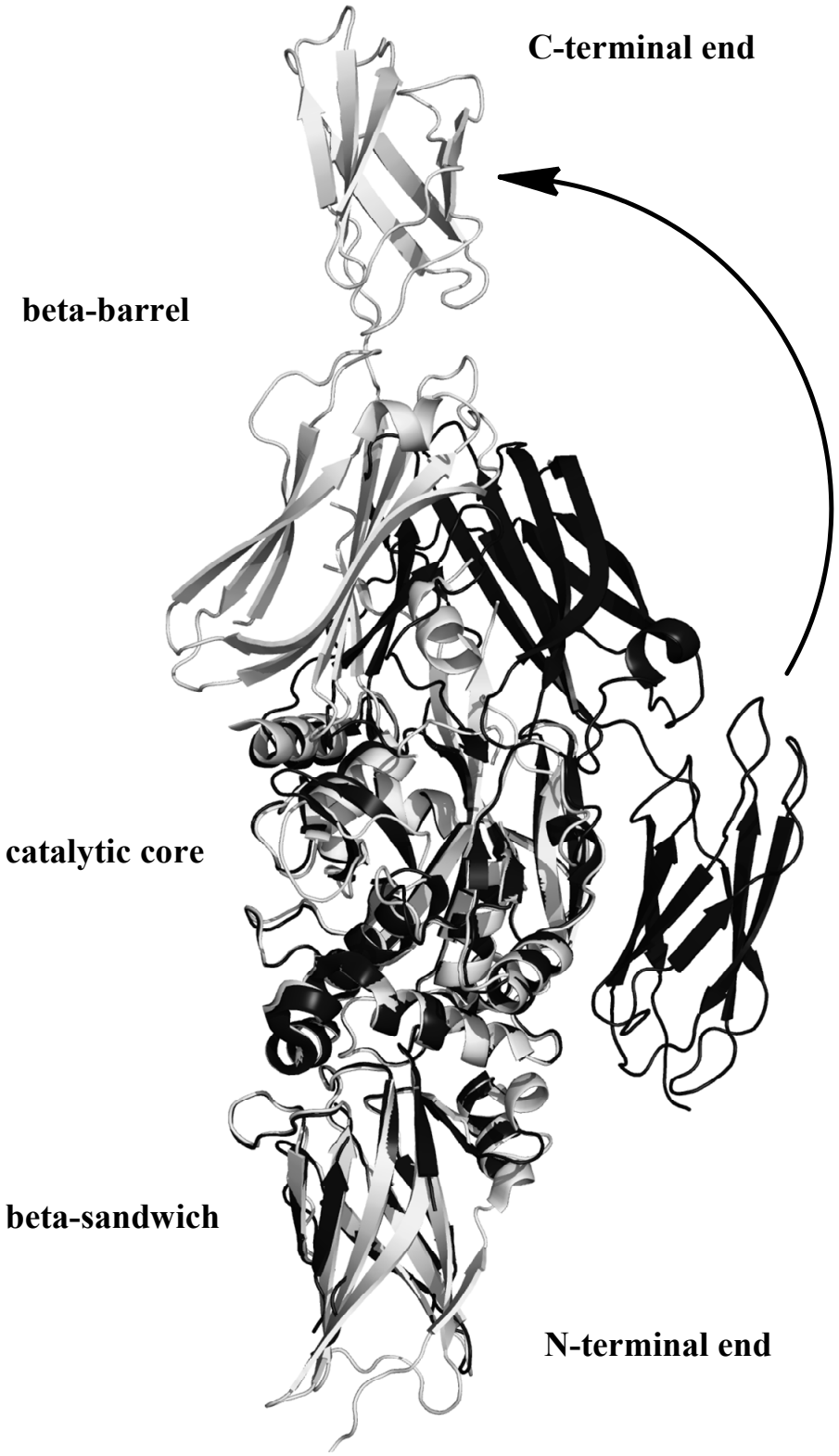
C-terminal end
beta-barrel
catalytic core
beta-sandwich
N-terminal end

substrate entrance was blocked by two loops within the first β-barrel domain at the C-terminal end of tTG. Most importantly, Tyr516, which is located within this loop region, formed a tight hydrogen bond with the hydroxyl group of Cys277, thus negating the catalytic activity (28). As a result, a plausible hypothesis for tTG activation involves the withdrawal of the two loops from the catalytic core, and the concomitant disruption of the hydrogen bond between Cys277 and Tyr516 (28). This hypothesis was confirmed by the more recently determined tTG structure in its "open" state, where the active conformation of tTG was, in effect, trapped by incubating this enzyme with an inhibitor that mimicked its gluten peptide substrate (29). Surprisingly, the inhibitor stabilized tTG in a conformation that significantly differed from its "closed" state (Figure 1.2). The N-terminal superimposition of the "open" and "closed" tTG structures revealed that the loops containing Tyr516 move away from the catalytic core region when the enzyme is in an active conformation, but with an unexpected swing angle of 120 degrees. How tTG achieves these dramatic structure changes is not yet fully understood.

Another significant finding associated with the "open" structure of tTG was the visualization of the "tryptophan tunnel" (29). Based on the comparison of the active sites between tTG and the structurally related cysteine proteases, Trp241 of tTG was proposed to be a critical residue for catalyzing the transamidation reaction through its ability to stabilize the first transition-state intermediate (49, 50). Consistent with this idea, Cys277 was found to be located within a hydrophobic tunnel bridged by Trp241 and Trp332, where the glutamine-containing substrate was proposed to enter from one

**Figure 1.3 The "tryptophan tunnel" Trp241 and Trp332 bridges the access of the two substrates to the catalytic site of tTG.** Trp241 and Trp332, as well as the catalytic triad Cys277, His335, and Asp358 of tTG, are displayed in stick mode, and all the other residues are drawn in opaque ribbon mode. Inactive tTG is presented in dark grey while active tTG is presented in light grey, which are superimposed through the alignment of respective N-terminal β-sandwich domain. The two arrows within the figure point out the approaching track of the glutamine-containing substrate and the lysine-containing substrate to tTG's catalytic site, respectively.

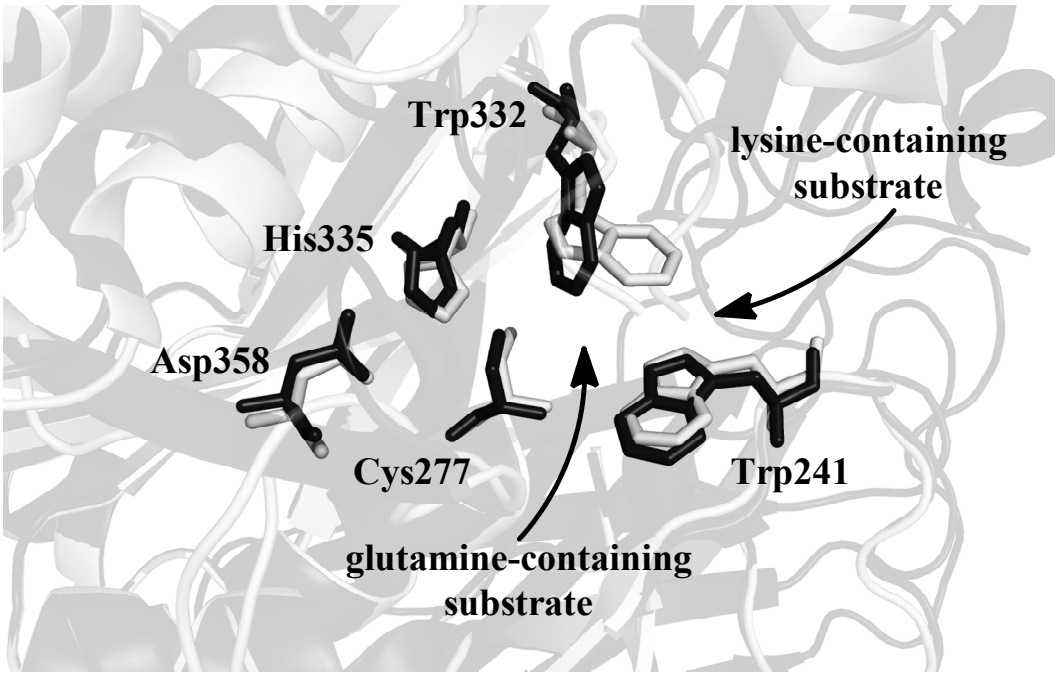
Trp332
lysine-containing
substrate
His335
Asp358
Cys277
Trp241
glutamine-containing
substrate

side, while the lysine-containing substrate entered from the opposite side (Figure 1.3). Substitution of Trp241 with Ala or Gly caused a more than 300-fold decrease in the catalytic rate constant (50), demonstrating the critical role of this tryptophan tunnel for transamidation activity.

*Function of tTG as a G-protein*

In 1992, Graham and his co-workers made the unexpected finding that rat tTG was involved in receptor-coupled signal transduction by functioning as a classical GTP-binding protein (G-protein), specifically, through its ability to mediate agonist-induced signaling events from the $\alpha_{1B/D}$-adrenergic receptor to its downstream effector phospholipase C δ1 (PLCδ1) (26). Subsequently, tTG was shown to mediate the activation of $Ca^{2+}$-activated $K^+$ channels in vascular smooth muscle cells (51). What made these findings particularly surprising was that the primary sequence of tTG did not contain any of the conventional guanine nucleotide-interacting motifs featured in the small or large G-proteins (52). However, the intrinsic ability of tTG to bind GDP/GTP and hydrolyze GTP to GDP argues that it contains a unique guanine nucleotide-interacting pocket which lacks obvious sequence similarity with those of the classical G-proteins. This was confirmed when the three dimensional structure for the "closed" conformation of tTG was determined, where one molecule of GDP was found to bind and co-crystalize with the inactive form of tTG (28). In large G-proteins, the Gα subunit often contains a helical domain adjacent to its guanine nucleotide-binding region to ensure the high affinity binding of guanine nucleotides, whereas small G-proteins lack the helical domain and instead use a bound $Mg^{2+}$ ion to

**Figure 1.4 The interaction of GDP with four positive-charged residues from tTG.** Lys173, Arg476, Arg478, and Arg580 from inactive tTG and the bound-GDP are shown in stick mode. The remaining residues are shown in opaque ribbon mode. The four positive-charged residues are displayed in light grey while GDP is drawn in dark grey. The hydrogen bonds are shown as dashed lines.

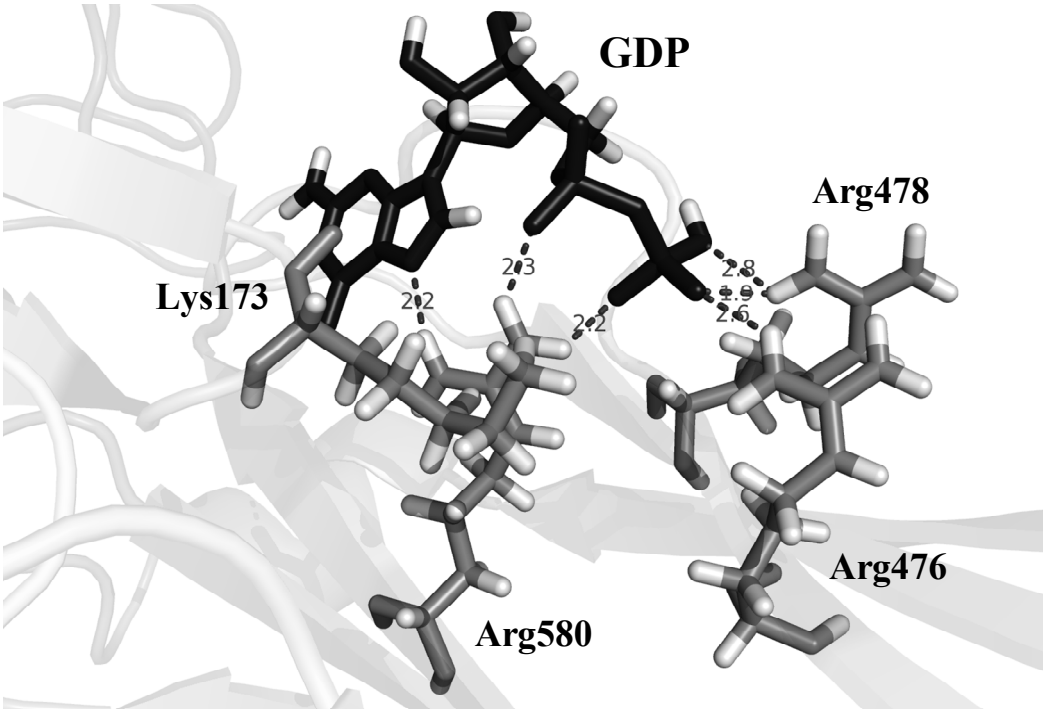
GDP
Arg478
Lys173
2.3
2.2
2.2
2.8
2.6
Arg476
Arg580

strengthen nucleotide-binding (53, 54). However, neither of these classical features was present in the tTG structure. Instead, surrounding the bound GDP molecule was a sequence of positive-charged residues (28), which were assumed to contribute to nucleotide-binding (Figure 1.4). These residues were located within the first β-strand and the following loop region of the first C-terminal β-barrel domain. Perhaps the most important of these residues was Arg580, which formed three hydrogen bonds with the guanine ring, the α-phosphate, and the β-phosphate of the GDP molecule, respectively (28). Substitutions at the corresponding position in rat tTG (Arg579) resulted in as much as a 100-fold reduction in GTP-binding affinity, as determined by isothermal titration calorimetry (55). In addition to Arg580, two other residues, Arg476 and Arg478, also helped properly position the GDP molecule in the pocket, through the formation of two hydrogen bonds between Arg478 and the β-phosphate group, and a single hydrogen bond contributed by Arg476 to the β-phosphate (28). The Arg476Ala and Arg478Ala substitutions attenuated the photo-affinity labeling of tTG with radioactive GTP, thus indicating that these residues contributed to the binding of guanine nucleotides (55). In addition to these three arginine residues that made direct contact with GDP, Lys173 was another positive-charged residue that drew significant attention. Changing Lys173 to asparagine did not alter the ability of tTG to bind guanine nucleotides, but it greatly impaired its GTP-hydrolytic capability (56). A plausible mechanism underlying this effect was that Lys173 plays an essential role in catalyzing GTP hydrolysis. Specifically, the fact that the β-phosphate group of GDP interacts with Arg476, Arg478 and Arg580 led to the prediction that the γ-phosphate group of GTP needed to point away from the arginine pocket in order to avoid steric

clash. Lys173 would presumably function to stabilize the transition-state for the GTP-hydrolytic reaction, because it is located close to the predicted position of the γ-phosphate group. An examination of the GTP hydrolysis-deficient Lys173Asn mutant in cells resulted in an interesting finding, namely, that the ability of tTG to mediate signals from the α-adrenergic receptor to PLCδ was independent of its GTP-hydrolysis capability (26, 56). This conclusion was demonstrated by the fact that the tTG Lys173Asn mutant stimulated the production of similar levels of inositol phosphate (i.e. the product of PLCδ) as wild-type tTG in COS-1 cells co-transfected with $\alpha_{1B}$-adrenergic receptor (26, 56). On the other hand, the Ser171Glu mutation in tTG, which disrupted the GTP-binding capability, as well as the Arg580Lys mutation seriously impaired the production of inositol phosphates in COS-1 cells, indicating that the guanine nucleotide-binding activity of tTG was necessary for mediating the signals from the α-adrenergic receptor (56).

*The role of tTG as a protective factor in cellular differentiation*

While there is now a growing appreciation for tTG in the progression of various types of human cancer (22-24, 39, 40, 57-59), as little as nine years ago this was far from the case. In fact, at that time tTG was widely considered as a protein that was important for either triggering the induction of apoptosis (18, 60-65) or for promoting cellular differentiation (14, 66-68), two cellular processes that are paradoxical with the development of the oncogenic state. The evidence implicating tTG as a regulator of cell death stemmed largely from a line of research being conducted at that time aimed at understanding the molecular mechanisms that underlie

the onset/progression of a class of neurodegenerative disorders, in particular Alzheimer's disease (AD), Huntington's disease (HD), and Parkinson's disease (PD), that are characterized by the presence of insoluble protein aggregates (69). In each of these disease states, the size and number of protein aggregates detected in the brains of affected individuals tend to increase with the severity of the disease, and protein aggregation has been suggested to directly contribute to neuronal cell dysfunction and death (70, 71). Interestingly, high levels of tTG expression and its enzymatic transamidation activity have been identified as hallmarks of AD, HD, and PD (72-76). Moreover, tTG was shown to cross-link components of the protein aggregates associated with each of these diseases (73, 75, 77-79). These findings, when coupled with the fact that inhibiting tTG-catalyzed transamidation activity suppresses protein aggregation and extends the lifespan of mouse models of HD and PD (77, 79, 80), provided some of the earliest and most intriguing data suggesting that tTG participated in the induction of cell death through the aberrant cross-linking of substrate proteins.

In addition to tTG being up-regulated in response to a variety of apoptosis-inducing cellular stresses (i.e. stressful conditions encountered by cells in neurodegenerative diseases), increases in its expression and activation were also shown to accompany cellular differentiation. For example, treatment of the human neuroblastoma cell line SH-SY5Y with the differentiation agent retinoic acid (RA) arrests their growth and stimulates the formation of neurite extensions (81, 82), making them a useful cell type to identify proteins which are important for neuronal differentiation. tTG was identified as one such protein (14, 66, 83). Not only was tTG expression and transamidation activity found to be significantly enhanced in SH-

SY5Y cells by RA stimulation, but inhibiting RA-induced tTG expression using an anti-sense construct blocked the ability of RA to arrest cell cycle progression, as well as to promote neurite extension (66). The study then went on to show that the ectopic expression of wild-type tTG in SH-SY5Y cells, but not a transamidation-defective form in which a cysteine residue within the catalytic triad of the enzyme active site was changed to a valine (tTG C277V), was sufficient to cause these cells to spontaneously undergo differentiation. Thus, these findings demonstrated that induction of tTG expression and activity in cells does not invariably result in cell death, but rather tTG may in certain contexts also promote cellular differentiation.

Our laboratory's interest in the functional consequences of tTG expression and activation started at about the same time that accumulating evidence, like those findings described above, were leading to the general belief that tTG participated in biological processes that resulted in apoptosis, and in a few instances limited cell growth through arresting the cell cycle. We were investigating the effects that the naturally occurring retinoid RA, as well as other synthetic retinoid analogs had on cell fate decisions. This question was particularly relevant at that time, since the growth inhibitory and differentiation activities associated with RA were prompting several research groups to examine the use of RA or RA-like synthetic derivatives as potential treatments for different types of human cancers ranging from prostate cancer to leukemia (84-87). Our laboratory, as well as other groups, was able to show that treatment of the human leukemia cell line HL60 with RA did indeed inhibit their growth (19, 88, 89). However, when the same cell line was cultured in the presence of a synthetically-derived analog that differs from RA by only the addition of a phenol

ring to its carbon backbone, and is referred to as N-(4-hydroxyphenol) retinamide (HPR or fenretinide), instead of inducing cell cycle arrest as is the case for RA, HPR elicited a potent apoptotic response in these cells (19, 90-92). Likewise, HPR was also found to be much more effective than RA at inducing cell death in NIH3T3 mouse fibroblasts (19), indicating that the abilities of these retinoids to differently influence cell fate decisions were not unique to a specific cell lineage.

How the highly related retinoid analogs RA and HPR gave rise to opposing cellular outcomes, such that RA promotes cell survival whereas HPR induces apoptosis, was puzzling and led us to consider possible mechanisms that could account for these effects. We obtained a clue as to how this may occur when we examined the effectiveness of HPR at inducing apoptosis in both HL60 leukemia cells and NIH3T3 fibroblasts that had first been stimulated with RA for different lengths of time (19). While short-term RA pre-treatments (up to 6 hours) caused little, if any, change in the ability of HPR to induce apoptosis in these cells, longer pre-treatments with RA did have effects. For example, HL60 and NIH3T3 cells that had been pre-incubated with RA for two days prior to being challenged with HPR became highly resistant to the apoptotic-inducing actions of HPR. Since pre-treating the cells with RA for extended lengths of time (on the order of days) was required in order to see the protective effects against HPR-induced apoptosis afforded by RA treatment, we began to favor the idea that RA-signaling might induce the expression of a distinct gene or set of genes that is crucial for ensuring cell viability during cellular differentiation.

While searching for potential candidate genes that were selectively up-regulated by RA, we considered tTG since the induction of its expression was already

known to be tightly coupled to the effects of RA-signaling in HL60 cells (88, 89), as well as some other cell types (i.e. SH-SY5Y cells) (14, 66, 83). In un-stimulated HL60 leukemia cells and NIH3T3 mouse fibroblasts, tTG is expressed at very low or almost undetectable levels (19, 62, 93). However, following the addition of RA to the cells, there was a progressive increase in the levels of tTG expression, with maximal expression being reached in both cell lines between 2-3 days after RA treatment (19). We then questioned how treating cells with HPR would influence tTG expression. In contrast to RA, HPR was found to be completely ineffective at increasing tTG expression levels beyond the nearly undetectable levels measured in un-stimulated HL60 or NIH3T3 cells. These findings not only identified the induction of tTG expression as a distinguishing feature between the signaling capabilities of RA and HPR, but they also opened the door to the possibility that tTG may be important for mediating the ability of RA to protect cells from HPR-induced apoptosis. This indeed appears to be the case, as ectopically expressing tTG in NIH3T3 cells was as effective as RA treatment at protecting the cells from challenges with HPR. Perhaps even more telling of the potential significance that tTG has in promoting cell survival came from another experiment in which its transamidation activity was blocked using monodansylcadaverine (MDC), a competitive inhibitor of the transamidation reaction, during the RA-induced differentiation of HL60 cells. Rather than undergoing cell cycle arrest and stimulating the formation of neurite extensions as occurs with RA treatment alone, RA treated HL60 cells cultured in the presence of MDC instead underwent apoptosis. These findings suggested for the first time that tTG can serve as a protective factor, particularly in cells that are undergoing differentiation. In these

instances, tTG expression and its corresponding transamidation activity are induced by RA to ensure that cells that are exiting the cell cycle as part of the cellular differentiation process survive without undergoing apoptosis.

*tTG and chemotherapy-resistance*

In addition to establishing a novel and unexpected role for tTG in maintaining the viability of HL60 leukemia cells and NIH3T3 fibroblasts undergoing RA-induced cellular differentiation (19), these initial findings also laid the foundation for subsequent investigations into whether tTG might provide a protective effect to cells under a number of other conditions. One area of study that has been developing rapidly over the last few years is the relationship between tTG and drug resistance in human cancer cells. Screening several different types of primary human tumor samples by immunohistochemistry for tTG expression has revealed that its expression levels are increased in a significant percentage of breast, pancreatic, ovarian, and brain tumors (19, 22, 24, 59, 94-96). Moreover, breast and pancreatic cancer cell lines that are resistant to chemotherapies also tend to have the highest levels of tTG expression and transamidation activity (38, 57, 59, 97, 98), suggesting that tTG may contribute to the drug-resistant phenotypes exhibited by some cancer cells. A case in point is the highly aggressive and chemotherapy-insensitive human breast carcinoma cell line MDAMB231. These cells constitutively express high levels of tTG, and when extracts from the cells were assayed for transamidation activity, it was determined that tTG was active (23, 38). Knocking-down tTG expression in these cancer cells using small interfering-RNAs (siRNAs) was found to be sufficient to sensitize them to the

chemotherapeutic agent doxorubicin (23). Likewise, treating MDAMB231 cells with the transamidation inhibitor MDC also made the cells susceptible to doxorubicin-induced apoptosis (38), indicating that the cross-linking activity of tTG is likely responsible for mediating its protective effects.

The notion that tTG provides a survival advantage to human cancer cells was further strengthened by demonstrating that the pro-survival signaling capabilities of the epidermal growth factor (EGF)-receptor are dependent on tTG in some cancer cell lines (38, 39). The EGF-receptor (EGFR) is a cell surface receptor tyrosine kinase that has been extensively investigated for its roles in promoting tumorigenesis (99-101). Upon binding EGF, the EGFR becomes activated and initiates the activation of numerous intracellular signal transduction pathways that work in concert to directly influence cellular processes, as well as to induce the expression of a specific set of genes that promote cancer cell growth and survival (99-101). The interplay that exists between EGFR-signaling and tTG in cancer cells was discovered when it was shown that the levels of tTG expression and its corresponding transamidation activity were markedly enhanced in the human breast cancer cell line SKBR3 after EGF stimulation (38). Consistent with the findings that RA-induced tTG activation protects HL60 leukemia cells and NIH3T3 fibroblasts from apoptotic challenges (19), inhibiting the EGF-stimulated transamidation activity of tTG using MDC also abolishes the ability of the EGFR to protect cells from doxorubicin-induced apoptosis, as well as from serum-deprivation-induced apoptosis (38, 39). Although it is currently unclear how often and in which cancer cell types the EGFR elicits a survival response by up-regulating tTG expression and activation, two additional pieces of evidence suggest

that this signaling mechanism is not limited to just SKBR3 breast cancer cells. First, it was shown that EGF stimulation was capable of potently inducing the expression and activation of tTG in two additional breast cancer cell lines, namely BT20 and MDAMB468 cells (38). Second, tTG was identified in a screen as one of the most highly up-regulated genes in a U87 brain tumor cell line that exogenously expresses a constitutively active mutant form of the EGFR (102). Thus, the coupling of EGFR-signaling to the induction of tTG expression and activation may be a common occurrence in human cancers, particularly in those cancer cells whose oncogenic potential is dependent on EGFR-signaling activities. Taken together, these findings suggest that the up-regulation of tTG expression and activation in human tumors represent a critical step during cancer progression where tumor cells are transitioning to a high grade, drug-resistant phenotype.

*How does tTG promote cell survival?*

In those cases where tTG has been implicated as a protective factor in both normal and cancer cells, its enzymatic transamidation activity has been shown to be essential (19, 24, 38, 39, 57, 97, 102). As a result of these findings, it should come as no surprise to learn that an important emphasis in the field has been to determine the identities of those proteins that are cross-linked by tTG to elicit survival responses in cancer cells. While virtually hundreds of proteins have been shown to serve as putative substrates for the transamidation activity of tTG using *in vitro* and high-throughput screening approaches (103, 104), determining which, if any, of these proteins are physiologically relevant substrates in different cellular contexts has

proven to be far more challenging. However, recent results have highlighted two proteins, that when covalently modified by tTG, can have significant implications on cell viability. The first is caspase-3 (also referred to as CPP32, YAMA, and apopain) (105), an important component of the apoptotic-inducing machinery in cells (106). Caspase-3, as well as the other members of the caspase family, is a cysteine protease that is expressed in cells as an inactive, proto-form of the enzyme. However, when a cell commits to undergoing programmed cell death or apoptosis, it initiates an irreversible activation of the caspase pathway which involves a series of cleavages that result in the conversion of inactive pro-caspases to active, functional caspases. Once activated, caspase-3 catalyzes the specific cleavage of several key proteins that are essential for maintaining cell viability, which results in cell death.

The findings showing that tTG can cross-link caspase-3 as a way to promote cell survival came from a study that was investigating how a HCT-116 colon carcinoma cell line that lacked Bax expression was insensitive to the apoptotic-inducing effects of thapsigargin (THG), an inhibitor of the endoplasmic reticulum $Ca^{2+}$-ATPase (105). The authors found by Western blot analysis that exposing Bax-deficient HCT-116 cells to THG for increasing lengths of time resulted in the progressive appearance of unusually high molecular weight forms of pro-caspase-3. Since the catalytic activity of tTG has been shown to induce the oligomerization of several different proteins (73, 75, 77, 79, 107), the ability of tTG to induce the oligomerization of pro-caspase-3 was examined as a possible explanation for the higher molecular weight forms of pro-caspase-3 detected in the cells treated with THG. Not only was it shown that THG potently induced tTG expression and activation in the

Bax-deficient HCT-116 colon carcinoma cells, but a recombinant form of pro-capase-3 could also be cross-linked by tTG *in vitro* (105). This raised the question of whether blocking the ability of tTG to cross-link proteins in THG-treated HCT-116 cells would influence the formation of the higher molecular weight species of pro-caspase-3, as well as sensitize these cells to THG. Indeed, knocking-down tTG expression using siRNA approaches or incubating HCT-116 cells with the tTG inhibitor MDC caused a significant reduction in the ability of THG to induce the formation of the larger forms of pro-caspase-3 (105). Coinciding with this effect, MDC treatment also made the cells susceptible to THG-induced apoptosis, indicating that tTG affords a protective effect to HCT-116 colon carcinoma cells from THG-induced apoptosis by cross-linking an important component of the cell death machinery, namely caspase-3, into non-functional oligomers (105).

The inhibitor of κBα (IκBα), a regulatory protein in the Rel/nuclear factor (NF)κB survival pathway, is the second example of a protein that can be cross-linked by tTG to potentiate cell survival (22). The central player in the NFκB survival pathway is NFκB itself, a transcription factor that can be rapidly and transiently activated by a variety of growth factors, and especially in response to harmful cellular stresses, to induce the expression of specific genes that promote cell survival, as well as cell growth (108, 109). The transcriptional activity of NFκB in un-stimulated cells is normally kept in check because NFκB is sequestered in the cytoplasm where it is found in a complex with its negative regulator IκBα (109). For NFκB to become activated by extracellular stimuli, a complex sequence of events must take place that

results in the phosphorylation of IκBα on two serine residues contained within its regulatory domain. This phosphorylated form of IκBα is then ubiquitinated and targeted for degradation in the proteosome. Once IκBα is degraded, NFκB is free to translocate from the cytoplasm to the nucleus where it functions to regulate the expression of various genes (109). While many of the genes up-regulated by NFκB promote cell survival and cell growth responses, NFκB also rapidly induces the expression of its own negative regulator IκBα, ensuring that NFκB activity is tightly controlled in normal cells (109).

Aberrant activation of the NFκB survival pathway has emerged as a hallmark of human cancers (109-112). Moreover, inactivating NFκB by siRNA knockdown or using NFκB inhibitors has been shown to block the growth and survival advantages associated with numerous cancer cell lines (109, 113), suggesting that de-regulation of the NFκB pathway may represent an important step during cancer progression. While searching for the mechanisms used by cancer cells to excessively stimulate NFκB activation, a connection with tTG emerged. It was noted that a strong correlation existed between the levels of tTG expression and the amount of constitutive NFκB activity detected in aggressive and drug-resistant forms of breast cancer cells (i.e. MDAMB231 cells), malignant melanoma cells (i.e. A375 cells), and pancreatic cancer cells (i.e. Panc-28 cells), as well as in primary pancreatic tumors (22). When the transamidation activity of tTG, associated with the Panc-28 pancreatic cancer cells, was inhibited by knocking-down tTG using siRNAs or treating the cells with MDC,

there was a corresponding reduction in NFκB activity, indicating that NFκB activation in Panc-28 cells is dependent on the catalytic function of tTG (22) .

So how does the transamidation activity of tTG stimulate NFκB activity? It appears to most likely involve the ability of tTG to cross-link IκBα, the critical negative regulator of NFκB activity. In support of this idea, tTG was found to induce the covalent oligomerization of IκBα both *in vitro* and within the Panc-28 cell line (22, 114). Interestingly, the recombinant form IκBα that was cross-linked by tTG was shown to bind NFκB more weakly than its non-cross-linked counterpart, suggesting that this tTG-induced modification of IκBα in cells functionally inactivates IκBα, resulting in the constitutive activation of NFκB (114). In line with these findings, a separate study looking at how tTG provides a protective effect to ovarian cancer cells challenged with the chemotherapeutic agent cisplatin also concluded that the tTG-stimulated chemo-resistance seen in these cancer cells was dependent on its ability to stimulate the activation of the NFκB survival pathway (97). Thus, it appears that the survival effects of tTG are coupled to NFκB activation in a number of cancer types.

Determining the mechanisms that give rise to drug-resistance in cancer cells is extremely important for the development of more effective strategies to treat patients with advanced forms of cancer. The increasing amounts of evidence showing that tTG expression and activation is frequently up-regulated in human cancers as a means of protecting cells from harmful cellular stresses (24, 38, 57, 59, 97, 98), has provided significant insights into how cancer cells become insensitive to chemotherapies. Thus, targeting tTG itself or its associated effects may prove to be an important strategy to

treat cancer patients with advanced and/or chemotherapy-insensitive forms of the disease.

*The role of tTG in cancer cell migration and invasion*

Directional cell migration is a fundamental cellular process that is required for proper embryonic development, tissue homeostasis, and immune responses in animals (115, 116). In order for a cell to efficiently migrate it must coordinate the activation and distribution of signaling molecules with changes in its actin-cytoskeleton network and plasma membrane. Although directional cell migration is a highly complicated, cyclic process that is still far from being completely understood, the general principles underlying cell migration are known (116). To migrate, a cell must first take on a polarized morphology, such that it has a front or leading edge (for forward movement) and a back (for retraction). Actin polymerization-dependent protrusions are then extended from the leading edge and make contact with the extracellular matrix. These newly formed sites of cell adhesion function to anchor the protrusions, allowing the body of the cell to shift forward. Cell contraction at the back end of the cell, as an outcome of actin bundling and de-polymerization, completes one cycle of the cell migration process. By repeating this sequence of events, a cell moves from one site to another (116).

Aside from its physiological relevance, cell migration is also a major factor in the development or progression of several different human pathologies, ranging from cardiovascular disease to cancer (115). For example, during tumor progression a subset of the cancer cells found within the primary tumor mass often acquire the

ability to move into or invade neighboring normal tissue. Tumors that exhibit this type of invasive behavior tend to be more aggressive in nature and correlate with a poor patient prognosis (115). Interestingly, tTG has recently been implicated as an important contributor to the migratory and invasive phenotype of human cancer cells (23, 25, 40, 58, 59, 96, 117).

One of the earliest indications that tTG is associated with cancer cell migration and tumor dissemination came from proteomic screens performed on primary and metastatic human lung and breast tumors, where tTG was identified as one of only eleven proteins that were consistently up-regulated in metastatic tumors (118). These findings were then followed up with a study that investigated the possible link between the constitutively expressed and activated tTG found in the human breast cancer cell line MDAMB231 and the excessive migration and invasive activity exhibited by these cells (23). Experiments performed comparing the migration and invasive capability of the parental MDAMB231 cells to a sub-line that was selected for its greatly reduced levels of tTG expression, revealed that tTG was required for MDAMB231 cells to exhibit these aggressive properties. The authors then went on to show that tTG was present at the plasma membrane of MDAMB231 cells where it was bound to β1, β4, and β5 integrins, members of a family of cell surface receptors that primarily function to attach cells to specific components in the extracellular matrix (i.e. fibronectin) and to promote cell migration (119, 120). tTG has been shown to interact with specific members of the integrin family in a variety of normal and cancer cell types (31, 96, 121), suggesting that its ability to interact with proteins that function in

cell attachment may likely contribute to its ability to stimulate cancer cell migration and invasion.

Signals that originate outside of the cell can play critical roles in directional cell motility. For example, simply adding growth factors like EGF to the culturing medium of normal fibroblasts or to HeLa cervical carcinoma cells can induce or enhance the ability of these cells to migrate (122, 123). These findings, combined with the fact that accumulating evidence suggests that the EGFR contributes to tumor invasion and metastasis (124-126), has generated a considerable amount of interest in determining the molecular mechanisms that link EGFR activation to the changes that cells must undergo in order to allow them to migrate and invade.

Our laboratory has recently implicated tTG as an important mediator of EGF-stimulated cancer cell migration and invasive activity (40). These studies stemmed from our long-standing interest in understanding how activation of the EGFR both initiates and orchestrates intracellular signaling events that give rise to cellular phenotypes that are characteristic of the oncogenic or transformed state. In this particular case, we set out to identify proteins that coupled the ability of the activated EGFR to give rise to an enhanced migratory and invasive capability in the human cervical carcinoma cell line HeLa. HeLa cell cultures exposed to EGF acquire the distinctive polarized cell morphology associated with actively migrating cells; with each cell having formed both a front or leading edge and a back. Since proteins that are localized to leading edges have consistently been shown to contribute to cell motility (115, 116), we began to look for proteins that accumulated at the leading edges of EGF-stimulated HeLa cells as a means to identify novel participants in cell

migration. Due to the earlier findings showing that tTG was vital for the aggressive phenotype exhibited by MDAMB231 breast cancer cells (23), we considered tTG as a possible candidate protein. Immunofluorescent studies carried-out on untreated HeLa cells revealed that tTG was primarily expressed throughout the cytoplasm of these cells (40). However, EGF treatment caused a dramatic change in the sub-cellular localization of tTG, such that it could be readily detectable in the leading edges of cells. Moreover, we found that EGF promotes the activation of tTG in HeLa cells, without having a significant effect on its expression, suggesting that tTG might play an important role in EGF-promoted cell migration (40). Indeed, treating HeLa cells with the tTG inhibitor MDC, or knocking-down tTG expression by siRNA, potently inhibited the migration- and invasion-promoting effects of EGF (40). Interestingly, however, MDC treatment appeared to have no effect on serum-induced HeLa cell migration, raising the possibility that tTG may not play a general role in cell migration, but rather is a specific component of the EGF-signaling pathway that promotes the motility of these cancer cells.

While these findings identify tTG as a crucial regulator of EGF-stimulated cell migration and invasion, they also raise a number of additional questions. The foremost of these being, what are the proteins that are covalently modified by tTG to promote cell migration and/or invasion? It is especially tempting to speculate that tTG is recruited to the leading edges of cells in order to cross-link another protein or specific set of proteins that are also present at the leading edge during cell migration. The cross-linking of these proteins by tTG would most likely affect their function in such a way as to allow EGF-stimulated cell migration to occur. However, we also recognize

the possibility that tTG might contribute to the development of the invasive/metastatic phenotype in cancer cells through additional mechanisms. In support of this idea, the aggressive nature of ovarian cancers was found to be coupled to the ability of tTG to regulate gene expression (25). More specifically, it was shown that tTG stimulated the expression of the transcriptional repressor Zeb1 through an NFκB-dependent mechanism. Since Zeb1 functions to limit the expression of proteins that are important for maintaining tissue homeostasis (i.e. E-cadherin) (127), ovarian tumors that over-express Zeb1 tend to disrupt tissue integrity, increasing the invasive and metastatic potential of these tumors.

## REFERENCES


1. Folk JE (1980) Transglutaminases. *Annu Rev Biochem* 49:517-531.

2. Greenberg CS, Birckbichler PJ, Rice RH (1991) Transglutaminases: multifunctional cross-linking enzymes that stabilize tissues. *Faseb J* 5:3071-3077.

3. Fujita K, et al. (1998) Alteration of enzymatic activities implicating neuronal degeneration in the spinal cord of the motor neuron degeneration mouse during postnatal development. *Neurochem Res* 23:557-562.

4. Tee AE, et al. (2009) The opposing effects of two tissue transglutaminase protein isoforms in neuroblastoma cell differentiation. *J Biol Chem*.

5. Aeschlimann D, Kaupp O, Paulsson M (1995) Transglutaminase-catalyzed matrix cross-linking in differentiating cartilage: identification of osteonectin as a major glutaminyl substrate. *J Cell Biol* 129:881-892.

6. Orlandi A, et al. (2009) Transglutaminase-2 differently regulates cartilage destruction and osteophyte formation in a surgical model of osteoarthritis. *Amino Acids* 36:755-763.

7. Raghunath M, et al. (1996) Cross-linking of the dermo-epidermal junction of skin regenerating from keratinocyte autografts. Anchoring fibrils are a target for tissue transglutaminase. *J Clin Invest* 98:1174-1184.

8. Haroon ZA, Hettasch JM, Lai TS, Dewhirst MW, Greenberg CS (1999) Tissue transglutaminase is expressed, active, and directly involved in rat dermal wound healing and angiogenesis. *Faseb J* 13:1787-1795.

9. Verderio EA, Johnson T, Griffin M (2004) Tissue transglutaminase in normal and abnormal wound healing: review article. *Amino Acids* 26:387-404.

10. Telci D, Griffin M (2006) Tissue transglutaminase (TG2)--a wound response enzyme. *Front Biosci* 11:867-882.

11. Jones RA, et al. (2006) Matrix changes induced by transglutaminase 2 lead to inhibition of angiogenesis and tumor growth. *Cell Death Differ* 13:1442-1453.

12. Mehta K, Lopez-Berestein G (1986) Expression of tissue transglutaminase in cultured monocytic leukemia (THP-1) cells during differentiation. *Cancer Res* 46:1388-1394.

13. Aeschlimann D, Wetterwald A, Fleisch H, Paulsson M (1993) Expression of tissue transglutaminase in skeletal tissues correlates with events of terminal differentiation of chondrocytes. *J Cell Biol* 120:1461-1470.

14. Singh US, et al. (2003) Tissue transglutaminase mediates activation of RhoA and MAP kinase pathways during retinoic acid-induced neuronal differentiation of SH-SY5Y cells. *J Biol Chem* 278:391-399.

15. Fesus L, et al. (1989) Apoptotic hepatocytes become insoluble in detergents and chaotropic agents as a result of transglutaminase action. *FEBS Lett* 245:150-154.

16. el Alaoui S, Mian S, Lawry J, Quash G, Griffin M (1992) Cell cycle kinetics, tissue transglutaminase and programmed cell death (apoptosis). *FEBS Lett* 311:174-178.

17. Zhang LX, Mills KJ, Dawson MI, Collins SJ, Jetten AM (1995) Evidence for the involvement of retinoic acid receptor RAR alpha-dependent signaling pathway in the induction of tissue transglutaminase and apoptosis by retinoids. *J Biol Chem* 270:6022-6029.

18. Oliverio S, Amendola A, Rodolfo C, Spinedi A, Piacentini M (1999) Inhibition of "tissue" transglutaminase increases cell survival by preventing apoptosis. *J Biol Chem* 274:34123-34128.

19. Antonyak MA, et al. (2001) Effects of tissue transglutaminase on retinoic acid-induced cellular differentiation and protection against apoptosis. *J Biol Chem* 276:33582-33587.

20. Boehm JE, Singh U, Combs C, Antonyak MA, Cerione RA (2002) Tissue transglutaminase protects against apoptosis by modifying the tumor suppressor protein p110 Rb. *J Biol Chem* 277:20127-20130.

21. Li B, et al. (2010) EGF potentiated oncogenesis requires a tissue transglutaminase-dependent signaling pathway leading to Src activation. *Proc Natl Acad Sci U S A* 107:1408-1413.

22. Mann AP, et al. (2006) Overexpression of tissue transglutaminase leads to constitutive activation of nuclear factor-kappaB in cancer cells: delineation of a novel pathway. *Cancer Res* 66:8788-8795.

23. Mangala LS, Fok JY, Zorrilla-Calancha IR, Verma A, Mehta K (2006) Tissue transglutaminase expression promotes cell attachment, invasion and survival in breast cancer cells. *Oncogene*.

24. Yuan L, et al. (2007) Transglutaminase 2 inhibitor, KCC009, disrupts fibronectin assembly in the extracellular matrix and sensitizes orthotopic glioblastomas to chemotherapy. *Oncogene* 26:2563-2573.

25. Shao M, et al. (2009) Epithelial-to-mesenchymal transition and ovarian tumor progression induced by tissue transglutaminase. *Cancer Res* 69:9192-9201.

26. Nakaoka H, et al. (1994) Gh: a GTP-binding protein with transglutaminase activity and receptor signaling function. *Science* 264:1593-1596.

27. Datta S, Antonyak MA, Cerione RA (2006) Importance of Ca(2+)-dependent transamidation activity in the protection afforded by tissue transglutaminase against doxorubicin-induced apoptosis. *Biochemistry* 45:13163-13174.

28. Liu S, Cerione RA, Clardy J (2002) Structural basis for the guanine nucleotide-binding activity of tissue transglutaminase and its regulation of transamidation activity. *Proceedings of the National Academy of Sciences of the United States of America.* 99:2743-2747.

29. Pinkas DM, Strop P, Brunger AT, Khosla C (2007) Transglutaminase 2 undergoes a large conformational change upon activation. *PLoS Biol* 5:e327.

30. Datta S, Antonyak MA, Cerione RA (2007) GTP-binding-defective forms of tissue transglutaminase trigger cell death. *Biochemistry* 46:14819-14829.

31. Akimov SS, Krylov D, Fleischman LF, Belkin AM (2000) Tissue transglutaminase is an integrin-binding adhesion coreceptor for fibronectin. *J Cell Biol* 148:825-838.

32. Fâesèus L, Szondy Z (2005) Transglutaminase 2 in the balance of cell death and survival. *FEBS letters.* 579:3297-3302.

33. Antonyak MA, et al. (2006) Two isoforms of tissue transglutaminase mediate opposing cellular fates. *Proc Natl Acad Sci U S A* 103:18609-18614.

34. Zemskov EA, Janiak A, Hang J, Waghray A, Belkin AM (2006) The role of tissue transglutaminase in cell-matrix interactions. *Front Biosci* 11:1057-1076.

35. Gandarillas A (2000) Epidermal differentiation, apoptosis, and senescence: common pathways? *Exp Gerontol* 35:53-62.

36. Antonyak MA, Boehm JE, Cerione RA (2002) Phosphoinositide 3-kinase activity is required for retinoic acid-induced expression and activation of the tissue transglutaminase. *J Biol Chem* 277:14712-14716.

37. Antonyak MA, McNeill CJ, Wakshlag JJ, Boehm JE, Cerione RA (2003) Activation of the Ras-ERK pathway inhibits retinoic acid-induced stimulation

of tissue transglutaminase expression in NIH3T3 cells. *J Biol Chem* 278:15859-15866.

38. Antonyak MA, et al. (2004) Augmentation of tissue transglutaminase expression and activation by epidermal growth factor inhibit doxorubicin-induced apoptosis in human breast cancer cells. *J Biol Chem* 279:41461-41467.

39. Li B, et al. (2010) EGF potentiated oncogenesis requires a tissue transglutaminase-dependent signaling pathway leading to Src activation. *Proc Natl Acad Sci U S A* (In Press).

40. Antonyak MA, et al. (2009) Tissue transglutaminase is an essential participant in the epidermal growth factor-stimulated signaling pathway leading to cancer cell migration and invasion. *J Biol Chem* 284:17914-17925.

41. Chen JS, Mehta K (1999) Tissue transglutaminase: an enzyme with a split personality. *The international journal of biochemistry & cell biology.* 31:817-836.

42. Hernandez AA, Roush WR (2002) Recent advances in the synthesis, design and selection of cysteine protease inhibitors. *Curr Opin Chem Biol* 6:459-465.

43. Lorand L, Conrad SM (1984) Transglutaminases. *Mol Cell Biochem* 58:9-35.

44. Iismaa SE, Mearns BM, Lorand L, Graham RM (2009) Transglutaminases and disease: lessons from genetically engineered mouse models and inherited disorders. *Physiol Rev* 89:991-1023.

45. Chica RA, Gagnon P, Keillor JW, Pelletier JN (2004) Tissue transglutaminase acylation: Proposed role of conserved active site Tyr and Trp residues revealed by molecular modeling of peptide substrate binding. *Protein Sci* 13:979-991.

46. Yee VC, et al. (1994) Three-dimensional structure of a transglutaminase: human blood coagulation factor XIII. *Proc Natl Acad Sci U S A* 91:7296-7300.

47. Yee VC, et al. (1994) Three-dimensional structure of a transglutaminase: human blood coagulation factor XIII. *Proceedings of the National Academy of Sciences of the United States of America.* 91:7296-7300.

48. Casadio R, et al. (1999) The structural basis for the regulation of tissue transglutaminase by calcium ions. *European journal of biochemistry / FEBS.* 262:672-679.

49. Murthy SN, et al. (2002) Conserved tryptophan in the core domain of transglutaminase is essential for catalytic activity. *Proc Natl Acad Sci U S A* 99:2738-2742.

50. Iismaa SE, et al. (2003) Evolutionary specialization of a tryptophan indole group for transition-state stabilization by eukaryotic transglutaminases. *Proc Natl Acad Sci U S A* 100:12636-12641.

51. Lee MY, Chung S, Bang HW, Baek KJ, Uhm D (1997) Modulation of large conductance Ca2+-activated K+ channel by Galphah (transglutaminase II) in the vascular smooth muscle cell. *Pflugers Arch* 433:671-673.

52. Cabrera-Vera TM, et al. (2003) Insights into G protein structure, function, and regulation. *Endocr Rev* 24:765-781.

53. Lambright DG, Noel JP, Hamm HE, Sigler PB (1994) Structural determinants for activation of the alpha-subunit of a heterotrimeric G protein. *Nature* 369:621-628.

54. Sprang SR, Coleman DE (1998) Invasion of the nucleotide snatchers: structural insights into the mechanism of G protein GEFs. *Cell* 95:155-158.

55. Begg GE, et al. (2006) Mutation of a critical arginine in the GTP-binding site of transglutaminase 2 disinhibits intracellular cross-linking activity. *J Biol Chem* 281:12603-12609.

56. Iismaa SE, Wu MJ, Nanda N, Church WB, Graham RM (2000) GTP binding and signaling by Gh/transglutaminase II involves distinct residues in a unique GTP-binding pocket. *J Biol Chem* 275:18259-18265.

57. Kim DS, Park SS, Nam BH, Kim IH, Kim SY (2006) Reversal of drug resistance in breast cancer cells by transglutaminase 2 inhibition and nuclear factor-kappaB inactivation. *Cancer Res* 66:10936-10943.

58. Hwang JY, et al. (2008) Clinical and biological significance of tissue transglutaminase in ovarian carcinoma. *Cancer Res* 68:5849-5858.

59. Verma A, et al. (2006) Increased expression of tissue transglutaminase in pancreatic ductal adenocarcinoma and its implications in drug resistance and metastasis. *Cancer Res* 66:10525-10533.

60. Melino G, et al. (1994) Tissue transglutaminase and apoptosis: sense and antisense transfection studies with human neuroblastoma cells. *Mol Cell Biol* 14:6584-6596.

61. Ou H, et al. (2000) Retinoic acid-induced tissue transglutaminase and apoptosis in vascular smooth muscle cells. *Circ Res* 87:881-887.

62. Nemes Z, Jr., Adany R, Balazs M, Boross P, Fesus L (1997) Identification of cytoplasmic actin as an abundant glutaminyl substrate for tissue

transglutaminase in HL-60 and U937 cells undergoing apoptosis. *J Biol Chem* 272:20577-20583.

63. Piacentini M, et al. (1991) The expression of "tissue" transglutaminase in two human cancer cell lines is related with the programmed cell death (apoptosis). *Eur J Cell Biol* 54:246-254.

64. Piredda L, et al. (1997) Lack of 'tissue' transglutaminase protein cross-linking leads to leakage of macromolecules from dying cells: relationship to development of autoimmunity in MRLIpr/Ipr mice. *Cell Death Differ* 4:463-472.

65. Piacentini M, et al. (2002) Transglutaminase overexpression sensitizes neuronal cell lines to apoptosis by increasing mitochondrial membrane potential and cellular oxidative stress. *J Neurochem* 81:1061-1072.

66. Tucholski J, Lesort M, Johnson GV (2001) Tissue transglutaminase is essential for neurite outgrowth in human neuroblastoma SH-SY5Y cells. *Neuroscience* 102:481-491.

67. Condello S, et al. (2008) Transglutaminase 2 and NF-kappaB interplay during NGF-induced differentiation of neuroblastoma cells. *Brain Res* 1207:1-8.

68. Chiocca EA, Davies PJ, Stein JP (1989) Regulation of tissue transglutaminase gene expression as a molecular model for retinoid effects on proliferation and differentiation. *J Cell Biochem* 39:293-304.

69. Ross CA, Poirier MA (2004) Protein aggregation and neurodegenerative disease. *Nat Med* 10 Suppl:S10-17.

70. Davies SW, et al. (1997) Formation of neuronal intranuclear inclusions underlies the neurological dysfunction in mice transgenic for the HD mutation. *Cell* 90:537-548.

71. Scherzinger E, et al. (1999) Self-assembly of polyglutamine-containing huntingtin fragments into amyloid-like fibrils: implications for Huntington's disease pathology. *Proc Natl Acad Sci U S A* 96:4604-4609.

72. Lesort M, Chun W, Johnson GV, Ferrante RJ (1999) Tissue transglutaminase is increased in Huntington's disease brain. *J Neurochem* 73:2018-2027.

73. Karpuj MV, et al. (1999) Transglutaminase aggregates huntingtin into nonamyloidogenic polymers, and its enzymatic activity increases in Huntington's disease brain nuclei. *Proc Natl Acad Sci U S A* 96:7388-7393.

74. Kim SY, Grant P, Lee JH, Pant HC, Steinert PM (1999) Differential expression of multiple transglutaminases in human brain. Increased expression

and cross-linking by transglutaminases 1 and 2 in Alzheimer's disease. *J Biol Chem* 274:30715-30721.

75. Junn E, Ronchetti RD, Quezado MM, Kim SY, Mouradian MM (2003) Tissue transglutaminase-induced aggregation of alpha-synuclein: Implications for Lewy body formation in Parkinson's disease and dementia with Lewy bodies. *Proc Natl Acad Sci U S A* 100:2047-2052.

76. Johnson GV, et al. (1997) Transglutaminase activity is increased in Alzheimer's disease brain. *Brain Res* 751:323-329.

77. Dedeoglu A, et al. (2002) Therapeutic effects of cystamine in a murine model of Huntington's disease. *J Neurosci* 22:8942-8950.

78. Kahlem P, Green H, Djian P (1998) Transglutaminase action imitates Huntington's disease: selective polymerization of Huntingtin containing expanded polyglutamine. *Mol Cell* 1:595-601.

79. Mastroberardino PG, et al. (2002) 'Tissue' transglutaminase ablation reduces neuronal death and prolongs survival in a mouse model of Huntington's disease. *Cell Death Differ* 9:873-880.

80. Karpuj MV, et al. (2002) Prolonged survival and decreased abnormal movements in transgenic model of Huntington disease, with administration of the transglutaminase inhibitor cystamine. *Nat Med* 8:143-149.

81. Pahlman S, Ruusala AI, Abrahamsson L, Mattsson ME, Esscher T (1984) Retinoic acid-induced differentiation of cultured human neuroblastoma cells: a comparison with phorbolester-induced differentiation. *Cell Differ* 14:135-144.

82. Preis PN, et al. (1988) Neuronal cell differentiation of human neuroblastoma cells by retinoic acid plus herbimycin A. *Cancer Res* 48:6530-6534.

83. Zhang J, Lesort M, Guttmann RP, Johnson GV (1998) Modulation of the in situ activity of tissue transglutaminase by calcium and GTP. *J Biol Chem* 273:2288-2295.

84. Sporn MB, Roberts AB (1983) Role of retinoids in differentiation and carcinogenesis. *Cancer Res* 43:3034-3040.

85. Breitman TR, Collins SJ, Keene BR (1981) Terminal differentiation of human promyelocytic leukemic cells in primary culture in response to retinoic acid. *Blood* 57:1000-1004.

86. Costa A, et al. (1994) Prospects of chemoprevention of human cancers with the synthetic retinoid fenretinide. *Cancer Res* 54:2032s-2037s.

87. Formelli F, Barua AB, Olson JA (1996) Bioactivities of N-(4-hydroxyphenyl) retinamide and retinoyl beta-glucuronide. *Faseb J* 10:1014-1024.

88. Breitman TR, Selonick SE, Collins SJ (1980) Induction of differentiation of the human promyelocytic leukemia cell line (HL-60) by retinoic acid. *Proc Natl Acad Sci U S A* 77:2936-2940.

89. Collins SJ, Robertson KA, Mueller L (1990) Retinoic acid-induced granulocytic differentiation of HL-60 myeloid leukemia cells is mediated directly through the retinoic acid receptor (RAR-alpha). *Mol Cell Biol* 10:2154-2163.

90. Delia D, et al. (1993) N-(4-hydroxyphenyl)retinamide induces apoptosis of malignant hemopoietic cell lines including those unresponsive to retinoic acid. *Cancer Res* 53:6036-6041.

91. Dipietrantonio A, Hsieh TC, Wu JM (1996) Differential effects of retinoic acid (RA) and N-(4-hydroxyphenyl) retinamide (4-HPR) on cell growth, induction of differentiation, and changes in p34cdc2, Bcl-2, and actin expression in the human promyelocytic HL-60 leukemic cells. *Biochem Biophys Res Commun* 224:837-842.

92. Ponzoni M, et al. (1995) Differential effects of N-(4-hydroxyphenyl)retinamide and retinoic acid on neuroblastoma cells: apoptosis versus differentiation. *Cancer Res* 55:853-861.

93. Nagy L, Thomazy VA, Chandraratna RA, Heyman RA, Davies PJ (1996) Retinoid-regulated expression of BCL-2 and tissue transglutaminase during the differentiation and apoptosis of human myeloid leukemia (HL-60) cells. *Leuk Res* 20:499-505.

94. Singer CF, et al. (2006) Tissue array-based expression of transglutaminase-2 in human breast and ovarian cancer. *Clin Exp Metastasis* 23:33-39.

95. Hettasch JM, et al. (1996) Tissue transglutaminase expression in human breast cancer. *Lab Invest* 75:637-645.

96. Satpathy M, et al. (2007) Enhanced peritoneal ovarian tumor dissemination by tissue transglutaminase. *Cancer Res* 67:7194-7202.

97. Cao L, et al. (2008) Tissue transglutaminase protects epithelial ovarian cancer cells from cisplatin-induced apoptosis by promoting cell survival signaling. *Carcinogenesis* 29:1893-1900.

98. Verma A, et al. (2008) Tissue transglutaminase regulates focal adhesion kinase/AKT activation by modulating PTEN expression in pancreatic cancer cells. *Clin Cancer Res* 14:1997-2005.

99. Yarden Y, Shilo BZ (2007) SnapShot: EGFR signaling pathway. *Cell* 131:1018.

100. Nicholson RI, Gee JM, Harper ME (2001) EGFR and cancer prognosis. *Eur J Cancer* 37 Suppl 4:S9-15.

101. Mendelsohn J, Baselga J (2000) The EGF receptor family as targets for cancer therapy. *Oncogene* 19:6550-6565.

102. Zhang R, Tremblay TL, McDermid A, Thibault P, Stanimirovic D (2003) Identification of differentially expressed proteins in human glioblastoma cell lines and tumors. *Glia* 42:194-208.

103. Esposito C, Caputo I (2005) Mammalian transglutaminases. Identification of substrates as a key to physiological function and physiopathological relevance. *FEBS J* 272:615-631.

104. Facchiano A, Facchiano F (2009) Transglutaminases and their substrates in biology and human diseases: 50 years of growing. *Amino Acids* 36:599-614.

105. Yamaguchi H, Wang HG (2006) Tissue transglutaminase serves as an inhibitor of apoptosis by cross-linking caspase 3 in thapsigargin-treated cells. *Mol Cell Biol* 26:569-579.

106. Kurokawa M, Kornbluth S (2009) Caspases and kinases in a death grip. *Cell* 138:838-854.

107. Hebert SS, et al. (2000) The mixed lineage kinase DLK is oligomerized by tissue transglutaminase during apoptosis. *J Biol Chem* 275:32482-32490.

108. Lee CH, Jeon YT, Kim SH, Song YS (2007) NF-kappaB as a potential molecular target for cancer therapy. *Biofactors* 29:19-35.

109. Basseres DS, Baldwin AS (2006) Nuclear factor-kappaB and inhibitor of kappaB kinase pathways in oncogenic initiation and progression. *Oncogene* 25:6817-6830.

110. Biswas DK, et al. (2004) NF-kappa B activation in human breast cancer specimens and its role in cell proliferation and apoptosis. *Proc Natl Acad Sci U S A* 101:10137-10142.

111. Nakshatri H, Bhat-Nakshatri P, Martin DA, Goulet RJ, Jr., Sledge GW, Jr. (1997) Constitutive activation of NF-kappaB during progression of breast cancer to hormone-independent growth. *Mol Cell Biol* 17:3629-3639.

112. Wang W, et al. (1999) The nuclear factor-kappa B RelA transcription factor is constitutively activated in human pancreatic adenocarcinoma cells. *Clin Cancer Res* 5:119-127.

113. Wu JT, Kral JG (2005) The NF-kappaB/IkappaB signaling system: a molecular target in breast cancer therapy. *J Surg Res* 123:158-169.

114. Lee J, et al. (2004) Transglutaminase 2 induces nuclear factor-kappaB activation via a novel pathway in BV-2 microglia. *J Biol Chem* 279:53725-53735.

115. Sahai E (2007) Illuminating the metastatic process. *Nat Rev Cancer* 7:737-749.

116. Le Clainche C, Carlier MF (2008) Regulation of actin assembly associated with protrusion and adhesion in cell migration. *Physiol Rev* 88:489-513.

117. Joshi S, Guleria R, Pan J, DiPette D, Singh US (2006) Retinoic acid receptors and tissue-transglutaminase mediate short-term effect of retinoic acid on migration and invasion of neuroblastoma SH-SY5Y cells. *Oncogene* 25:240-247.

118. Jiang D, et al. (2003) Identification of metastasis-associated proteins by proteomic analysis and functional exploration of interleukin-18 in metastasis. *Proteomics* 3:724-737.

119. Hynes RO (2002) Integrins: bidirectional, allosteric signaling machines. *Cell* 110:673-687.

120. Humphries MJ, Travis MA, Clark K, Mould AP (2004) Mechanisms of integration of cells and extracellular matrices by integrins. *Biochem Soc Trans* 32:822-825.

121. Akimov SS, Belkin AM (2001) Cell surface tissue transglutaminase is involved in adhesion and migration of monocytic cells on fibronectin. *Blood* 98:1567-1576.

122. Zuo X, et al. (2006) Exo70 interacts with the Arp2/3 complex and regulates cell migration. *Nat Cell Biol* 8:1383-1388.

123. Katz M, et al. (2007) A reciprocal tensin-3-cten switch mediates EGF-driven mammary cell migration. *Nat Cell Biol* 9:961-969.

124. Micallef J, et al. (2009) Epidermal growth factor receptor variant III-induced glioma invasion is mediated through myristoylated alanine-rich protein kinase C substrate overexpression. *Cancer Res* 69:7548-7556.

125. Cui X, et al. (2006) Epidermal growth factor induces insulin receptor substrate-2 in breast cancer cells via c-Jun NH(2)-terminal kinase/activator protein-1 signaling to regulate cell migration. *Cancer Res* 66:5304-5313.

126. Ricono JM, et al. (2009) Specific cross-talk between epidermal growth factor receptor and integrin alphavbeta5 promotes carcinoma cell invasion and metastasis. *Cancer Res* 69:1383-1391.

127. Wellner U, et al. (2009) The EMT-activator ZEB1 promotes tumorigenicity by repressing stemness-inhibiting microRNAs. *Nat Cell Biol* 11:1487-1495.

# CHAPTER 2

## *EGF potentiated oncogenesis requires a tissue transglutaminase-dependent signaling pathway leading to Src activation

### Introduction

The EGFR is expressed on the surface of various types of human cancer cells where the ligand-dependent induction of its kinase activity triggers signaling pathways that promote cancer cell growth, motility, and chemo-resistance (1). Moreover, the EGFR or one of its ligands is often found overexpressed or mutated in tumors, with these events being linked to enhanced tumorigenicity (2, 3). The close connection between excessive EGFR-signaling activities and cancer progression has led to the development of EGFR-targeted therapeutic strategies that are currently being used to treat patients with lung, colon, and pancreatic cancer (1, 4). However, many of these patients either fail to respond or develop resistance to these treatments, suggesting that alternative strategies that target EGFR-signaling activities are needed and could be therapeutically beneficial in these cases (5).

Determining the molecular mechanisms that underlie the ability of the EGFR to stimulate malignant transformation represents a crucial step in the development of more effective and/or alternative cancer treatments. Indeed, several of the signaling proteins that have been shown to function downstream of the EGFR, including Ras, PI3K, and Src, have been extensively investigated for their roles in mediating oncogenic transformation and are now considered as viable targets for intervention

*Published previously as Li B & Antonyak MA, et al. (2010) *PNAS* 107:1408-1413.

**Figure 2.1 tTG is required for EGF-stimulated growth of human breast cancer cells. (A)** Equal numbers of SKBR3 cells were plated and maintained in medium containing 2% FBS, supplemented without or with EGF. The cell cultures were counted every other day for a week and their growth rates recorded. Error bars represents standard deviation from two repeated experiemts. **(B)** Anchorage-independent growth assays were performed on SKBR3 cells treated without or with EGF. Shown are images of the resulting colonies that formed. **(C)** Graph quantifying the number of colonies that SKBR3 cells formed in these assays. All of the assays were performed 3 times and the results were averaged together and plotted. **(D and E)** Serum-starved SKBR3 cells (D) and BT20 cells (E) were treated without or with EGF for 2 days and then were lysed. The cell extracts were immunoblotted with tTG and actin antibodies (insets) and assayed for transamidation activity as read-out by the incorporation of BPA into lysate proteins. The results from 3 separate assays were quantified using ImageJ software, averaged together, and graphed (graphs). **(F)** Serum-starved SKBR3 cells were treated without or with 150 ng/mL heregulin for 2 days and then were lysed. The cell extracts were immunoblotted with tTG and actin antibodies (insets) and assayed for transamidation activity by the incorporation of BPA into lysate proteins. The results from 3 separate assays were quantified using ImageJ software, averaged together, and graphed (graph). **(G and H)** Two sets each of SKBR3 cells (G) or BT20 cells (H) transfected with control siRNA or tTG siRNAs (denoted tTG-1 or tTG-2), or incubated without or with MDC, were stimulated without or with EGF as indicated. One set of cells was lysed and immunoblotted with tTG and actin antibodies (insets). Anchorage-independent growth assays were performed on the second set of cells. The results from 3 separate assays were averaged together and graphed (graphs)**. (I)** Equal numbers of SKBR3 cells transfected with control siRNA or tTG siRNAs, or incubated without or with MDC, were plated and then maintained in medium containing 2% FBS supplemented without or with EGF. The cell cultures were counted at the indicated times and their growth rates recorded. Experiemts were repeated twice. All the error bars shown from (C) to (I) represent standard deviation.

A

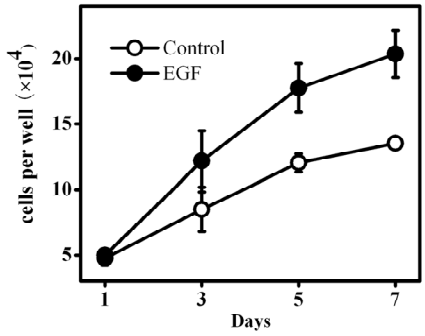
Control
EGF
cells per well (×10^4)
20
15
10
5
1
3
5
7
Days

B

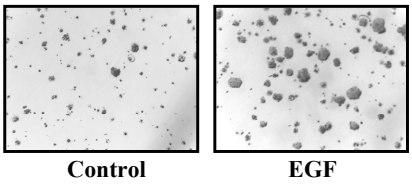
Control
EGF

C

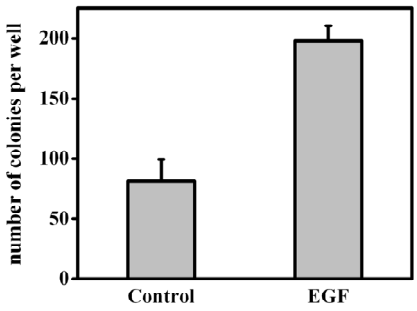
number of colonies per well
200
150
100
50
0
Control
EGF

**Figure 2.1 (Continued)**

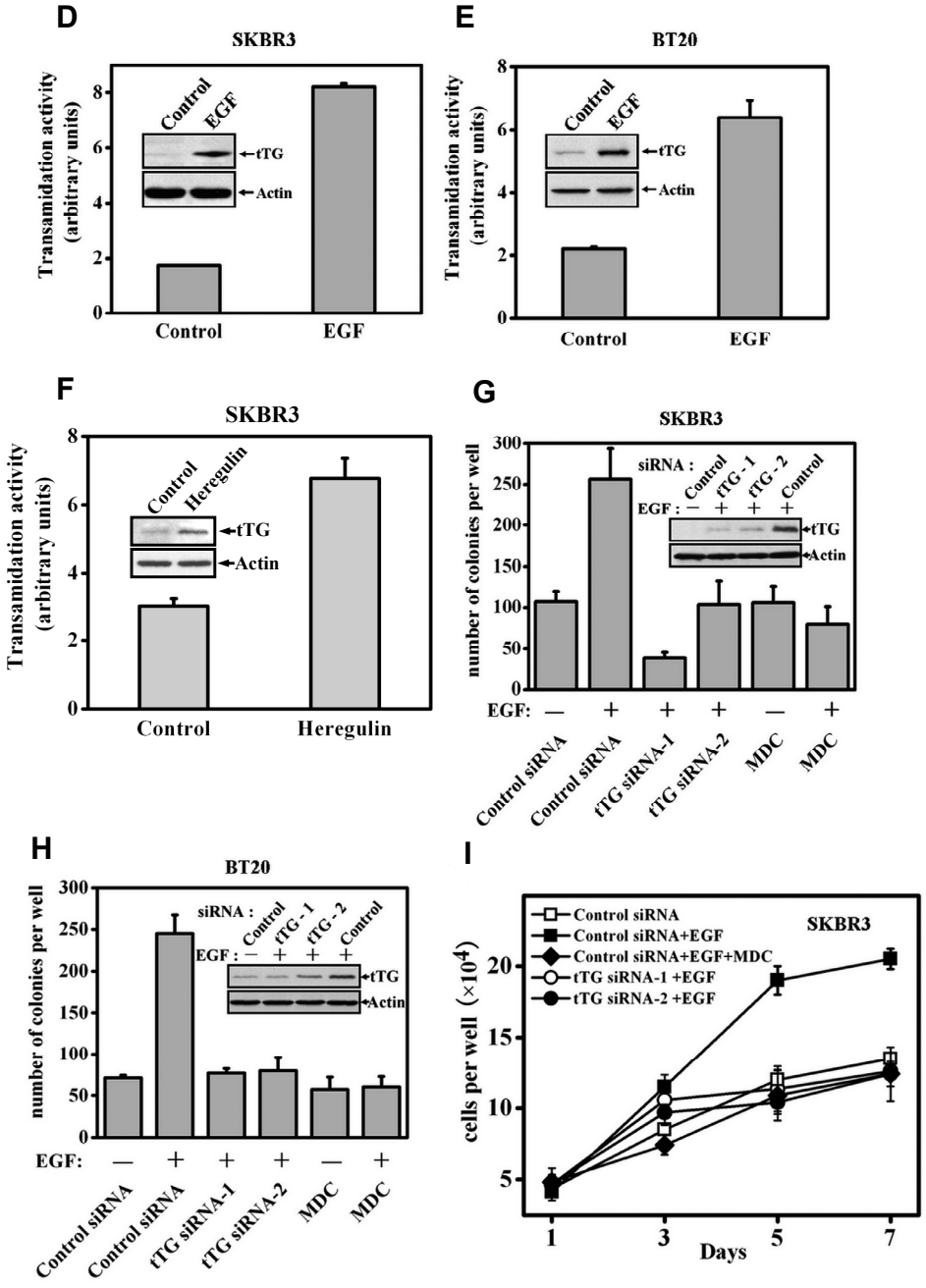

against various types of human cancer (3, 6, 7). In addition, the EGFR regulates the expression of a number of proteins likely to contribute to cell growth control and to malignant transformation, and these proteins offer an additional group of potential therapeutic targets. Here I show that tTG, which is capable of GTP-binding/GTPase activity and acyl-transferase activity (8, 9), represents one such protein whose expression is strongly stimulated by EGF in human breast cancer cells. I go on to demonstrate how tTG expression is up-regulated by EGFR-signaling activities and that it plays an essential role through a novel mechanism in EGFR-driven oncogenic transformation.

**Results**

*tTG mediates the growth-promoting effects of EGF in human breast cancer cells*

The human breast cancer cell line, SKBR3, when grown in medium containing EGF shows enhanced proliferation compared to control cells (Figure 2.1*A*), and an increased ability to form colonies in soft agar (Figure 2.1*B* and 2.1*C*), an *in vitro* measure of tumorigenicity. Efforts to identify proteins in these breast cancer cells whose expression was up-regulated by EGF and therefore potentially contribute to its growth-promoting activity, led me to tTG, a dual function enzyme that couples an ability to bind and hydrolyze GTP with a transamidation activity that cross-links proteins via glutamine-lysine or glutamine-polyamine linkages. While there have been suggestions that chronic tTG expression and/or activation associated with some human cancers is linked to their malignant transformation (10-16), an understanding of how tTG is regulated in cancer cells and whether there is a functional relationship between

**Figure 2.2 EGFR and ErbB2 expression levels are correlated to tTG expression levels in human mammary tumor tissues.** Human breast cancer tissue arrays (catalog # BR1921, U.S. Biomax) containing 80 cases of invasive ductal breast cancer tissue and 16 normal ductal mammary tissues were subjected to immunohistochemical analysis with tTG, EGFR, and ErbB2 antibodies according to the manufacturer's protocol. The resulting staining obtained with each antibody was quantified using ImageJ software. (**A**) The expression levels of tTG detected in the normal mammary tissues and mammary tumor tissues were plotted. Each circle represents a normal mammary tissue, whereas each square represents a mammary tumor tissue. (**B**) Representative immunohistochemical images of a normal mammary tissue and a mammary tumor tissue stained for tTG (magnification: ×20). (**C**) Chart summarizing the numbers and percentages of ductal mammary tumors that were screened and exhibited tTG overexpression (column 2, designated positive) or showed no overexpression of tTG (column 2, designated negative) versus the overexpression of EGFR or ErbB2 (column 3).

**A**

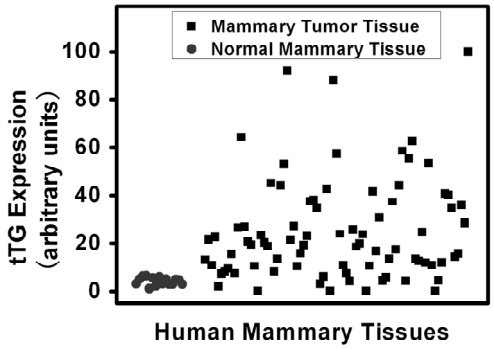


**B**

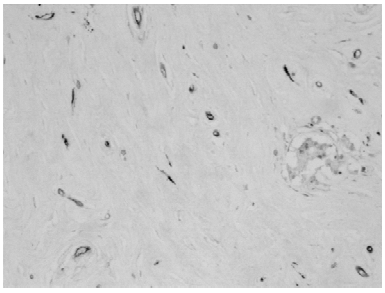

**Normal Mammary Tissue**

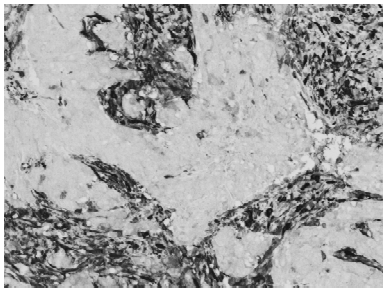

**Mammary Tumor Tissue**

**C**

| Tumor type and Grading | tTG Status | EGFR and ErbB2 Status |
|---|---|---|
| Human Ductal Mammary Carcinoma (80 Cases*) | Positive: 64/80 (80%) | EGFR Positive: 44/64 (69%)<br>ErbB2 Positive: 44/64 (69%) |
| | Negative:16/80 (20%) | EGFR Positive: 5/16 (31%)<br>ErbB2 Positive: 6/16 (39%) |

*Grade 1: 3/80 (4%) ; Grade 2: 63/80 (78%) ; Grade 3: 14/80 (18%)

this protein and EGF-promoted tumor growth has been lacking. Figure 2.1*D*, *inset* shows that EGF induced a strong up-regulation of tTG expression in SKBR3 cells, compared to the nearly undetectable amounts in untreated cells, as well as stimulated its enzymatic activity as assayed by the incorporation of biotinylated pentylamine (BPA) into lysate proteins (Figure 2.1*D*, *graph*). Similarly, EGF caused the up-regulation and activation of tTG in other breast cancer cell lines such as BT20 cells (Figure 2.1*E*, *inset and graph*).

I further established a link between growth factor signaling and tTG in human breast cancer cells by providing two additional pieces of evidence. First, I found that heregulin, a ligand that activates the EGFR family member ErbB2, which has been implicated in breast cancer progression (1), was nearly as effective as EGF at inducing tTG expression and activation in SKBR3 cells (Figure 2.1*F*). Second, immunohistochemical analysis of a human breast cancer tissue array shows that the expression levels of both the EGFR and ErbB2 correlate significantly to tTG expression (Figure 2.2*A*-*C*). Taken together, these findings suggest that tTG may be a critical mediator of EGF- and heregulin-promoted oncogenic processes.

I then asked whether knocking-down tTG expression by siRNA (Figure 2.1*G* and 2.1*H, insets*) or the addition of monodansylcadaverine (MDC), an inhibitor of tTG-catalyzed transamidation, affected the growth-promoting characteristics of EGF. Soft agar assays showed that the EGF-stimulated colony formation of SKBR3 and BT20 cells was reduced to essentially basal levels (i.e. the number of colonies that form in the absence of EGF stimulation) by either the introduction of siRNAs targeting tTG or by treatment with MDC (Figure 2.1*G* and 2.1*H, graphs*). In addition,

**Figure 2.3 Ras- and Cdc42-dependent signaling stimulate tTG expression. (A)** Extracts of serum-starved SKBR3 cells ectopically expressing either the vector-only (treated without or with EGF) or one of the activated forms of the indicated signaling proteins for 2 days were immunoblotted with tTG, HA, and actin antibodies as indicated. **(B)** Serum-deprived cells expressing the vector-only (treated without or with EGF) or various combinations of the activated forms of Ras (Ras G12V) and Cdc42 (Cdc42 F28L) were lysed and then immunoblotted with the indicated antibodies. **(C)** SKBR3 cells cultured in serum-free medium supplemented without or with EGF, plus either LY294002, PD98059, or BAY 11-7082 for 2 days were lysed and the extracts immunoblotted with tTG and actin antibodies. The level of tTG expression detected in each sample was quantified using ImageJ software and the results listed below the tTG blot (Fold tTG expression). **(D)** Extracts of serum-deprived SKBR3 cells ectopically expressing the vector, the oncogenic Dbl protein (onco-Dbl), or the indicated combinations of activated forms of RhoA (RhoA F30L) and Cdc42 (Cdc42 F28L), were immunoblotted with the indicated antibodies. **(E)** SKBR3 cells expressing Ras G12V and/or Cdc42 F28L were incubated without or with either LY294002 or BAY 11-7082 for 2 days and then were lysed. The extracts were immunoblotted with the indicated antibodies.

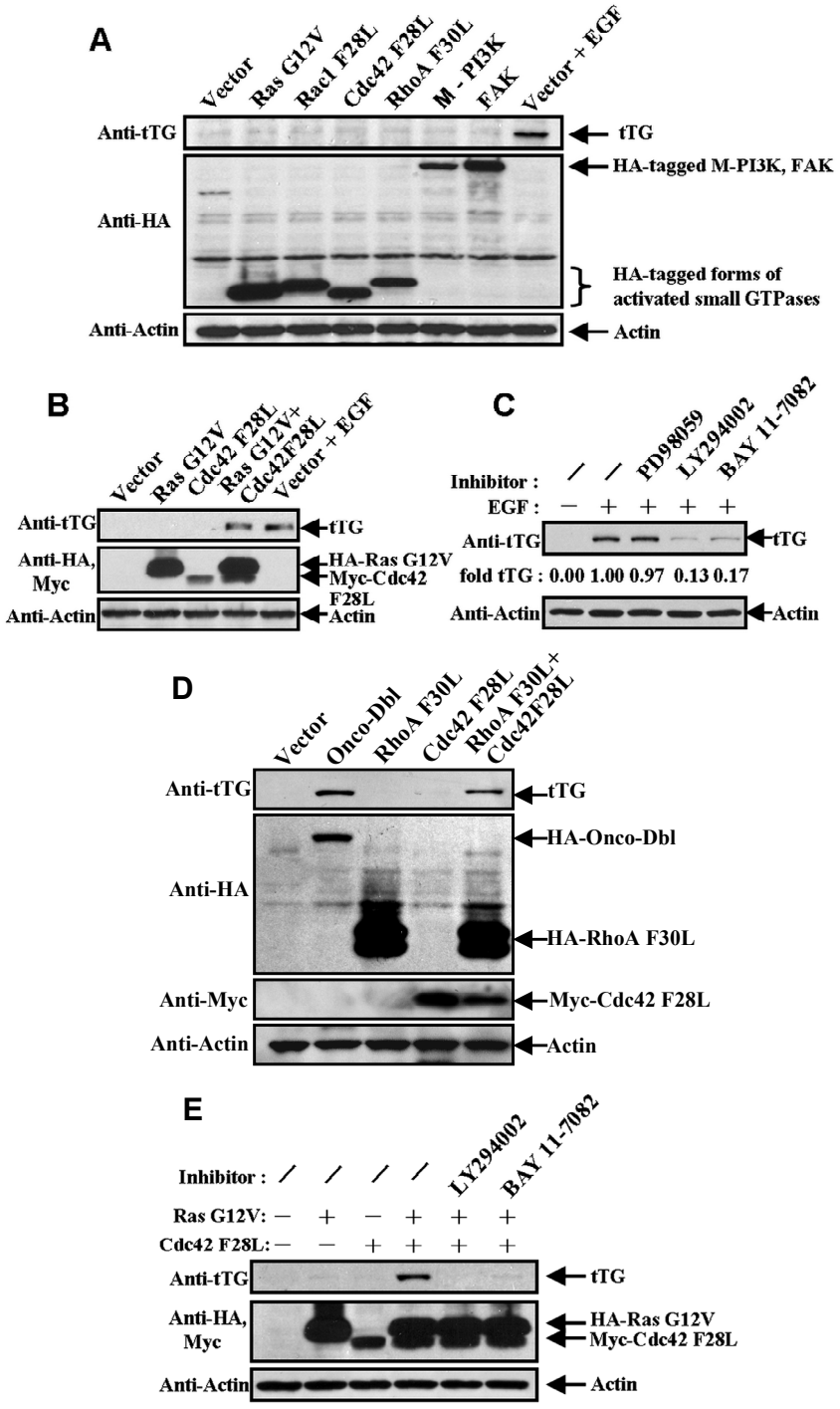
A
Vector
Ras G12V
Rac1 F28L
Cdc42 F28L
RhoA F30L
M - PI3K
FAK
Vector + EGF
Anti-tTG
tTG
HA-tagged M-PI3K, FAK
Anti-HA
HA-tagged forms of activated small GTPases
Anti-Actin
Actin
B
Vector
Ras G12V
Cdc42 F28L
Ras G12V+ Cdc42F28L
Vector + EGF
Anti-tTG
tTG
Anti-HA, Myc
HA-Ras G12V
Myc-Cdc42 F28L
Anti-Actin
Actin
C
Inhibitor :
PD98059
LY294002
BAY 11-7082
EGF : − + + + +
Anti-tTG
tTG
fold tTG : 0.00 1.00 0.97 0.13 0.17
Anti-Actin
Actin
D
Vector
Onco-Dbl
RhoA F30L
Cdc42 F28L
RhoA F30L+ Cdc42F28L
Anti-tTG
tTG
HA-Onco-Dbl
Anti-HA
HA-RhoA F30L
Anti-Myc
Myc-Cdc42 F28L
Anti-Actin
Actin
E
Inhibitor :
LY294002
BAY 11-7082
Ras G12V: − + − + + +
Cdc42 F28L: − − + + + +
Anti-tTG
tTG
Anti-HA, Myc
HA-Ras G12V
Myc-Cdc42 F28L
Anti-Actin
Actin

as shown in Figure 2.1*I*, knock-downs of tTG or treatment with MDC also inhibited the ability of EGF to stimulate the growth of SKBR3 cells in monolayer.

*Co-activation of the Ras- and Cdc42-signaling cascades promotes tTG expression*

To determine how EGF promotes the up-regulation of tTG expression, I examined several signaling proteins known to act down-stream of the EGFR including the small GTPases Ras, Rac1, Cdc42, and RhoA, as well as PI3K and focal adhesion kinase (FAK) (17). Figure 2.3*A* shows the results obtained when I introduced activated forms of these different GTPases, PI3K [myristoylated (M)-PI3K], or wild-type FAK, into SKBR3 cells and assayed for changes in the expression levels of tTG. Despite expressing considerable amounts of each protein (Figure 2.3*A*, *middle panel*), none was capable of enhancing tTG expression (Figure 2.3*A*, *top panel*). This suggested that the ability of EGF to induce tTG expression is likely not mediated by a single signaling cascade, but rather results from the combined activation of two or more pathways. In fact, I found that when different combinations of activated Ras and Rho GTPases (e.g. Cdc42) were expressed in SKBR3 cells, there was a marked up-regulation of tTG expression that fully mimicked the actions of EGF (Figure 2.3*B*). While combinations of activated Ras and Cdc42, or Ras and Rac1, appeared to be most effective at restoring tTG expression, different combinations of Rho GTPases in the absence of activated Ras (e.g. Cdc42 and RhoA), or the expression of oncogenic Dbl, a guanine nucleotide-exchange factor for Cdc42 and RhoA (18), will at least partially mirror the actions of EGF in up-regulating tTG (Figure 2.3*D*).

The ability of the activated Ras and Rho proteins to work together to up-regulate tTG expression led to the question of what might be functioning downstream from these GTPases. One of the best known signaling effectors for activated Ras is ERK, and so I examined how blocking ERK activity using the inhibitor PD98059 affected EGF-stimulated tTG expression. The results in Figure 2.3*C* show that the EGF-stimulated expression of tTG in SKBR3 cells was unaffected under conditions where ERK activity was inhibited. However, another well known signaling target for activated Ras, PI3K (19), appears to be essential, as treatment of SKBR3 cells with the PI3K inhibitor LY294002 blocked the ability of EGF to induce the up-regulation of tTG in SKBR3 cells, consistent with our earlier findings that PI3K activation is necessary for tTG expression (10). Likewise, inhibiting PI3K activity prevented the combination of Ras and Cdc42 from up-regulating tTG expression (Figure 2.3*E*).

Because my findings suggested that a signaling target capable of responding to one or more different Rho GTPases contributes to the EGF-induced expression of tTG, I also examined NF B. I felt that NF B represented an attractive candidate because it is activated by Cdc42, Rac1, and RhoA, and participates in the malignant transformation of breast cancer cells (20, 21). Indeed, the results shown in Figure 2.3*C* and 2.3*E* demonstrate that blocking NF B activation using the small molecule BAY 11-7082, which prevents the phosphorylation and ensuing degradation of the NF B-negative regulator, IκB , significantly compromised the ability of EGF, as well as the combination of activated Ras and Cdc42, to up-regulate tTG expression.

*Overexpression of tTG in SKBR3 cells mimics the growth-promoting effects of EGF*

**Figure 2.4 Overexpression of tTG in SKBR3 cells promotes cell cycle progression, chemoresistance, anchorage-independent growth, and xenograft tumor formation. (A)** Extracts of SKBR3 cells stably expressing the vector-only or Myc-tagged forms of tTG WT and tTG C277V were immunoblotted with tTG and actin antibodies (top two panels) and assayed for transamidation activity as read-out by the incorporation of BPA into lysate proteins. Shown is an autoradiogram of these results (bottom panel). **(B)** Immunofluorescence was performed on the stable cell lines using a Myc antibody and DAPI. **(C)** Equal numbers of each stable cell line were seeded and maintained in medium containing 5% FBS. The cells were counted at the indicated times and their growth rates recorded. Experiemts were repeated twice. SKBR3 cells stably expressing the vector or Myc-tagged forms of tTG WT or tTG C277V were **(D)** incubated with BrdU for 30 minutes and then were washed and fixed with ethanol. The fixed cells were stained with a BrdU antibody and then analyzed by fluorescence microscopy. Those cells that incorporated BrdU into their DNA were considered actively proliferating and counted. The experiments were performed 3 times and the results were averaged together and graphed; **(E)** treated without or with 0.5 μM or 1.5 μM doxorubicin (Dox) for 24 hours. The stable cell lines were then fixed and stained with 4, 6-diamidino-2-phenylindole (DAPI) for viewing by fluorescence microscopy. Apoptotic cells were identified by nuclear condensation and blebbing. The experiment was performed in triplicate and the average percentage of cell death was plotted; **(F)** subjected to anchorage-independent growth assays. The results from 3 separate assays were averaged together and graphed. Insets are representative images of the assays; **(G)** injected subcutaneously into nude mice (6 mice for each cell line). The tumors were allowed to grow for 1 month before their final volumes were determined. The relative tumor volume for each of the stable cell lines was then graphed. Experiemts were repeated twice. All the errors bars shown from (C) to (G) represent standard deviation.

*The experiments described in (E) and (G) were performed by Marc A. Antonyak and Bo Li.

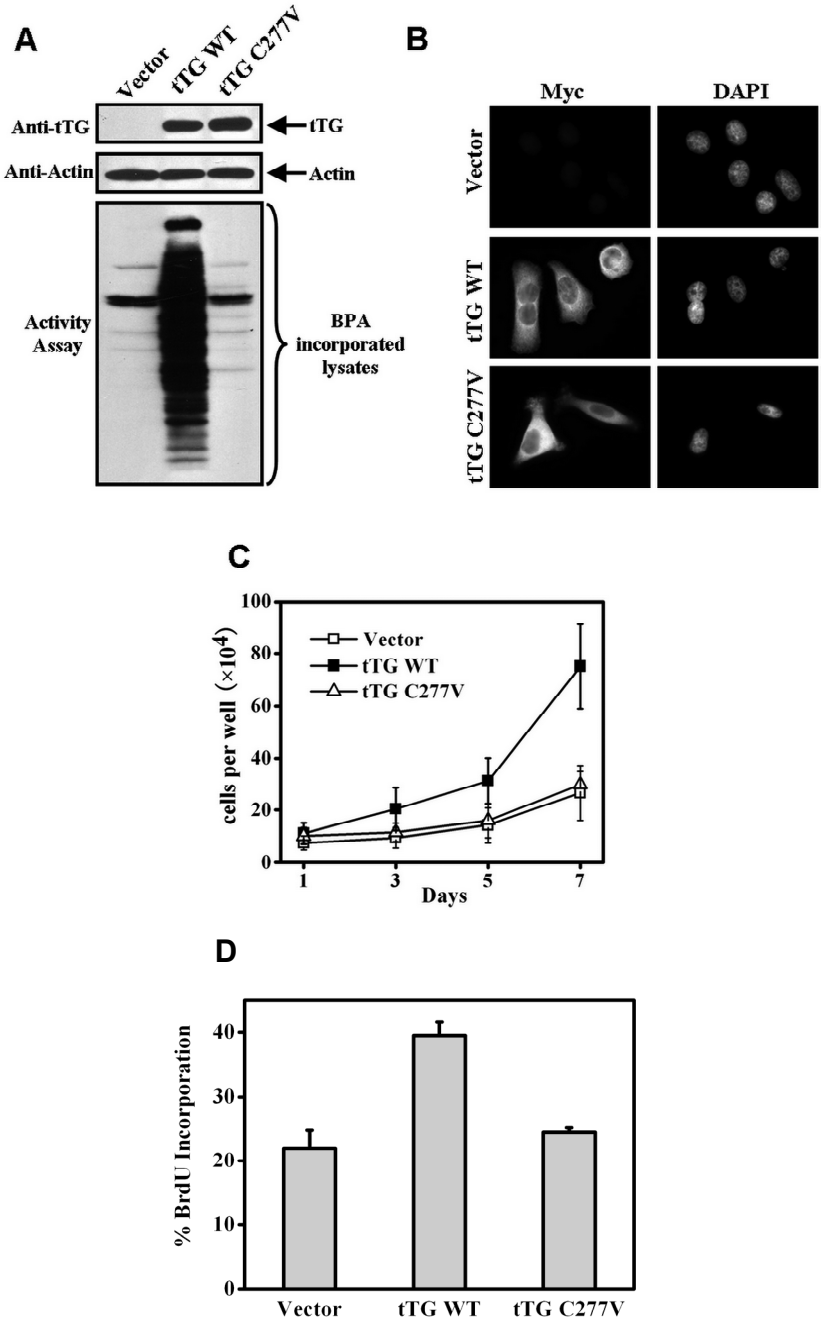
A
Vector
tTG WT
tTG C277V
Anti-tTG
tTG
Anti-Actin
Actin
Activity Assay
BPA incorporated lysates
B
Myc
DAPI
Vector
tTG WT
tTG C277V
C
cells per well (×10⁴)
100
80
60
40
20
0
Vector
tTG WT
tTG C277V
1
3
5
7
Days
D
% BrdU Incorporation
40
30
20
10
0
Vector
tTG WT
tTG C277V

**Figure 2.4 (Continued)**

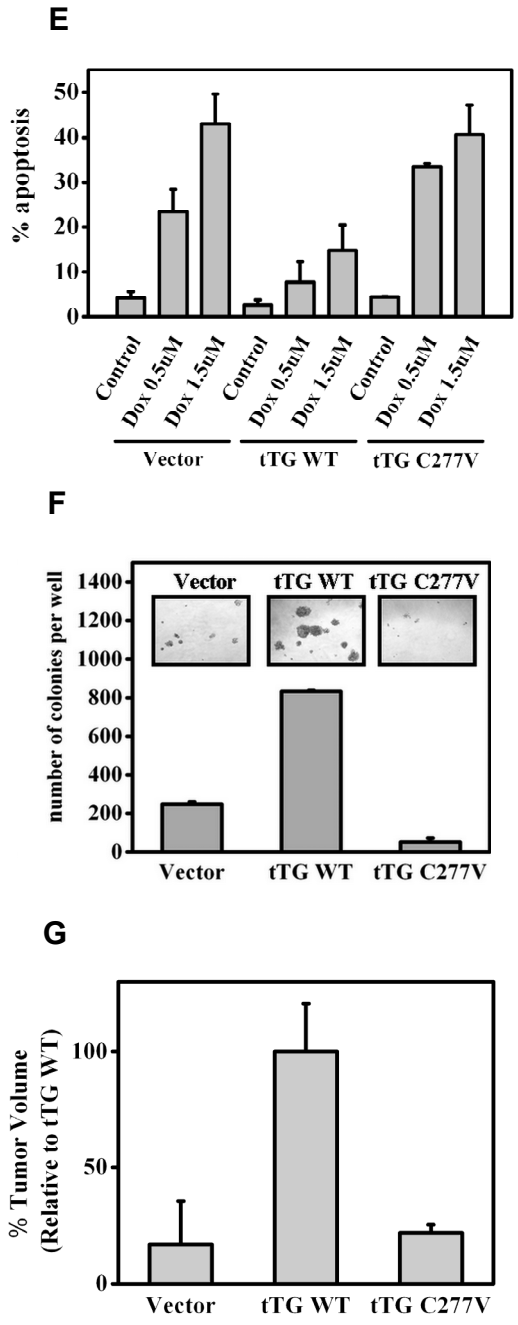

Since the induction of tTG expression by EGF is required for its growth-promoting effects in SKBR3 cells, I was interested in determining whether overexpressing tTG in these cells was sufficient to mirror the actions of this growth factor. Therefore, SKBR3 cells that stably expressed either vector alone, Myc-tagged wild-type tTG (tTG WT), or a Myc-tagged transamidation-defective form of tTG (tTG C277V), were generated. The expression of the different tTG constructs was similar in these cells (Figure 2.4*A*, *top panel*), and as expected, the overexpression of wild-type tTG was accompanied by clearly detectable transamidation activity when assaying the incorporation of BPA into cell lysate proteins, whereas the activity in cells expressing the tTG C277V mutant was similar to that of the vector-control cells (Figure 2.4*A*, *bottom panel*). Immunofluorescent analysis of the stable cell lines revealed that both wild-type tTG and tTG C277V exhibited a similar cytoplasmic, non-nuclear distribution, indicating that eliminating the ability of tTG to transamidate substrates does not affect its cellular localization (Figure 2.4*B*).

These stable cell lines were used to examine whether tTG overexpression is sufficient to mimic the actions of EGF and enhance the transformed phenotype of SKBR3 cells. Figure 2.4*C* shows that SKBR3 cells overexpressing wild-type tTG had a marked growth advantage over the vector-control cells, whereas the growth rates of cells expressing the tTG C277V mutant were similar to control cells. Moreover, overexpression of wild-type tTG in SKBR3 cells resulted in a 2-fold increase in 5-bromo-deoxyuridine (BrdU) incorporation over control cells (Figure 2.4*D*), as well as provided a protective effect from doxorubicin-induced apoptosis (Figure 2.4*E*). I then

examined the ability of the different stable cell lines to form colonies in soft agar. Consistent with my findings with parental SKBR3 cells (see Figure 2.1*C*), SKBR3 cells expressing the vector alone were capable of forming colonies in soft agar (Figure 2.4*F*, *inset and graph)*. The overexpression of wild-type tTG resulted in a ~4-fold increase in colony formation, with the average size of the colonies being larger than the background colonies formed by the control cells. In contrast, SKBR3 cells expressing tTG C277V failed to grow under anchorage-independent conditions (Figure 2.4*F*, *inset and graph*). In fact, the transamidation-defective tTG C277V mutant behaved like a dominant-negative inhibitor by effectively eliminating anchorage-independent growth such that it was well below the basal levels observed in the vector-control cells. Tumor formation assays performed in mice using these same stable cell lines yielded results that further demonstrated that tTG enhanced the transformed phenotype of SKBR3 cells (Figure 2.4*G*).

*The ability of tTG to enhance the growth and transforming phenotypes of breast cancer cells is due to its activation of Src*

How does increasing the levels of tTG expression in breast cancer cells enhance their oncogenic potential? To address this question, I asked whether overexpressing tTG in SKBR3 cells led to the activation of signaling proteins that have been implicated in cell growth and transformation. Extracts were prepared from serum-deprived SKBR3 cells stably expressing vector alone, wild-type tTG (tTG WT), or the transamidation-defective tTG C277V and then immunoblotted with antibodies that recognize the activated forms of different mitogenic signaling proteins. I found

**Figure 2.5 tTG-stimulated Src tyrosine kinase activity promotes aberrant cell growth. (A)** Extracts of serum-starved SKBR3 cells stably expressing the vector, Myc-tagged tTG WT, or Myc-tagged tTG C277V were immunoblotted with antibodies that detect the activated forms of the indicated signaling proteins. **(B)** The same cell extracts were also immunoblotted with an anti-phospho-tyrosine antibody. A distinct protein doublet ($M_r$ ~60-65 kDa) detected in each cell lysate (arrow) was **(C)** quantified using ImageJ software. The experiemts were preformed in triplicate, and the results were averaged and graphed. **(D)** Immunoprecipitations with a total-Src antibody (IP: Total Src) were performed on extracts of the indicated SKBR3 stable cell lines and the resulting immunocomplexes were immunoblotted with phospho-Src and total-Src antibodies. The extent of Src activity detected in each sample was quantified using ImageJ software and listed below its corresponding band in the Anti-Phospho-Src blot (Fold Phospho-Src*)*. To confirm equal amounts of each cell extract were used for the immunoprecipitations, the whole cell extracts were immunoblotted with Myc and actin antibodies (Input). **(E)** tTG stable cell lines deprived of serum were stimulated with EGF for increasing lengths of time and then lysed. The cell extracts were immunoblotted with the indicated antibodies. **(F and G)** SKBR3 cells overexpressing vector-only or tTG WT (F), or parental SKBR3 cells treated without or with EGF (G), were incubated without or with 5 μM PP2, and then subjected to anchorage-independent growth assays. The results from 3 separate assays were averaged together and graphed. All the errors bars shown in (C), (F) and (G) represent standard deviations.

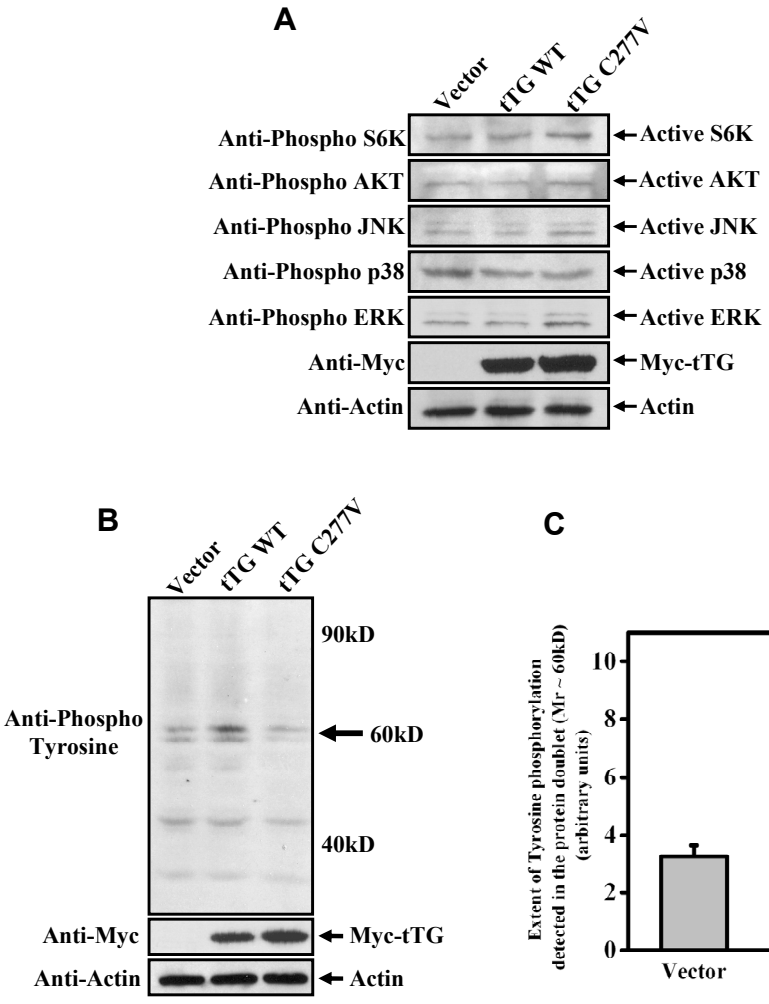
A
Vector
tTG WT
tTG C277V
Anti-Phospho S6K
Active S6K
Anti-Phospho AKT
Active AKT
Anti-Phospho JNK
Active JNK
Anti-Phospho p38
Active p38
Anti-Phospho ERK
Active ERK
Anti-Myc
Myc-tTG
Anti-Actin
Actin
B
Vector
tTG WT
tTG C277V
90kD
Anti-Phospho Tyrosine
60kD
40kD
Anti-Myc
Myc-tTG
Anti-Actin
Actin
C
Extent of Tyrosine phosphorylation detected in the protein doublet (Mr ~ 60kD) (arbitrary units)
0
2
4
6
8
10
Vector
tTG WT
tTG C277V

**Figure 2.5 (Continued)**

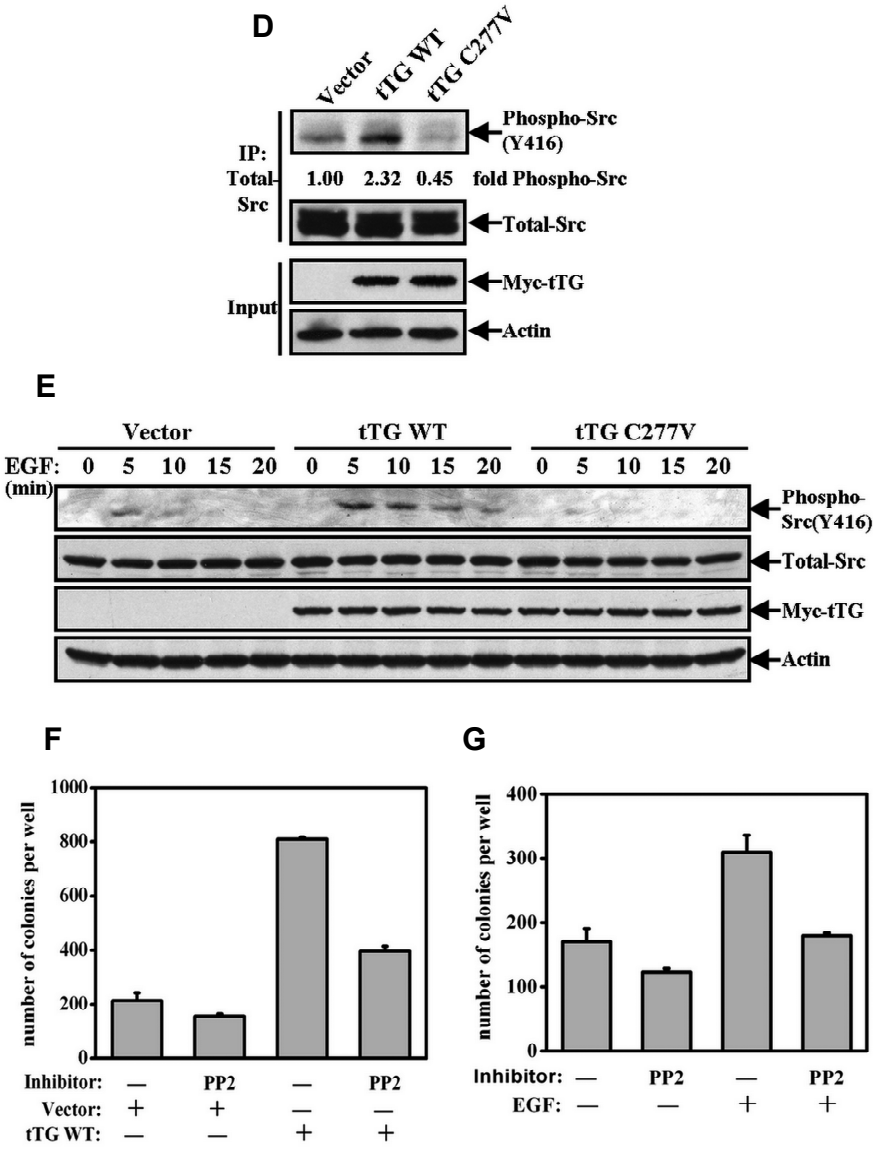

that the overexpression of tTG in SKBR3 cells did not increase the activities of AKT or S6K, nor did it activate the MAP-kinases JNK, ERK, or p38, relative to their activities in vector-control cells (Figure 2.5*A*). However, when the same cell extracts were subjected to immunoblot analysis using an anti-phospho-tyrosine antibody, a protein doublet with an apparent molecular mass in the 60-65 kDa area was enhanced in SKBR3 cells overexpressing wild-type tTG (Figure 2.5*B* and 2.5*C*). Because c-Src is a phospho-tyrosine-containing protein with $M_r \sim 60$ kDa, I examined whether tTG might be capable of enhancing the auto-phosphorylation of Src in cells. Indeed, I found that there was a better than 2-fold increase in Src auto-phosphorylation (i.e. a measure of Src activation) in cells expressing wild-type tTG compared to the vector-control cells (Figure 2.5*D*), whereas in cells expressing the tTG C277V mutant, the extent of Src activation was about half of that for control cells. Figure 2.5*E* shows that the magnitude and duration of EGF-dependent Src activation in SKBR3 cells was also potentiated by tTG overexpression. I then demonstrated that blocking Src activity using the small molecule PP2 inhibited the anchorage-independent growth of SKBR3 cells caused by tTG overexpression (Figure 2.5*F*), as well as by EGF stimulation (Figure 2.5*G*). Thus, the ability of tTG to stimulate Src kinase activity is directly responsible for the role that it plays in the EGF-stimulated growth and transformation of breast cancer cells.

*tTG activates Src through its interaction with keratin-19*

I then set out to determine how tTG influences Src kinase activity. While I was able to co-immunoprecipitate tTG with HA-tagged c-Src from SKBR3 cells (Figure

**Figure 2.6 A tTG-K19 interaction enhances the ability of tTG to bind to and stimulate Src kinase activity.** Immunoprecipitations with a HA antibody (IP: HA) were performed on the extracts of SKBR3 cells co-expressing HA-tagged Src and either the vector-only or Myc-tagged tTG WT **(A)**, as well as BT20 or MDAMB468 cells co-expressing HA-tagged Src and Myc-tagged tTG WT **(B)**. The resulting immunocomplexes were immunoblotted with Myc and HA antibodies. These cell extracts were also immunoblotted with Myc and HA antibodies (Input). **(C)** Protein pull-down assays were carried-out by incubating recombinant His-tagged tTG alone or together with GST-tagged forms of either Src or fibronectin. Glutathione-agarose beads were then added to each sample and the resulting protein complexes that formed were precipitated and subjected to immunoblot analysis with tTG and GST antibodies (GST Pull-down). An equivalent volume of each sample was removed just prior to the addition of the glutathione-agarose beads and immunoblotted with tTG and GST antibodies to show the relative amounts of the recombinant proteins present in each sample (Input). **(D)** Immunoprecipitations with a Myc antibody (IP: Myc) were performed on extracts of SKBR3 cells stably expressing the vector-only, Myc-tagged tTG WT, or Myc-tagged tTG C277V. The resulting immunocomplexes were resolved by SDS-PAGE and then Silver-stained to detect proteins that co-immunoprecipitated with Myc-tTG WT. **(E)** The protein ($M_r$ ~40 kDa) that was detected by Silver staining was identified as K19 by Mass Spectroscopy. Shown is the protein sequence of human K19. The peptide fragments identified by Mass Spectroscopy are shaded. Immunoprecipitations with a Myc antibody (IP: Myc) were performed on the extracts of SKBR3 cells stably overexpressing Myc-tTG WT or Myc-tTG C277V mutant **(F)**, or on the lysates from BT20 or MDAMB468 cells overexpressing Myc-tagged tTG WT **(G)**. The resulting immunocomplexes were immunoblotted with K19 and Myc antibodies. **(H)** An *in vitro* transamidation activity assay was performed on recombinant K19 by incubating it with BPA without or with either recombinant His-tagged tTG WT or recombinant His-tagged tTG C277A. Shown is an autoradiogram of the results (top panel). The reactions were also immunoblotted with tTG and K19 antibodies to show the relative amounts of each of the recombinant proteins (Input). **(I)** HA immunoprecipitations were performed on the extracts of SKBR3 cells co-expressing Myc-tTG and HA-Src and transfected with either control siRNA or K19 siRNAs (denoted K19 siRNA-1 or K19 siRNA-2). The immunocomplexes (IP: HA) were immunoblotted with Myc and HA antibodies. **(J)** Total-Src immunoprecipitations were performed on lysates of SKBR3 cells expressing Myc-tTG WT and transfected with either control or K19 siRNAs. The immunocomplexes (IP: Total Src) were immunoblotted with phospho-Src and total-Src antibodies. All cell extracts were also immunoblotted with the indicated antibodies (Input). The extent of Src activity detected in each sample was quantified using ImageJ software and listed below its corresponding band in the Anti-Phospho-Src blot (Fold Phospho-Src). **(K)** SKBR3 cells stably expressing the vector-only or Myc-tTG WT were transfected with control siRNA or K19 siRNAs (inset) and then subjected to anchorage-independent growth assays. The results from 3 separate assays were averaged together and graphed (graph). Errors bars represent standard deviations.

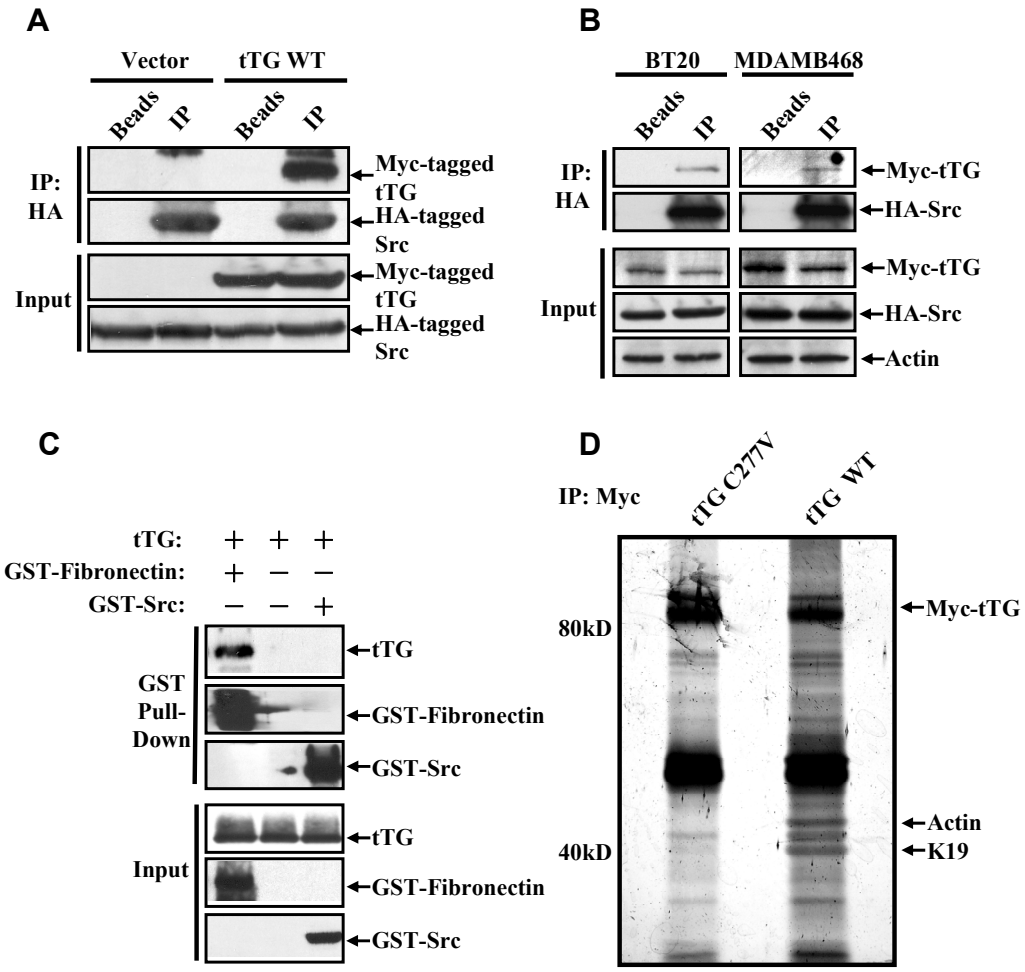


E

MTSYSYRQSSATSSFGGLGGGSVRFGPGVAFRAPSIHGGSGGRGVSVSSARFVSSSSSGAYGG
GYGGVLTASDGLLAGNEKLTMQNLNDRLASYLDKVRALEAANGELEVKIRDWYQKQGPGPSRDY
SHYYTTIQDLRDKILGATIENSRIVLQIDNARLAADDFRTKFETEQALRMSVEADINGLRRVLDELTL
ARTDLEMQIEGLKEELAYLKKNHEEEISTLRGQVGGQVSVEVDSAPGTDLAKILSDMRSQYEVMA
EQNRKDAEAWFTSRTEELNREVAGHTEQLQMSRSEVTDLRRTLQGLEIELQSQLSMKAALEDTLA
ETEARFGAQLAHIQALISGIEAQLGDVRADSERQNQEYQRLMDIKSRLEQEIATYRSLLE
GQEDHYNNLSASKVL

Figure 2.6 (Continued)

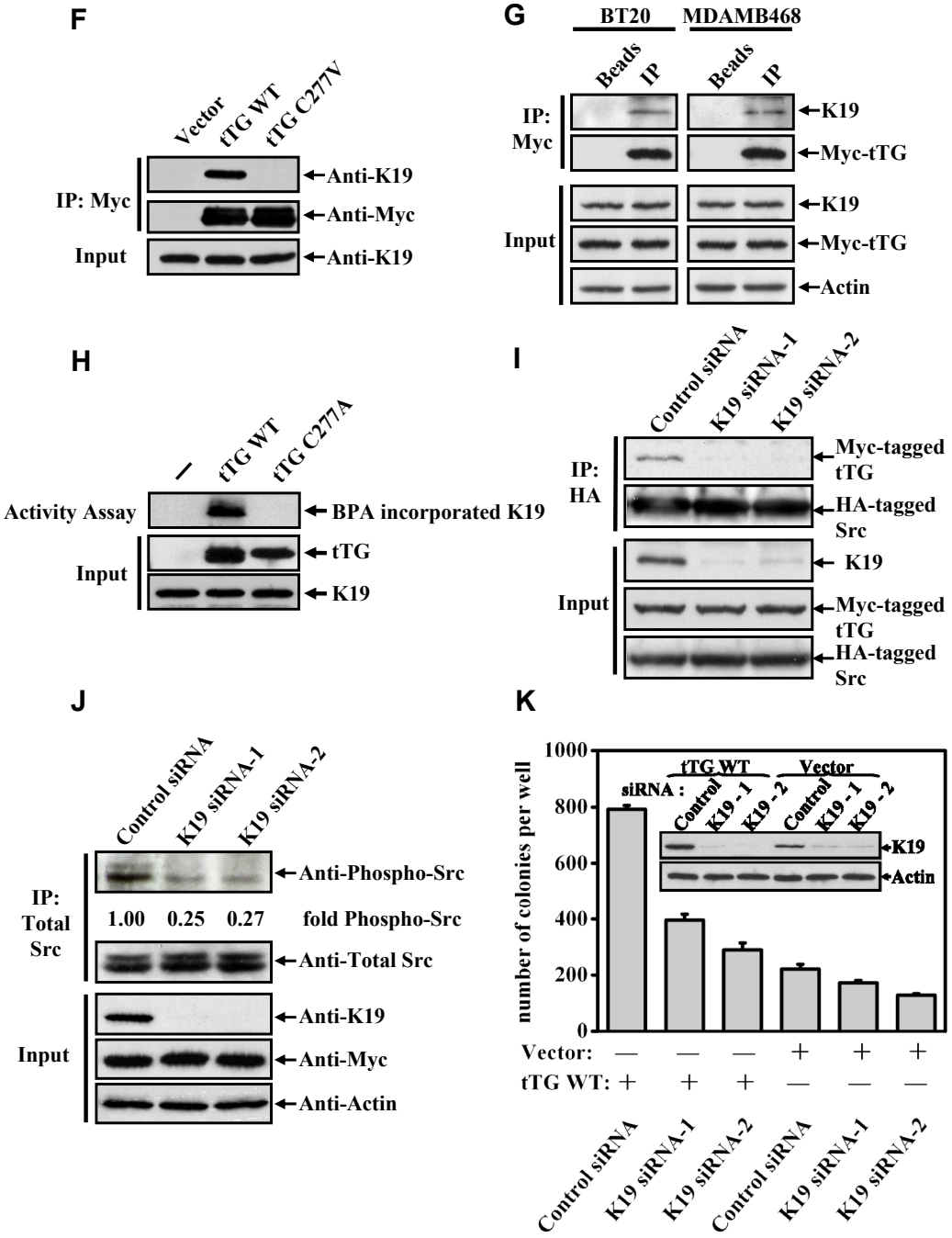

2.6*A*), as well as from BT20 and MDAMB468 cells (Figure 2.6*B*), I was unable to demonstrate a direct interaction between purified recombinant tTG and c-Src under conditions where I could detect an interaction between tTG and one of its best-known binding partners, fibronectin (22) (Figure 2.6*C*). This suggested that an intermediate protein was involved in mediating the effects of tTG on Src activity. Given that only transamidation-competent tTG, and not a transamidation-defective mutant, was capable of increasing Src activity and enhancing the transforming phenotypes of breast cancer cells, I wanted to search for candidate transamidation substrates of tTG that might serve to mediate the tTG-dependent regulation of Src. Thus, I used Myc-tagged wild-type tTG and the transamidation-defective tTG C277V mutant to screen lysates of SKBR3 cells for tTG-interacting proteins. The idea was that candidate substrates should be able to form a stable acyl-intermediate with the active site cysteine residue of wild-type tTG but not with the C277V mutant. The ectopically expressed forms of tTG were immunoprecipitated from these extracts using an anti-Myc antibody, and then the resulting immunocomplexes were resolved by SDS-PAGE and Silver-stained to detect proteins that co-immunoprecipitated with the Myc-tagged tTG constructs. Two proteins of Mr ~40 kDa and ~45 kDa specifically associated with Myc-tagged wild-type tTG (Figure 2.6*D*, *arrows*). The ~45 kDa protein was determined to be actin by co-immunoprecipitation and subsequent immunoblot analysis with an anti-actin antibody, a known transamidation substrate of tTG (23). The identity of the smaller protein was initially determined by sequencing (Figure 2.6*E*), and subsequently confirmed by co-immunoprecipitation and immunoblot analysis (Figure 2.6*F*), to be the intermediate filament protein keratin-19 (K19). I also determined that K19

associates with tTG in two additional breast cancer cell lines, namely in BT20 and MDAMB468 cells (Figure 2.6*G*). Moreover, I showed that tTG is capable of labeling K19 with BPA in an *in vitro* transamidation assay (Figure 2.6*H*), indicating that tTG can both bind and transamidate K19.

Interestingly, K19 is a human breast tumor marker (24-26). This, coupled with the recent finding that the related family member, K17, can promote epithelial cell growth by acting as a scaffold protein to bring together the necessary signaling proteins to trigger the PI3K/AKT- and mTOR-dependent activation of p70 ribosomal S6 kinase (27), led me to consider the possibility that K19 may serve to mediate the tTG-dependent activation of c-Src. This in fact turned out to be the case, as shown by the data in Figure 2.6*I* where the ability of tTG to be co-immunoprecipitated with HA-tagged Src from SKBR3 cells was dependent on K19, i.e. knock-downs of K19 blocked the ability of tTG to interact with Src. Moreover, the ability of tTG to activate Src is dependent on K19 as indicated by the loss of this activation when K19 expression is knocked-down by RNAi (Figure 2.6*J*), and K19 is necessary for the ability of tTG to enhance the anchorage-independent growth of SKBR3 cells (Figure 2.6*K*).

**Discussion**

Excessive activation of the EGFR contributes to oncogenesis by stimulating the growth and survival of cancer cells, while small molecule inhibitors or antibody-based approaches that target the EGFR or its immediate downstream effectors, have shown some promise as treatments for certain human cancers (1, 2, 4, 5). Therefore,

**Figure 2.7 Diagram depicting how tTG participates in an EGFR/Src signaling pathway that leads to enhanced cancer cell growth.**

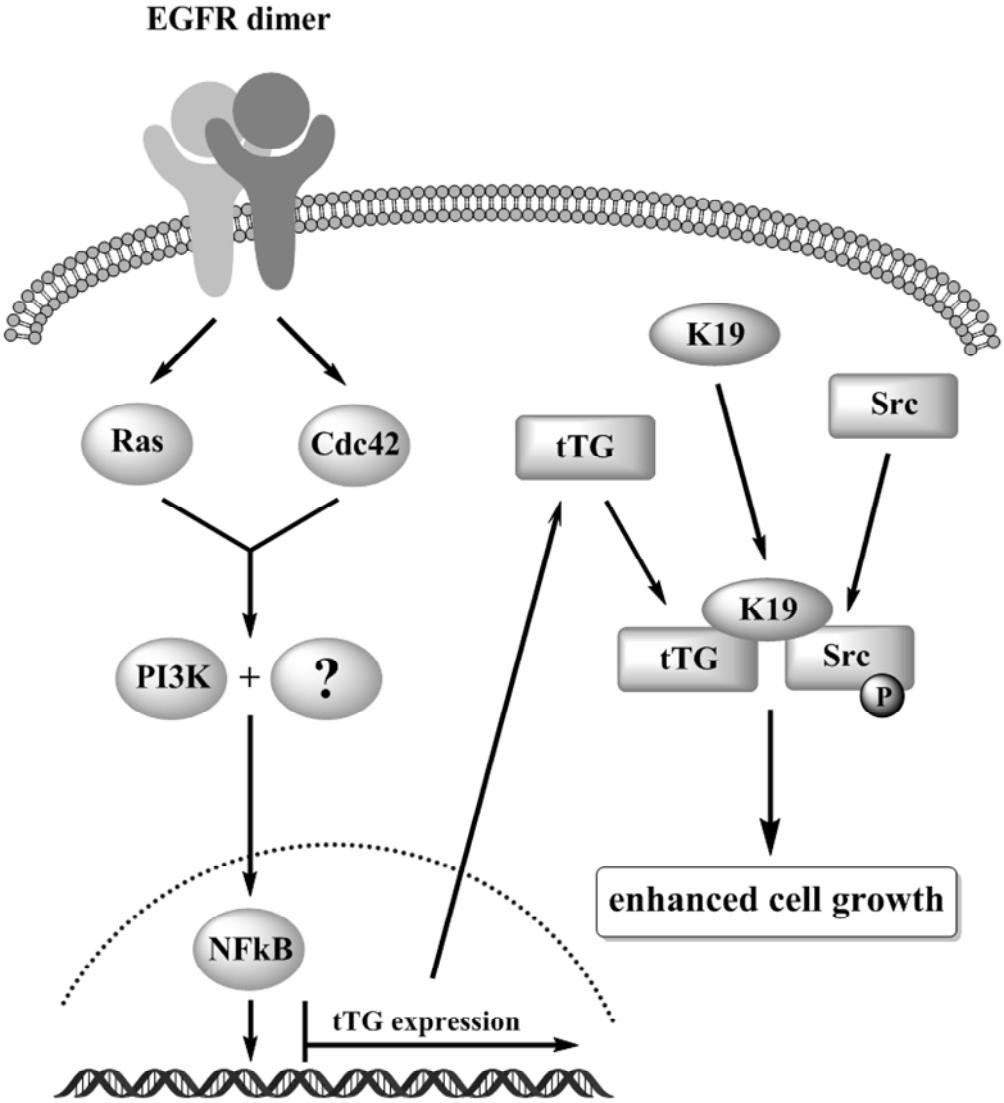
EGFR dimer
Ras
Cdc42
PI3K
+
?
NFkB
tTG expression
tTG
K19
Src
K19
tTG
Src
P
enhanced cell growth

continuing efforts to better understand the mechanisms by which the EGFR stimulates cancer progression will play a critical part in the development of alternative strategies to treat cancers. While it is generally appreciated that the EGFR modifies global gene expression patterns in cells, the identities of those gene products whose induction is most important for cell growth and/or survival are largely unknown. Here, I have identified tTG, a dual function GTPase/acyl-transferase, as one such protein. The initial indication for this came from the finding that stimulating SKBR3 or BT20 breast cancer cells with EGF not only increased their proliferative capacity and ability to form colonies in soft agar, but also resulted in the induction of tTG expression and activation. Suppressing tTG expression or activity potently inhibited the EGF-induced growth advantages in each of these cell lines. I further showed that overexpression of wild-type tTG in SKBR3 cells could fully recapitulate the growth-stimulatory actions of EGF, therefore implicating tTG as a key participate in EGFR-promoted cellular transformation.

Thus far, very little has been known about the signaling pathways that mediate EGF-induced tTG expression. However, I have begun to delineate some of the events that must occur to stimulate tTG expression and cellular transformation, as summarized in Figure 2.7. Although the individual ectopic expression of activated forms of various signaling proteins in SKBR3 cells did not induce tTG expression, I found that the Ras- and Cdc42-signaling pathways cooperated to up-regulate tTG. I then showed that the induction of tTG expression by either EGF stimulation or co-expression of activated Ras and Cdc42 was sensitive to the PI3K inhibitor LY294002, as well as the NFκB inhibitor BAY 11-7082.

Increasing the levels of tTG expression in SKBR3 breast cancer cells enhances their oncogenic potential, and thus mirrors the actions of EGF-treatment. Surprisingly, I discovered that this is due to the ability of tTG to activate c-Src. Consistent with these results, as well as with several lines of evidence linking Src kinase activity to tumor progression, the anchorage-independent growth advantage afforded to SKBR3 cells by either EGF-stimulation or tTG overexpression was severely compromised when these cells were cultured in the presence of the Src inhibitor PP2. Overall, these findings highlight an interesting connection between the overexpression of tTG observed in increasing numbers of breast cancer as well as other human cancers and the presence of elevated Src activity.

An intriguing question concerns how tTG expression leads to increased Src activity in cells. I obtained a clue when I found that Src co-immunoprecipitated with tTG from SKBR3 cell lysates, but that the recombinant forms of these two proteins failed to show a similar association *in vitro*, implying that the tTG-Src interaction in cells was indirect and most likely mediated by another protein. Indeed, I identified the intermediate filament K19 as a tTG-binding partner that is essential for the ability of tTG to associate with Src in cells, as well as for the enhanced Src activity observed in the SKBR3 cells stably overexpressing tTG. Moreover, I demonstrated that K19 is capable of being transamidated by tTG *in vitro*. Thus, the tTG-catalyzed crosslinking of K19 might enable it to act as a signaling scaffold that binds and favors the activated state of c-Src, an idea that I am currently investigating. Interestingly, K19 belongs to a family of cytokeratins, many of which, including K19, are overexpressed in a large number of human cancer types (28, 29) and are routinely used as diagnostic indicators

of metastasis and tumor aggressiveness (24-26). Given the connections between K19 and human cancers, an important question has been whether the cytokeratins directly contribute to oncogenesis. My findings that K19 serves to bridge the interaction between tTG and Src, resulting in enhanced Src kinase activity and aberrant cell growth, point to a novel and rather unexpected role for K19 in EGFR-promoted cellular transformation.

In summary, the findings presented in this study demonstrate for the first time to my knowledge that the induction of tTG expression and activation by EGF is both necessary and sufficient for mediating the growth-promoting actions of EGF in human breast cancer cells. Interestingly, a recent proteomic screen of the U87 brain tumor cell line overexpressing a highly oncogenic form of the EGFR known as EGFR variant type III (EGFRvIII) showed that tTG was one of three proteins whose expression was enhanced by this mutant EGFR (30). Whether tTG is important for promoting the oncogenic potential of EGFRvIII remains to be determined. However, my findings now point to an important relationship between EGFR-mediated transformation and tTG expression and suggest that tTG may represent a potentially valuable therapeutic target.

**Materials and Methods**

*Materials.* Cell culture reagents, EGF, Lipofectamine, Lipofectamine 2000, protein G-beads, glutathione-agarose beads, tTG and K19 RNAis, and the HA, GST, and Myc antibodies were from Invitrogen. LY 294002, PP2, PD 98059, BAY11-7082, DAPI and MDC were from Calbiochem. The 5-(biotinamido) pentylamine was from Pierce.

The tTG, actin, and K19 antibodies were from Neomarkers, while antibodies recognizing total or activated Src, AKT, JNK, P38, p70 S6-kinase, and ERK, as well as the anti-phospho-tyrosine antibody, were from Cell Signaling.

*Cell Culture.* SKBR3 and BT20 cell lines were grown in RPMI 1640 medium containing 10% FBS. Expression constructs were transfected into cells using Lipofectamine, while RNAis were introduced into cells using Lipofectamine 2000. Cells stably expressing Myc-tagged pcDNA3 vector, Myc-tTG WT or Myc-tTG C277V were generated by selection with growth medium supplemented with 800 μg/ml G418. Where indicated, cells were treated with various combinations of 0.1 μg/ml EGF, 20 μM MDC, 10 μM LY294002, 20 μM PD98059, 2 μM BAY 11-7082, or 5 μM PP2.

*Immunoblot Analysis.* Cells were lysed with lysis buffer (25 mM Tris, 100 mM NaCl, 1% Triton X-100, 1 mM EDTA, 1 mM DTT, 1 mM $NaVO_4$, 1 mM β-glycerol phosphate, and 1 μg/mL aprotinin), and then the lysates were resolved by SDS-PAGE and the proteins transferred to PDVF membranes. The filters were incubated with the various primary antibodies diluted in TBST (20 mM Tris, 135 mM NaCl, and 0.02% Tween 20). The primary antibodies were detected with horseradish peroxidase-conjugated secondary antibodies followed by exposure to ECL reagent.

*Immunofluorescence.* SKBR3 cells expressing the Myc-pCDNA3 vector, Myc-tTG WT, or Myc-tTG C277V, were fixed using 5% formaldehyde, permeabilized with

0.2% Triton X-100, and then incubated with a Myc antibody. The Myc antibody was detected using an Oregon green 488-conjugated secondary antibody and DAPI was used to stain nuclei.

*Transamidation Assay.* These assays were performed as previously described (10).

*Cell growth assays.* Parental SKBR3 cells or the SKBR3 stable cell lines were plated in dishes at a density of $5\times10^4$ cells/dish and cultured in medium containing 2% FBS, without or with EGF, MDC, or PP2. Every other day for one week, one set of cells was collected and counted, while the medium on the remaining sets of cells was replenished.

*Soft agar assays.* Parental SKBR3 and BT20 cells or the SKBR3 stable cell lines were plated at a density of $6\times10^3$ cells/ml in medium containing 0.3% agarose, without or with EGF, MDC, or PP2 onto underlays composed of growth medium containing 0.6% agarose in six-well dishes. The cultures were fed one week later, and after 14 days of growth the colonies were counted.

*Immunoprecipitation.* Cell extracts (typically 600 μg) were pre-cleared with protein G beads before incubating with a particular antibody for 2 hours, followed by addition of protein G beads for 1 hour. The beads were washed with cell lysis buffer before being boiled with Laemmli's sample buffer and subjected to SDS-PAGE and Western-blotting.

*Silver-staining and MS-peptide sequence identification.* Silver-staining of proteins resolved by SDS-PAGE was performed based on the manufacturer's instructions (Bio-Rad). Protein bands of interest were excised from the gel and washed 3 times with 50% acetonitrile. The samples were analyzed at the Harvard Microchemistry and Proteomics Analysis Facility by micro-capillary reverse-phase HPLC nano-electrospray tandem mass spectrometry on a Thermo LTQ-Orbitrap mass spectrometer.

*Immunihistochemistry.* Human breast cancer tissue arrays (catalog # BR1921, U.S. Biomax) containing 80 cases of invasive ductal breast cancer tissue and 16 normal ductal mammary tissues were subjected to immunohistochemical analysis with tTG, EGFR, and ErbB2 antibodies. Briefly, the tissue array slides were deparaffinized by baking at 60 °C for 30 minutes and then rehydrated in distilled water containing 3% $H_2O_2$ for 30 min. After washing with PBS, the slides were boiled for 10 min in 10 mM sodium citrate buffer (pH 6.0) and allowed to cool to room temperature. The slides were then blocked with 2.5% horse serum and with Avidin and Biotin blocking solutions (Avidin/Biotin Blocking Kit, Vector Labs). The tissue arrays were then incubated with the various primary antibodies, followed by biotinylated secondary antibodies, and then a 30 minute treatment with the Elite ABC reagent (Universal R.T.U. Vectastain Elite ABC Kit, Vector Labs). After washing with PBS, the slides were processed with chromogen solution (ImmPACT DAB Substrate, Vector Labs). The slides were then dehydrated and mounted.

## REFERENCES


1. Mendelsohn J, Baselga J (2000) The EGF receptor family as targets for cancer therapy. *Oncogene* 19:6550-6565.

2. Nicholson RI, Gee JM, Harper ME (2001) EGFR and cancer prognosis. *Eur J Cancer* 37 Suppl 4:S9-15.

3. Roberts PJ, Der CJ (2007) Targeting the Raf-MEK-ERK mitogen-activated protein kinase cascade for the treatment of cancer. *Oncogene* 26:3291-3310.

4. Dutta PR, Maity A (2007) Cellular responses to EGFR inhibitors and their relevance to cancer therapy. *Cancer Lett* 254:165-177.

5. Bianco R, Troiani T, Tortora G, Ciardiello F (2005) Intrinsic and acquired resistance to EGFR inhibitors in human cancer therapy. *Endocr Relat Cancer* 12 Suppl 1:S159-171.

6. Chen YL, Law PY, Loh HH (2005) Inhibition of PI3K/Akt signaling: an emerging paradigm for targeted cancer therapy. *Curr Med Chem Anticancer Agents* 5:575-589.

7. Ishizawar R, Parsons SJ (2004) c-Src and cooperating partners in human cancer. *Cancer Cell* 6:209-214.

8. Folk JE (1980) Transglutaminases. *Annu Rev Biochem* 49:517-531.

9. Ariens RA, Lai TS, Weisel JW, Greenberg CS, Grant PJ (2002) Role of factor XIII in fibrin clot formation and effects of genetic polymorphisms. *Blood* 100:743-754.

10. Antonyak MA, et al. (2004) Augmentation of tissue transglutaminase expression and activation by epidermal growth factor inhibit doxorubicin-induced apoptosis in human breast cancer cells. *The Journal of biological chemistry.* 279:41461-41467.

11. Morley S, Wagner J, Kauppinen K, Sherman M, Manor D (2006) Requirement for Akt-mediated survival in cell transformation by the dbl oncogene. *Cell. Signal.*

12. Kim DS, Park SS, Nam BH, Kim IH, Kim SY (2006) Reversal of drug resistance in breast cancer cells by transglutaminase 2 inhibition and nuclear factor-kappaB inactivation. *Cancer Res* 66:10936-10943.

13. Mann AP, et al. (2006) Overexpression of tissue transglutaminase leads to constitutive activation of nuclear factor-kappaB in cancer cells: delineation of a novel pathway. *Cancer Res* 66:8788-8795.

14. Mangala LS, Fok JY, Zorrilla-Calancha IR, Verma A, Mehta K (2007) Tissue transglutaminase expression promotes cell attachment, invasion and survival in breast cancer cells. *Oncogene* 26:2459-2470.

15. Mehta K, Fok J, Miller FR, Koul D, Sahin AA (2004) Prognostic significance of tissue transglutaminase in drug resistant and metastatic breast cancer. *Clin Cancer Res* 10:8068-8076.

16. Verma A, et al. (2006) Increased expression of tissue transglutaminase in pancreatic ductal adenocarcinoma and its implications in drug resistance and metastasis. *Cancer Res* 66:10525-10533.

17. Yarden Y, Shilo BZ (2007) SnapShot: EGFR signaling pathway. *Cell* 131:1018.

18. Cerione RA, Zheng Y (1996) The Dbl family of oncogenes. *Curr. Opin. Cell Biol.* 8:216-222.

19. Wells V, Downward J, Mallucci L (2007) Functional inhibition of PI3K by the betaGBP molecule suppresses Ras-MAPK signalling to block cell proliferation. *Oncogene* 26:7709-7714.

20. Cammarano MS, Minden A (2001) Dbl and the Rho GTPases activate NF kappa B by I kappa B kinase (IKK)-dependent and IKK-independent pathways. *J Biol Chem* 276:25876-25882.

21. Wu YW, Tsai YH (2006) A rapid transglutaminase assay for high-throughput screening applications. *J Biomol Screen* 11:836-843.

22. Jeong JM, Murthy SN, Radek JT, Lorand L (1995) The fibronectin-binding domain of transglutaminase. *J Biol Chem* 270:5654-5658.

23. Nemes Z, Jr., Adany R, Balazs M, Boross P, Fesus L (1997) Identification of cytoplasmic actin as an abundant glutaminyl substrate for tissue transglutaminase in HL-60 and U937 cells undergoing apoptosis. *J. Biol. Chem.* 272:20577-20583.

24. Nakata B, Takashima T, Ogawa Y, Ishikawa T, Hirakawa K (2004) Serum CYFRA 21-1 (cytokeratin-19 fragments) is a useful tumour marker for detecting disease relapse and assessing treatment efficacy in breast cancer. *Br J Cancer* 91:873-878.

25. Takada M, et al. (1995) Measurement of cytokeratin 19 fragments as a marker of lung cancer by CYFRA 21-1 enzyme immunoassay. *Br J Cancer* 71:160-165.

26. Uenishi T, et al. (2003) Cytokeratin-19 fragments in serum (CYFRA 21-1) as a marker in primary liver cancer. *Br J Cancer* 88:1894-1899.

27. Kim S, Wong P, Coulombe PA (2006) A keratin cytoskeletal protein regulates protein synthesis and epithelial cell growth. *Nature* 441:362-365.

28. Uenishi T, et al. (2003) Cytokeratin 19 expression in hepatocellular carcinoma predicts early postoperative recurrence. *Cancer Sci* 94:851-857.

29. Zhang DH, Tai LK, Wong LL, Sethi SK, Koay ES (2005) Proteomics of breast cancer: enhanced expression of cytokeratin19 in human epidermal growth factor receptor type 2 positive breast tumors. *Proteomics* 5:1797-1805.

30. Zhang R, Tremblay TL, McDermid A, Thibault P, Stanimirovic D (2003) Identification of differentially expressed proteins in human glioblastoma cell lines and tumors. *Glia* 42:194-208.

# CHAPTER 3

## *Cancer cell-derived microvesicles induce transformation by transferring tissue transglutaminase and fibronectin to recipient cells

### Introduction

The release of MVs or oncosomes from different types of high-grade or aggressive forms of human cancer cells into their surroundings is becoming increasingly recognized as a feature of tumor biology (1-3), yet how these structures are generated and their importance in cancer progression are only just beginning to be appreciated. Of particular interest are the recent findings showing that at least some of the MVs generated by aggressive brain, breast, and prostate cancer cells involve the direct budding or shedding of vesicles from their plasma membranes. These membrane-bound structures range in size up to ~2.0 microns in diameter and contain a variety of cell surface receptors, intracellular signaling proteins, cytoskeletal components, as well as RNA transcripts encoding mitogenic factors, depending upon their cellular origin (4-8). Interestingly, they have been shown to be taken-up by recipient cancer cells where the transferred cargo can promote the activation of survival and mitogenic signaling proteins, including AKT and ERK (5, 7, 9).

By determining that MVs provide a means for cancer cells to share intracellular proteins and genetic information with each other, the above findings have begun to shed some light on a poorly understood but potentially important mechanism underlying the onset and development of human cancers. However, numerous

*Published previously as Antonyak MA & Li B, et al. (2011) *PNAS* 108:4852-4857.

**Figure 3.1 Distinct types of human cancer cells generate MVs.** (**A**) MDAMB231 cells were analyzed by SEM (left image) and immunofluorescent microscopy using rhodamine-conjugated phalloidin to detect F-actin (right image). Some of the largest MVs are indicated with arrows. (**B**) Quantification of MV production by various cell lines cultured under serum-starved or EGF-stimulated conditions. Cells generating MVs were detected by labeling the samples with rhodamine-conjugated phalloidin. The data shown represents the mean ± s.d. from three independent experiments. (**C**) Images of cells from the experiment performed in (B). Some of the MVs are denoted with arrows. **(D**) MDAMB231 cells transiently expressing a GFP-tagged form of the plasma membrane-targeting sequence from the Lyn tyrosine kinase (GFP-PM) were subjected to live-imaging fluorescent microscopy. Shown are a series of time-lapsed images taken in 2 minute intervals of a transfectant. The arrow denotes a MV that forms and is shed from a cell. (**E**) Serum-deprived MDAMB231 cells that were either mock transfected or transfected with pEGFP (a plasmid encoding GFP) were lysed, and the MVs shed into the medium by the transfectants were isolated and lysed as well. The whole cell lysates (WCLs) and the MV lysates were then immunoblotted with antibodies against GFP, the MV-marker flotillin-2, and the cytosolic-specific-marker IκBα. MDAMB231 cells that were either mock transfected or transfected with a plasmid encoding GFP (pEGFP) were placed in serum-free medium for a day. The conditioned medium from the transfectants were collected and the intact MVs present in the medium were isolated and subjected to FACS analysis by gating for GFP-positive MVs that are between ~1-3 μm in diameter. (**F**) The results obtained when the MVs isolated from the mock transfected MDAMB231 cells were analyzed. (**G**) The results obtained when the MVs isolated from MDAMB231 cells transiently expressing GFP were analyzed.

*The experiments described in (B) and (C) were performed by Marc A. Antonyak and Bo Li. The experiments described in (F) and (G) were performed by Kristen L. Bryant.

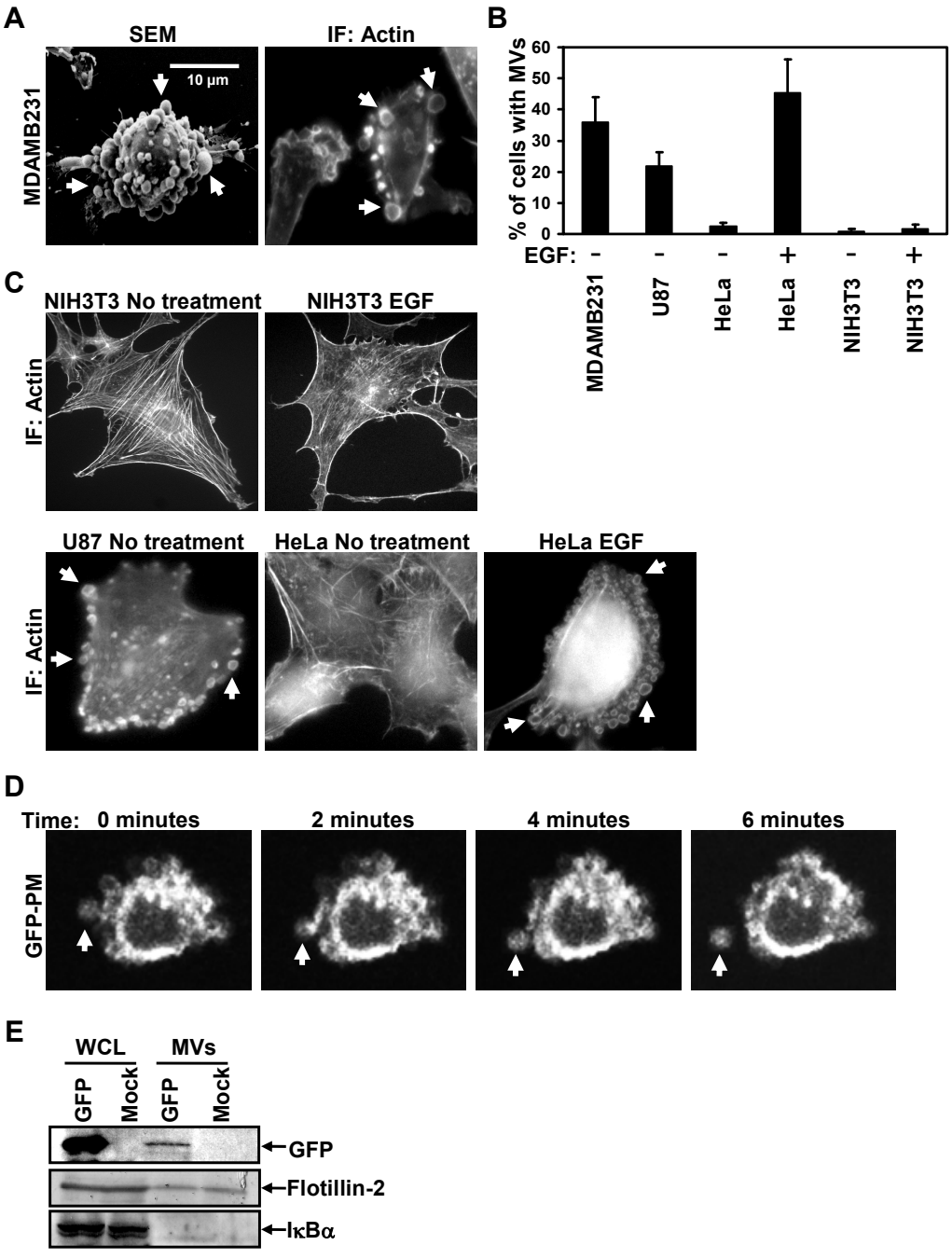
A
SEM
IF: Actin
MDAMB231
10 µm
B
% of cells with MVs
60
50
40
30
20
10
0
EGF: - - - + - +
MDAMB231
U87
HeLa
HeLa
NIH3T3
NIH3T3
C
NIH3T3 No treatment
NIH3T3 EGF
IF: Actin
U87 No treatment
HeLa No treatment
HeLa EGF
IF: Actin
D
Time: 0 minutes
2 minutes
4 minutes
6 minutes
GFP-PM
E
WCL
MVs
GFP
Mock
GFP
Mock
GFP
Flotillin-2
IκBα

**Figure 3.1 (Continued)**

**F**

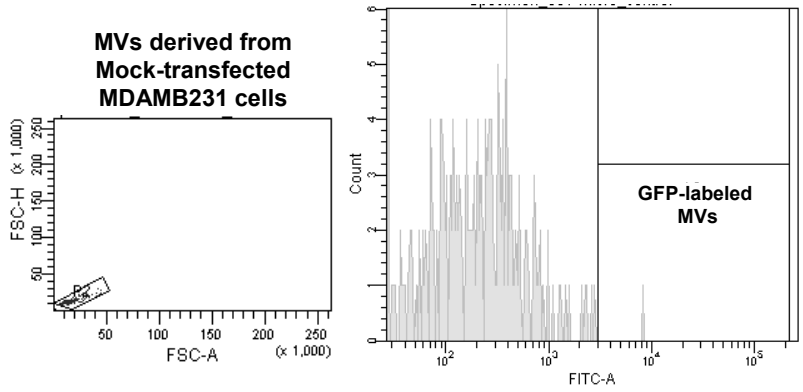


**G**

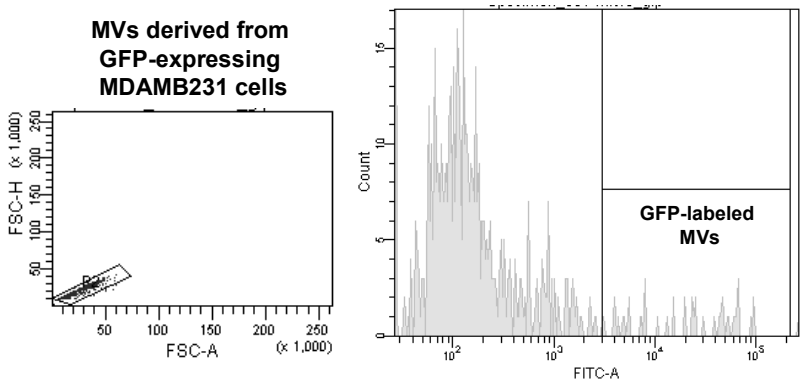

questions regarding MV biogenesis and function need to be addressed in order to more thoroughly understand the significance of this unconventional form of cell communication in oncogenesis. Here I will describe findings that suggest a novel role for MVs in cancer progression, as well as identify the proteins that are essential to this function.

**Results**

Analysis of serum-starved cultures of the highly aggressive human breast cancer cell line MDAMB231 by scanning electron microscopy (SEM) (Figure 3.1*A*, *left image*) or by fluorescent microscopy performed on cells stained for F-actin (Figure 3.1*A*, *right image*) showed that MVs ranging in size from ~0.2-2.0 microns in diameter were present on the surface of ~35% of these cells (Figure 3.1*B*). MVs were also detected on ~25% of serum-deprived U87 human glioblastoma cells, while their formation was induced in HeLa cervical carcinoma cells by epidermal growth factor (EGF) stimulation (Figure 3.1*B* and 3.1*C*). In contrast, MVs were not detected on the surface of normal NIH3T3 fibroblasts cultured under serum-starved or EGF-stimulated conditions, indicating that some cell types may not generate MVs. Moreover, I determined that MVs were actively shed from these cancer cells as demonstrated by time-lapsed images of the release of a GFP-labeled MV from the plasma membrane of a MDAMB231 cell transfected with a pEGFP plasmid encoding the plasma membrane targeting sequence of the Lyn tyrosine kinase (GFP-PM) (Figure 3.1*D*), as well as through the detection of MVs containing GFP in the culturing medium collected from pEGFP-only expressing transfectants by immunoblot

**Figure 3.2 MDAMB231 and U87 cancer cell-derived MVs are capable of transforming normal fibroblasts and normal mammary epithelial cells.** (**A**) Whole cell lysates (WCLs) of serum-starved MDAMB231 and U87 cells, as well as lysates of the MVs shed by these cells, were immunoblotted with antibodies against the MV-markers actin and flotillin-2, the cytosolic-specific-marker IκBα, and the activated (phospho)-EGF-receptor. Multiple sets of serum-deprived NIH3T3 fibroblasts were incubated with serum-free medium, medium containing 2% calf serum (CS), or medium supplemented with intact MVs derived from either MDAMB231 or U87 cells as indicated. (**B**) One set of cells was lysed after being exposed to the various culturing conditions for the indicated lengths of time and then immunoblotted with antibodies that recognize the activated and total forms of AKT and ERK. Two additional sets of fibroblasts were evaluated for their abilities to (**C**) undergo serum-deprivation-induced cell death and (**D**) grow in low serum (2% CS). For the growth assays, the culturing medium (including the MVs) was replenished daily. (**E**) NIH3T3 fibroblasts incubated without or with MVs derived from either MDAMB231 or U87 cells were subjected to anchorage-independent growth assays. The soft agar cultures were re-fed (including adding freshly prepared MVs) every third day. NIH3T3 cells expressing Cdc42 F28L was used as a positive control for these experiments. (**F**) Images of the resulting colonies that formed in (E). The data shown in (C), (D), and (E) represent the mean ± s.d. from at least three independent experiments. (**G**) Cell death assays were performed on MCF10A cells that were cultured for 3 days in serum-free medium, medium containing 2% fetal bovine serum (FBS), or serum-free medium supplemented with intact MVs derived from 5.0 x $10^6$ MDAMB231 cells. (**H**) Anchorage-independent growth assays were performed on MCF10A cells incubated with MVs derived from 5.0 x $10^6$ MDAMB231 cells treated without or with the tTG inhibitor T101. (**I**) Anchorage-independent growth assays were performed on NIH3T3 fibroblasts incubated with U87 cell-derived MVs treated without or with the EGF receptor inhibitor AG1478. The culturing medium (including the MVs, T101, and AG1478) for the soft agar assays performed in (H) and (I) was replenished every third day for 12 days, at which time the colonies that formed were counted. The data shown in (G), (H), and (I) represent the mean ± s.d. from three independent experiments.

*The experiments described in (C) and (G) were performed by Marc A. Antonyak and Bo Li.

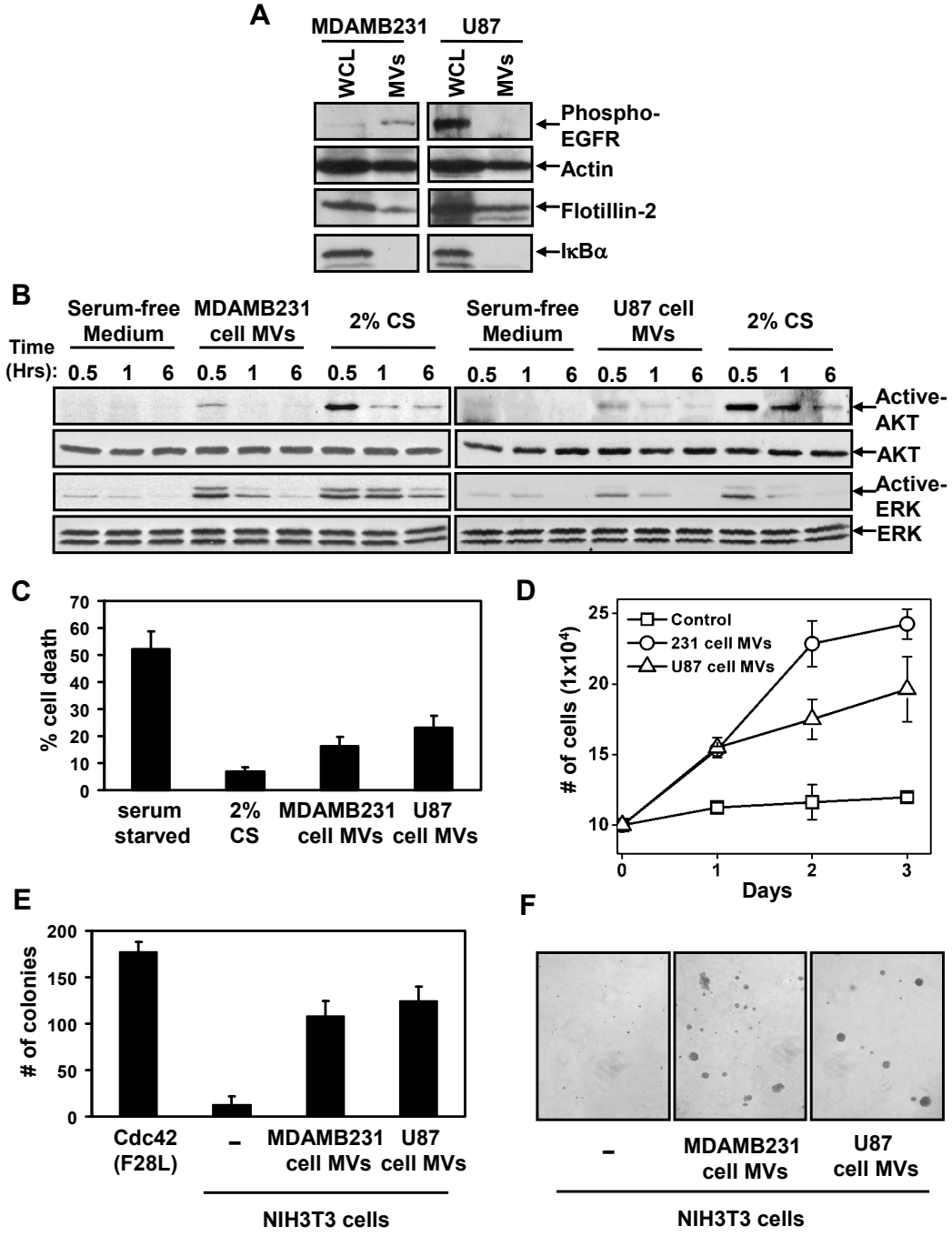
A
MDAMB231
U87
WCL
MVs
WCL
MVs
Phospho-EGFR
Actin
Flotillin-2
IκBα
B
Time (Hrs):
Serum-free Medium
MDAMB231 cell MVs
2% CS
Serum-free Medium
U87 cell MVs
2% CS
0.5 1 6 0.5 1 6 0.5 1 6 0.5 1 6 0.5 1 6 0.5 1 6
Active-AKT
AKT
Active-ERK
ERK
C
% cell death
70
60
50
40
30
20
10
0
serum starved
2% CS
MDAMB231 cell MVs
U87 cell MVs
D
# of cells (1x10⁴)
25
20
15
10
Control
231 cell MVs
U87 cell MVs
0
1
2
3
Days
E
# of colonies
200
150
100
50
0
Cdc42 (F28L)
–
MDAMB231 cell MVs
U87 cell MVs
NIH3T3 cells
F
–
MDAMB231 cell MVs
U87 cell MVs
NIH3T3 cells

Figure 3.2 (Continued)

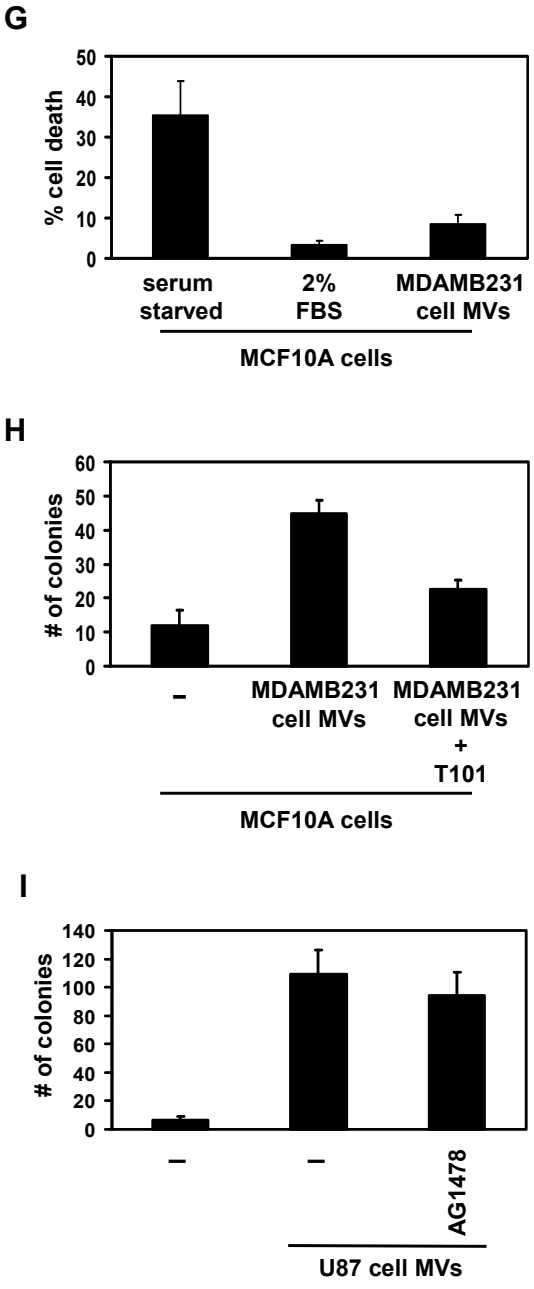

analysis (Figure 3.1*E*) and fluorescence-activated cell sorting (FACS) analysis (Figure 3.1*F* and 3.1*G*).

While MVs had been previously reported to share their cargo between cancer cells, I was interested in seeing whether MVs might be capable of conferring onto normal (non-transformed) recipient cells some of the transformed characteristics of the donor cancer cells. Thus, I isolated MVs constitutively shed by MDAMB231 breast cancer cells and U87 brain tumor cells from their serum-free culturing medium (Figure 3.2*A*) and added them to cultures of non-transformed NIH3T3 fibroblasts. The MVs generated by either of these cancer cell lines were capable of stimulating the activities of the signaling protein kinases AKT and ERK in the recipient fibroblasts (Figure 3.2*B*), similar to what has been observed when cancer cell-derived MVs were incubated with other cancer cells or endothelial cells (5, 7, 9). Moreover, when NIH3T3 fibroblasts were incubated with MVs derived from MDAMB231 cells or U87 cells, they exhibited two phenotypes characteristic of cancer cells, namely an enhanced survival capability (Figure 3.2*C*) and an ability to grow under low serum conditions (Figure 3.2*D*). I then asked whether the cancer cell-derived MVs, when added to normal cells, could induce cellular transformation as read-out by anchorage-independent growth (i.e. colony formation in soft agar). Figure 3.2*E* and 3.2*F* show that while the control NIH3T3 fibroblasts failed to form colonies in soft agar, sustained treatment of fibroblasts with MVs collected from either MDAMB231 cells or U87 cells conferred upon them the ability to grow under anchorage-independent conditions. MDAMB231 cell-derived MVs similarly promoted the survival (Figure 3.2*G*) and aberrant growth (Figure 3.2*H*) of the normal human mammary epithelial

**Table 3.1 Proteins common to both MDAMB231 cell- and U87 cell-derived MVs.** Proteomic analysis was performed on MVs shed by either MDAMB231 breast cancer cells or U87 brain tumor cells. A list was compiled (based on general cellular function) of those proteins that were identified in the MVs from both MDAMB231 and U87 cells. The complete list of proteins identified in each MV samples is attached in the Appendix.

**Proteomic analyses of microvesicles shed by MDAMB231 cells and U87 cells**

***Nucleic Acid-binding Proteins***
eukaryotic translation elongation factor 1
eukaryotic translation elongation factor 2
histone cluster 1
histone cluster 2
RuvB-like protein 1
RuvB-like protein 2

***Extracellular Matrix and Plasma Membrane-associated Proteins***
annexin A2
CD9 antigen
collagen
Ecto-5'-nucleotidase
EGF-like repeats and discoidin I-like domains-containing protein 3
fibronectin
galectin 3 binding protein
integrin beta 1
laminin
lysyl hydroxylase precursor
major histocompatibility complex
Na+/K+ -ATPase
transglutaminase 2 isoform a

***Metabolic Proteins***
aldolase A
enolase
ferritin
glyceraldehyde-3-phosphate dehydrogenase
L-lactate dehydrogenase A
nicotinamide phosphoribosyltransferase precursor
phosphoglycerate kinase 1
pyruvate kinase
UDP-glucose pyrophosphorylase

***Cytoskeletal Proteins***
actin
actinin
chaperonin
moesin
T-complex protein 1
tubulin
vimentin

***Signaling,Trafficking, and other functional proteins***
adenylyl cyclase-associated protein
alpha-2-macroglobulin precursor
heat shock protein 70kDa
heat shock protein 90kDa
HtrA serine peptidase 1 precursor
valosin-containing protein

cell line MCF10A. Thus, the continuous MV-mediated transfer of cargo from cancer cells to normal cells is indeed capable of endowing these cells with the characteristics induced by oncogenic transformation.

I then asked what MV-associated protein(s) is responsible for mediating the transfer of transforming capability. I initially considered the EGF-receptor (EGFR) as a possible candidate protein, since it was shown that activated forms of this receptor can be shared between brain cancer cells via MVs (5, 6, 9). However, it is unlikely that the EGFR accounts for the similar transforming abilities associated with the MVs derived from MDAMB231 breast cancer cells and U87 glioblastoma cells (Figure 3.2*C-E*), given that activated EGFRs cannot be detected in the MVs shed from U87 cells (Figure 3.2*A*). This was further supported by the finding that the anchorage-independent growth advantage imparted to NIH3T3 cells by U87 cell-derived MVs is insensitive to treatment with the EGFR tyrosine kinase inhibitor AG1478 (Figure 3.2*I*).

To identify proteins potentially involved in the transforming actions of these MVs, proteomic screens were carried-out. Proteins common to MVs derived from MDAMB231 cells and U87 cells are listed in Table 3.1. Notably among the MV-associated proteins was tTG, a protein cross-linking enzyme that has been linked to the chemoresistance and aberrant cell growth exhibited by some cancer cells (10-15), and is secreted from cells by an unknown mechanism (15-17). I confirmed that tTG is a component of MVs derived from MDAMB231 and U87 cells by immunoblot analysis (Figure 3.3*A*) and demonstrated that the MVs on the surfaces of MDAMB231 cells were detectable when immunostained with a tTG antibody (Figure 3.3*B, top images*), but not when stained with only the secondary antibody (Figure 3.3*B, bottom-*

**Figure 3.3 MVs shed by cancer cells contain tTG on the outer leaflet of MV membrane.** (**A**) Whole cell lysates (WCLs) of serum-starved MDAMB231 and U87 cells, as well as lysates of the MVs shed by these cells, were immunoblotted with several antibodies, including one against tTG. (**B**) Top images- MDAMB231 cells immuno-stained with a tTG antibody. The boxed area was enlarged and arrows are used to denote certain MVs. Bottom images- a MDAMB231 cell co-stained with just the secondary antibody (left image) and Rhodamine-conjugated phalloidin to label the MVs (right image). (**C**) Images of serum-starved U87 glioblastoma cells and HeLa cervical carcinoma cells that were left untreated or stimulated with EGF for 15 minutes as indicated, and then immuno-stained with a tTG antibody. Pronounced MVs are denoted with arrows. (**D**) Whole cell lysates (WCLs) of MDAMB231 cells ectopically expressing either GFP-only or GFP-tTG, as well as lysates of the MVs shed by these transfectants into their culturing medium, were immunoblotted with antibodies against GFP, the MV-marker flotillin-2, and the cytosolic-specific-marker IκBα. (**E**) Fluorescent images of permeabilized and non-permeabilized samples of MDAMB231 cells stained with antibodies against tTG and the intracellular protein Rheb, and DAPI to label nuclei. (**F**) Intact MDAMB231 cell-derived MVs were isolated, fixed, immuno-stained with a tTG antibody, and then processed for detection by SEM. Shown is a representative SEM image of a MV. Note the detection of tTG on the surface of the MV. (**G**) The transamidation activity of a fixed concentration of purified recombinant tTG (1 μM) incubated with increasing concentrations of the tTG inhibitor T101 was assayed. The IC50 of T101 (dashed lines) was determined to be ~1.5 μM. This experiment was repeated two additional times, with comparable results. (**H**) Transamidation activity assays, as readout by the incorporation of BPA into lysate proteins, were performed on the cell extracts of MDAMB231 cells that had been cultured in medium supplemented without or with 200 μM T101 (a 133-fold greater concentration than the IC50 calculated for this inhibitor in B) for ~10 hours prior to being washed extensively and then lysed (cell cultures). Equal amounts of a MDAMB231 cell extract were left untreated or were incubated with 10 μM T101 15 minutes before being subjected to a transamidation activity assay (cell extracts). Data are mean ± s.d. from three independent experiments. (**I**) Whole cell lysates (WCLs) of serum-starved MDAMB231 cells, as well as intact MVs generated by these cells treated without or with the tTG inhibitors T101 (cell-impermeable) or MDC (cell-permeable), were assayed for transamidation activity as readout by the incorporation of BPA into casein. The samples were then immunoblotted with antibodies against tTG, flotillin-2, and IκBα.

*The experiments described in (B), (C) and (E) were performed by Marc A. Antonyak and Bo Li.

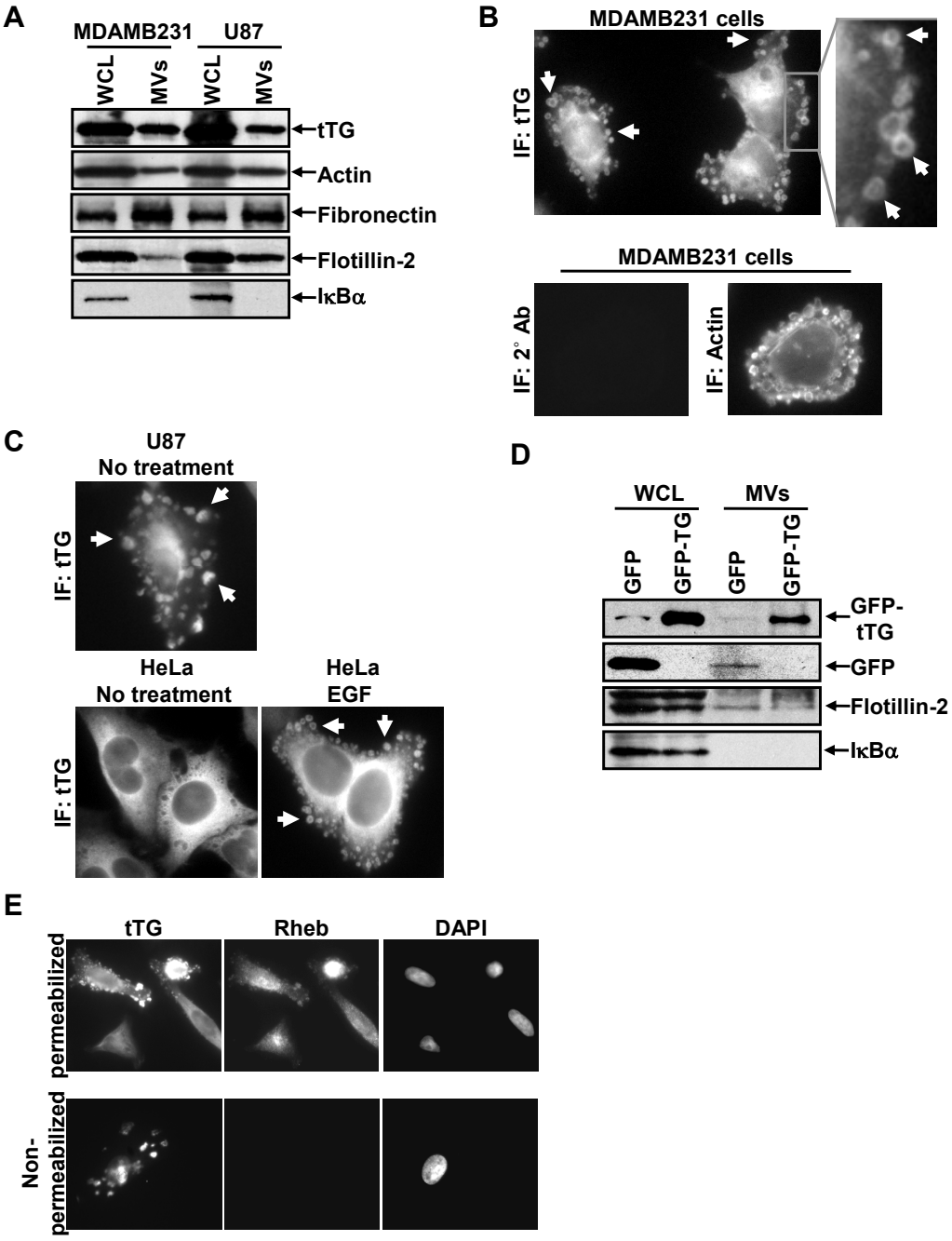
A
MDAMB231
U87
WCL
MVs
WCL
MVs
tTG
Actin
Fibronectin
Flotillin-2
IκBα
B
MDAMB231 cells
IF: tTG
MDAMB231 cells
IF: 2° Ab
IF: Actin
C
U87
No treatment
IF: tTG
HeLa
No treatment
HeLa
EGF
IF: tTG
D
WCL
MVs
GFP
GFP-TG
GFP
GFP-TG
GFP-tTG
GFP
Flotillin-2
IκBα
E
tTG
Rheb
DAPI
permeabilized
Non-permeabilized

Figure 3.3 (Continued)

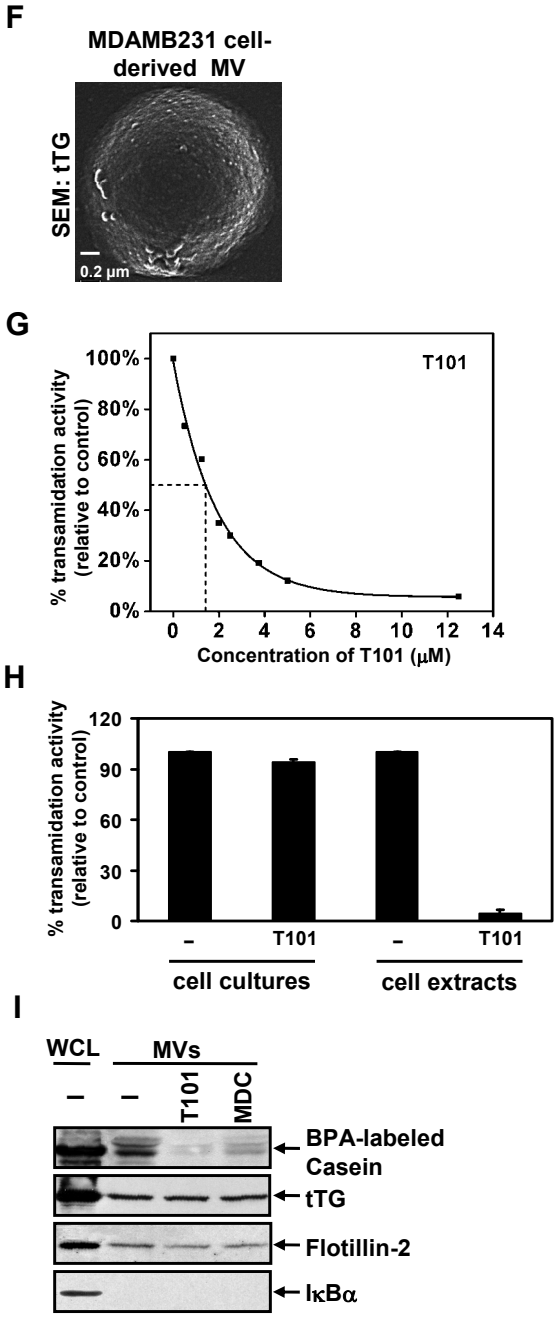

*left image*). Likewise, the MVs generated by U87 cells and HeLa cervical carcinoma cells stimulated with EGF also contained tTG (Figure 3.3*C*). These findings, when coupled with the fact that a GFP-tagged form of tTG is more efficiently incorporated into MVs shed by MDAMB231 compared to GFP alone (Figure 3.3*D*), demonstrate that tTG is targeted to MVs generated by distinct types of cancer cells and in response to specific cell culturing conditions.

As shown in Figure 3.3*B*, tTG was frequently enriched in the membranes of MVs, as indicated by the ring-shaped staining patterns detected with a tTG antibody in cells actively forming MVs. The same tTG antibody also labeled MVs that protruded from the plasma membranes of non-permeabilized MDAMB231 cells (Figure 3.3*E*), as well as detected tTG on the surfaces of individually isolated MVs from MDAMB231 cells by immuno-SEM (Figure 3.3*F*). The top panel in Figure 3.3*I* shows that tTG expressed in whole cell lysates (WCL) from MDAMB231 cells, or in intact MVs shed by these cells, was enzymatically active as readout by its ability to catalyze the incorporation of biotinylated pentylamine (BPA) into casein. Pre-treatment of the intact MDAMB231 cell-derived MVs with the cell permeable tTG inhibitor monodansylcadaverine (MDC) greatly diminished the levels of BPA-labeled casein detected in the assay. Interestingly, the cell impermeable tTG inhibitor T101 (Figure 3.3*G* and 3.3*H*) also effectively blocked the cross-linking activity associated with MVs derived from MDAMB231 cells (Figure 3.3*I*), suggesting that tTG is predominantly localized and activated on the outer leaflet of MV membranes.

**Figure 3.4 tTG is not important for the ability of human cancer cells to generate MVs.** (**A**) Serum-starved MDAMB231 cells treated without or with T101, MDC, BFA, or Exo1, were immuno-stained with a tTG antibody. Shown are representative images of the cells exposed to the various inhibitors. Cells forming MVs are denoted with arrows. (**B**) Serum-starved MDAMB231 cells treated without or with the tTG inhibitors T101 and MDC (left panel), transfected with either control siRNA (siCont) or two distinct tTG siRNAs (siTG-1 and siTG-2) (middle panel), or treated without or with the inhibitors of classical secretion, BFA and Exo1 (right panel), were lysed (WCLs) and the MVs released into the medium by the cells were also collected and lysed. The extracts were immunoblotted with antibodies against tTG, the MV-marker flotillin-2, and the cytosolic-specific-marker IκBα. (**C**) Whole cell lysates (WCLs) of MDAMB231 cells ectopically expressing vector-only or Myc-tagged forms of wild-type tTG (TG WT), a transamidation-defective form of tTG (TG C277V), or a GTP-binding-defective form of tTG (TG R580L), as well as lysates of the MVs shed by the transfectants, were immunoblotted with antibodies against the Myc-tag, flotillin-2, and IκBα.

*The experiments described in (A) were performed by Marc A. Antonyak and Bo Li.

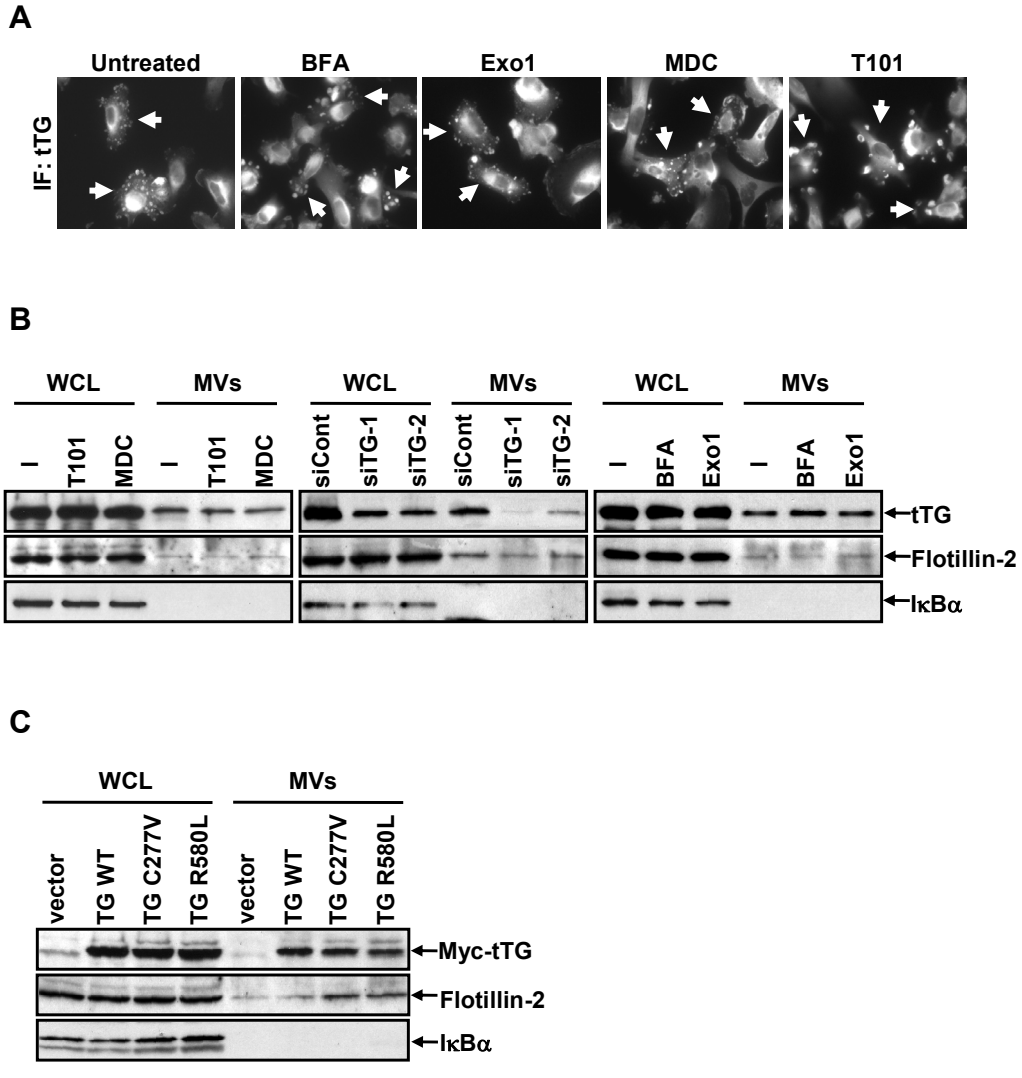
A
Untreated
BFA
Exo1
MDC
T101
IF: tTG
B
WCL
MVs
WCL
MVs
WCL
MVs
I
T101
MDC
I
T101
MDC
siCont
siTG-1
siTG-2
siCont
siTG-1
siTG-2
I
BFA
Exo1
I
BFA
Exo1
tTG
Flotillin-2
IκBα
C
WCL
MVs
vector
TG WT
TG C277V
TG R580L
vector
TG WT
TG C277V
TG R580L
Myc-tTG
Flotillin-2
IκBα

The MVs derived from MDAMB231 breast cancer cells were not sensitive to the traditional secretory inhibitors, BFA or ExoI, which block Arf GTPase activation (18), as indicated by monitoring MV formation by immunofluorescence staining of vesicle-associated tTG (Figure 3.4*A*). I then considered the possibility that the ability of tTG to cross-link proteins was important for the formation and/or shedding of MVs by cancer cells. Immunofluorescent analysis with a tTG antibody revealed that exposing MDAMB231 cells to the tTG inhibitors MDC and T101 had no effect on MV formation (Figure 3.4*A*). The shedding of MVs by MDAMB231 cells also did not require tTG enzymatic activity, nor was it affected by ExoI or BFA, as shown by the detection of nearly equivalents amounts of the MV-marker flotillin-2 (5) and tTG in MVs isolated from the culturing medium of control cells or cells treated with different inhibitors (Figure 3.4*B, left and right panels*). Correspondingly, knocking-down tTG in MDAMB231 cells, which depleted the expression of tTG in the MVs, caused little change in the amount of MVs shed by these cells as read-out by the flotillin-2 marker (Figure 3.4*B, middle panel*). Moreover, tTG mutants, defective in their ability to cross-link substrates (tTG C277V) or to bind GTP (tTG R580L), when ectopically expressed in MDAMB231 cells were targeted to MVs as efficiently as ectopically expressed, wild-type tTG (Figure 3.4*C*). Thus, these results indicate that tTG is not essential for the ability of cancer cells to form or shed MVs, nor is the enzymatic activity of tTG needed for its targeting to MVs.

I then examined whether tTG might function as MV cargo and be transferred to recipient cells. NIH3T3 fibroblasts were incubated for 30 minutes with MVs

**Figure 3.5 tTG can be transferred from MDAMB231 cells or U87 cells to recipient fibroblasts via MVs.** Extracts of serum-starved NIH3T3 fibroblasts that were incubated with serum-free medium or serum-free medium supplemented with MDAMB231 cell (**A**) or U87 cell (**B**) -derived MVs that had been pre-treated without or with the tTG inhibitor T101 for 30 minutes were immunoblotted with tTG and actin antibodies. (**C**) NIH3T3 cells incubated for 30 minutes with serum-free medium supplemented without or with intact MVs generated by either MDAMB231 or U87 cells were immuno-stained with a tTG antibody and rhodamine-conjugated phalloidin to detect actin. Shown are representative fluorescent images of the fibroblasts. Note that tTG is only detected in the fibroblasts that were incubated with cancer cell-derived MVs. Lysates of fibroblasts incubated for 30 minutes with MDAMB231 cell (**D**) or U87 cell (**E**) -derived MVs that had been pre-treated without or with T101 were assayed for transamidation activity as read-out by the incorporation of BPA into lysate proteins. Data shown in (D) and (E) are mean ± s.d. from three independent experiments.

*The experiments described in (C) were performed by Marc A. Antonyak and Bo Li.

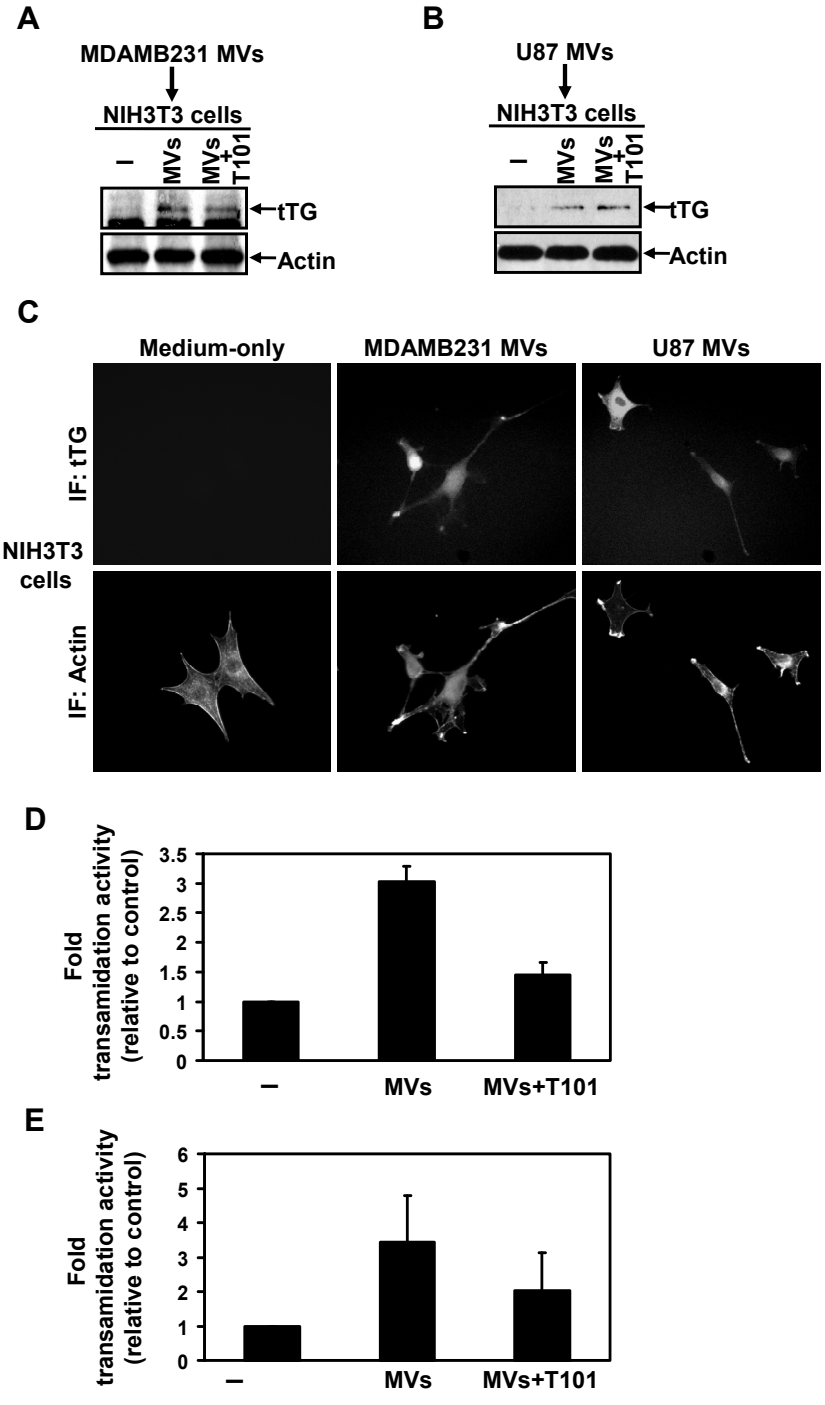
A
MDAMB231 MVs
NIH3T3 cells
–
MVs
MVs+T101
tTG
Actin
B
U87 MVs
NIH3T3 cells
–
MVs
MVs+T101
tTG
Actin
C
Medium-only
MDAMB231 MVs
U87 MVs
IF: tTG
NIH3T3 cells
IF: Actin
D
Fold transamidation activity (relative to control)
3.5
3
2.5
2
1.5
1
0.5
0
–
MVs
MVs+T101
E
Fold transamidation activity (relative to control)
6
5
4
3
2
1
0
–
MVs
MVs+T101

derived from serum-starved cultures of either MDAMB231 cells or U87 cells and then analyzed for tTG expression by immunoblot analysis (Figure 3.5*A* and 3.5*B*) and immunofluorescent microscopy (Figure 3.5*C*). The results from these experiments show that the levels of tTG were significantly increased in fibroblasts that had been incubated with the cancer cell-derived MVs relative to the barely discernible levels of tTG in control fibroblasts.

These findings then raised the question of whether the MV-mediated transfer of activated tTG into recipient fibroblasts might be important for conferring these cells with enhanced survival capability and the characteristics of transformation. To address this I took advantage of my earlier findings that tTG is localized on the surfaces of MVs such that its cross-linking activity is susceptible to inhibition by the cell impermeable, irreversible inhibitor T101 (Figure 3.3*B,* 3.3*E* and 3.3*I*). By pre-treating cancer cell-derived MVs with T101 before adding them to fibroblast cultures, I was able to selectively and irreversibly inhibit the cross-linking activity of the MV-associated tTG (Figure 3.5*D* and 3.5*E*). Using this approach, I compared how the survival advantage afforded to NIH3T3 fibroblasts by MVs collected from cancer cells would be affected under conditions where tTG activity was inhibited. Figure 3.6*A* and 3.6*B* show that pre-treatment of the MVs derived from either MDAMB231 or U87 cells with T101 severely compromised their ability to protect the recipient fibroblasts from serum-deprivation-induced cell death. Importantly, the extent of cell survival achieved by culturing NIH3T3 cells in medium supplemented with a nominal amount of calf serum (2% CS) was unchanged by the addition of T101, indicating that the ability of this small molecule inhibitor to abolish the protection afforded by the cancer

**Figure 3.6 The ability of MDAMB231 cell or U87 cell-derived MVs to induce cellular transformation requires the transfer of active tTG from MVs to recipient cells.** Cell death assays were performed on fibroblasts maintained in serum-free medium, 2% CS-medium, or serum-free medium containing MDAMB231 cell (**A**) or U87 cell (**B**) -derived MVs. Each culturing medium was further supplemented without or with the tTG inhibitors T101 (cell-impermeable) or MDC (cell-permeable) as indicated. (**C)** The MVs shed from serum-starved MDAMB231 cells transfected with either control siRNA (siCont) or two different tTG siRNAs (siTG-1 and siTG-2) were collected and resuspended in serum-free DMEM. NIH3T3 cells plated in each well of a 6-well dish were then placed in serum-free medium or serum-free medium containing the different MV preparations for ~35 hours, at which time the cell death rates of the different cell cultures were determined. **(D**) Anchorage-independent growth assays were performed on fibroblasts incubated with MDAMB231 cell-derived MVs treated without or with T101, the RGD-peptide, or the control RGE-peptide. (**E**) Anchorage-independent growth assays were performed on NIH3T3 fibroblasts incubated with the different MV preparations as indicated. The soft agar cultures were re-fed (including the addition of freshly prepared MVs) every third day for 12 days, at which time the colonies that formed were counted. (**F**) Anchorage-independent growth assays were performed on control NIH3T3 fibroblasts or on fibroblasts incubated with MVs derived from U87 cells treated with either T101, the RGD-peptide, the RGE-control-peptide, or untreated. (**G**) Anchorage-independent growth assays were also performed on NIH3T3 cells stably expressing vector alone or an activated form of Cdc42 (Cdc42 F28L) treated with 200 μM T101 or untreated. Note that the ability of Cdc42 F28L to induce colony formation is insensitive to T101. Data shown in (A) though (G) are all mean ± s.d. from three independent experiments. (**H**) Tumor formation assays were performed in which 5 x $10^5$ mitotically-arrested (using mitomycin-C) MDAMB231 cells (denoted as Mito-C-MDAMB231) expressing either control siRNA (siCont) or tTG siRNAs (denoted as siTG-1 or siTG-2) were subcutaneously injected singly, or combined with 5 x $10^5$ NIH3T3 fibroblasts, into nude mice. As controls, untreated MDAMB231 and NIH3T3 cells were injected into nude mice. The resulting tumors that formed for each condition were counted and the results shown in the table..

*The experiments described in (A), (B), (C) and (H) were performed by Marc A. Antonyak and Bo Li.

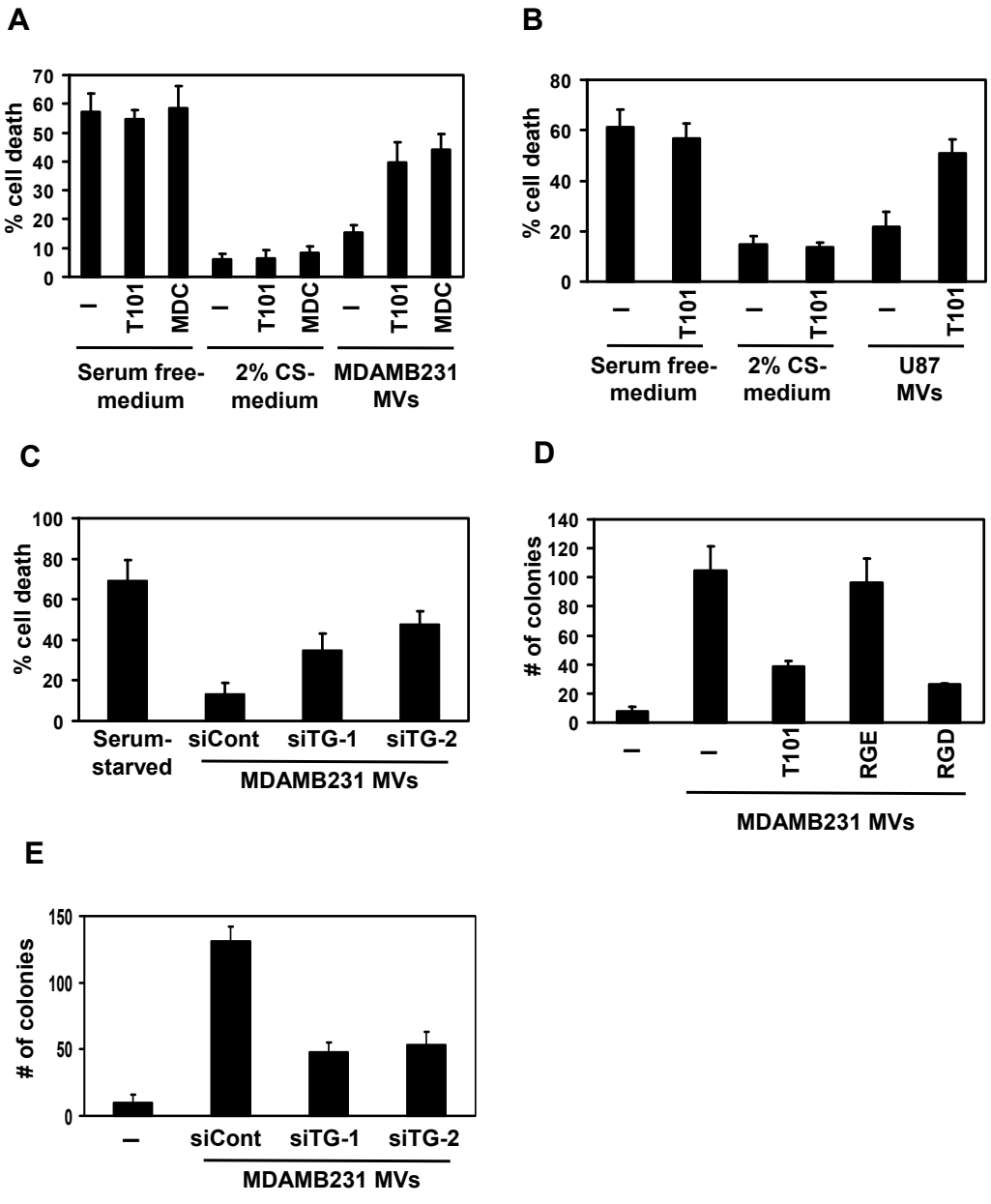
A
% cell death
70
60
50
40
30
20
10
0
–
T101
MDC
–
T101
MDC
–
T101
MDC
Serum free-medium
2% CS-medium
MDAMB231 MVs
B
% cell death
80
60
40
20
0
–
T101
–
T101
–
T101
Serum free-medium
2% CS-medium
U87 MVs
C
% cell death
100
80
60
40
20
0
Serum-starved
siCont
siTG-1
siTG-2
MDAMB231 MVs
D
# of colonies
140
120
100
80
60
40
20
0
–
–
T101
RGE
RGD
MDAMB231 MVs
E
# of colonies
150
100
50
0
–
siCont
siTG-1
siTG-2
MDAMB231 MVs

Figure 3.6 (Continued)

F

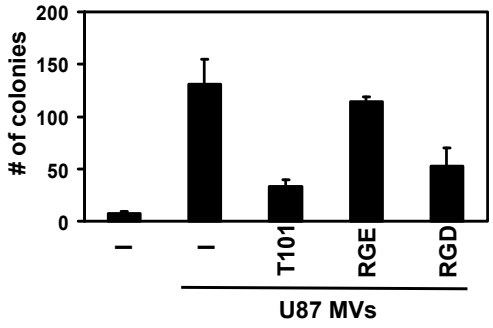


G

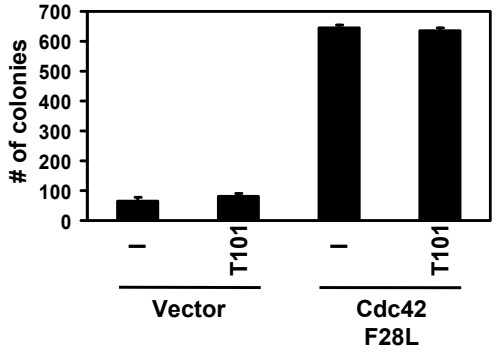


H

| Cells Injected | Tumors/Injection | Cells Injected | Tumors/Injection |
|---|---|---|---|
| MDAMB231 | 4/4 | Mito-C-MDAMB231(siCont) + NIH3T3 | 4/6 |
| NIH3T3 | 0/6 | Mito-C-MDAMB231(siTG-1) + NIH3T3 | 0/6 |
| Mito-C-MDAMB231 | 0/6 | Mito-C-MDAMB231(siTG-2) + NIH3T3 | 0/6 |

cell-derived MVs was not due to off-target effects that sensitized the fibroblasts to apoptosis. Analogous experiments were then performed where either MDAMB231 cell-derived MVs were incubated with serum-starved NIH3T3 cells in the presence of the cell permeable tTG inhibitor MDC (Figure 3.6*A*), or MVs collected from MDAMB231 cells in which tTG had been knocked-down (Figure 3.4*B*) were added to serum-starved NIH3T3 cells (Figure 3.6*C*). Collectively, the results from these experiments point to a critical role for tTG in mediating the survival advantage imparted to fibroblasts by cancer cell-derived MVs.

I then asked whether the transforming abilities of the cancer cell-derived MVs were dependent upon tTG. As shown previously in Figure 3.2*E* and 3.2*H*, and again in Figure 3.6*D*, 3.6*E* and 3.6*F*, incubating normal NIH3T3 fibroblasts and MCF10A epithelial cells with MVs derived from MDAMB231 cells or U87 cells induced their ability to grow (i.e. to form colonies) under anchorage-independent conditions. However, when recipient fibroblasts or epithelial cells were incubated with MV preparations that had been pre-treated with T101 (Figure 3.6*D*, 3.2*H* and 3.6*F*), or in which tTG had been knocked-down (Figure 3.6*E*), the number of colonies that formed in each case was reduced. I then verified that T101 did not generally inhibit cellular transformation by showing that this inhibitor had no influence on the ability of NIH3T3 cells expressing an activated form of the small GTPase Cdc42 (Cdc42 F28L) to grow under anchorage-independent conditions, even when a 5-fold excess of T101 was used (Figure 3.6*G*).

These findings prompted me to then consider whether cancer cell-derived MVs might function similarly *in vivo* and promote tumor growth by causing normal cells in

**Figure 3.7 tTG functionally cooperates with FN to mediate the transforming actions of MVs on recipient fibroblasts**. (**A**) Lysates of NIH3T3 cells stably overexpressing vector alone or Myc-tTG were immunoblotted with Myc and actin antibodies, and assayed for transamidation activity as readout by the incorporation of BPA into lysate proteins. (**B**) Cell death assays were performed on the NIH3T3 stable cell lines maintained in serum-free medium that was treated with T101, MDC, or 2% CS-medium, or was untreated. (**C**) Anchorage-independent growth assays were performed on the NIH3T3 stable cell lines. Vector-control fibroblasts were incubated with MDAMB231 cell-derived MVs, as a positive control. Data shown in (B) and (C) are mean ± s.d. from two independent experiments. (**D**) Whole cell lysates (WCLs) of MDAMB231 and lysates of the MVs shed by these cells were either immunoblotted (Input), or subjected to immunoprecipitation using a tTG antibody (IP: tTG) and then immunoblotted, with FN, tTG, and actin antibodies. Note the detection of crosslinked FN in the MV lanes (FN dimer). (**E**) Intact MVs collected from MDAMB231 or U87 cells were treated without or with T101 prior to being lysed. The MV extracts were then subjected to immunoprecipitation using a tTG antibody (IP: tTG). The resulting immunocomplexes were immunoblotted with FN and tTG antibodies. (**F**) Intact MVs collected from MDAMB231 or U87 cells were treated without or with T101 prior to being lysed. The MV extracts were then immunoblotted with FN and tTG antibodies. Note that the crosslinked forms of FN detected in the MV samples (FN dimer) were significantly reduced by T101 treatment. (**G**) Lysates of fibroblasts that were incubated without or with MVs derived from MDAMB231 and U87 cells that had been pre-treated without or with T101, or the RGD-peptide, were immunoblotted with antibodies against FAK and ERK, or with antibodies that specifically recognize the activated forms of these protein kinases. (**H**) Diagram depicting how MVs transform recipient cells. MVs containing tTG and fibronectin are generated and released from the surfaces of human cancer cells. The MVs can then be taken-up by, or directly alter the microenvironment of, neighboring normal cells, where the co-transfer of tTG and FN function cooperatively on the recipient cells to induce signaling events that promote cell survival and aberrant cell growth.

*The experiments described in (B) were performed by Marc A. Antonyak and Bo Li.

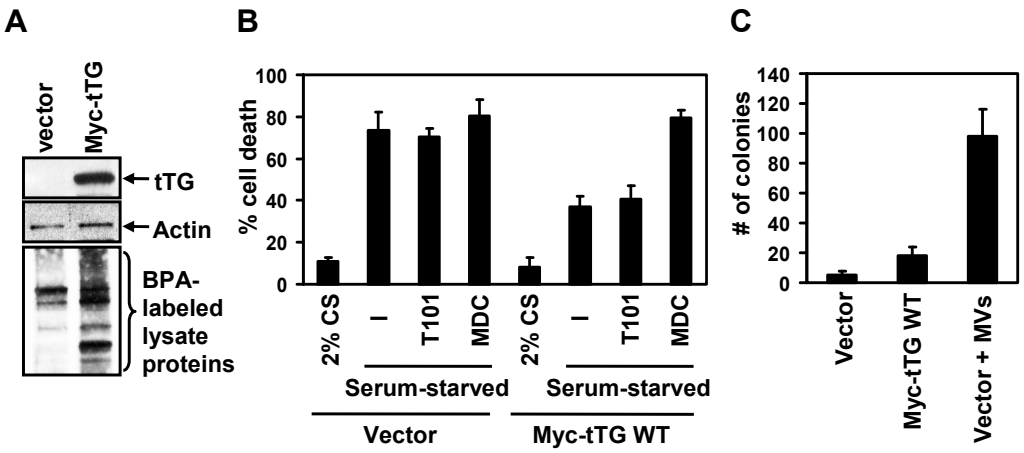
A
vector
Myc-tTG
tTG
Actin
BPA-labeled lysate proteins
B
% cell death
100
80
60
40
20
0
2% CS
–
T101
MDC
2% CS
–
T101
MDC
Serum-starved
Serum-starved
Vector
Myc-tTG WT
C
# of colonies
140
120
100
80
60
40
20
0
Vector
Myc-tTG WT
Vector + MVs

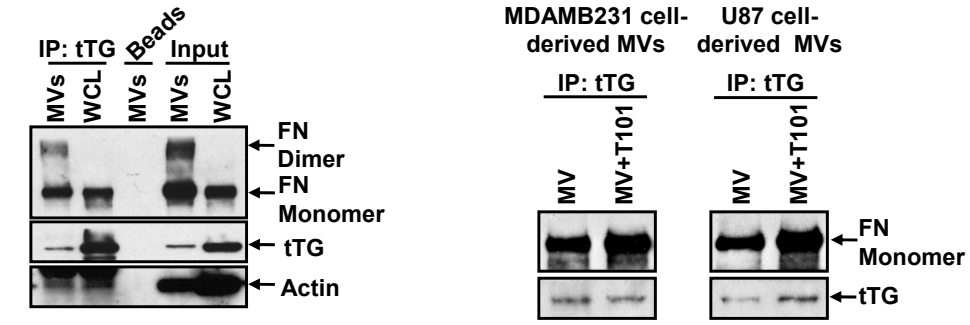
D
IP: tTG
Beads
Input
MVs
WCL
MVs
MVs
WCL
FN Dimer
FN Monomer
tTG
Actin
E
MDAMB231 cell-derived MVs
U87 cell-derived MVs
IP: tTG
IP: tTG
MV
MV+T101
MV
MV+T101
FN Monomer
tTG

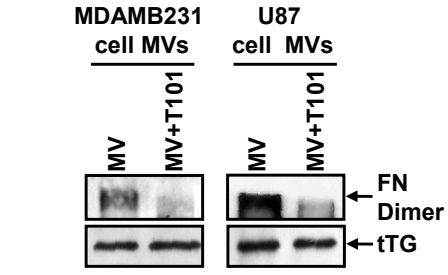
F
MDAMB231 cell MVs
U87 cell MVs
MV
MV+T101
MV
MV+T101
FN Dimer
tTG

Figure 3.7 (Continued)

G

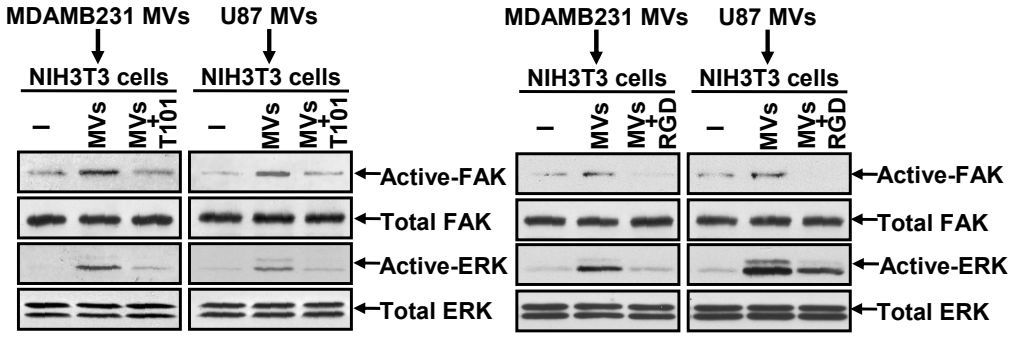


H

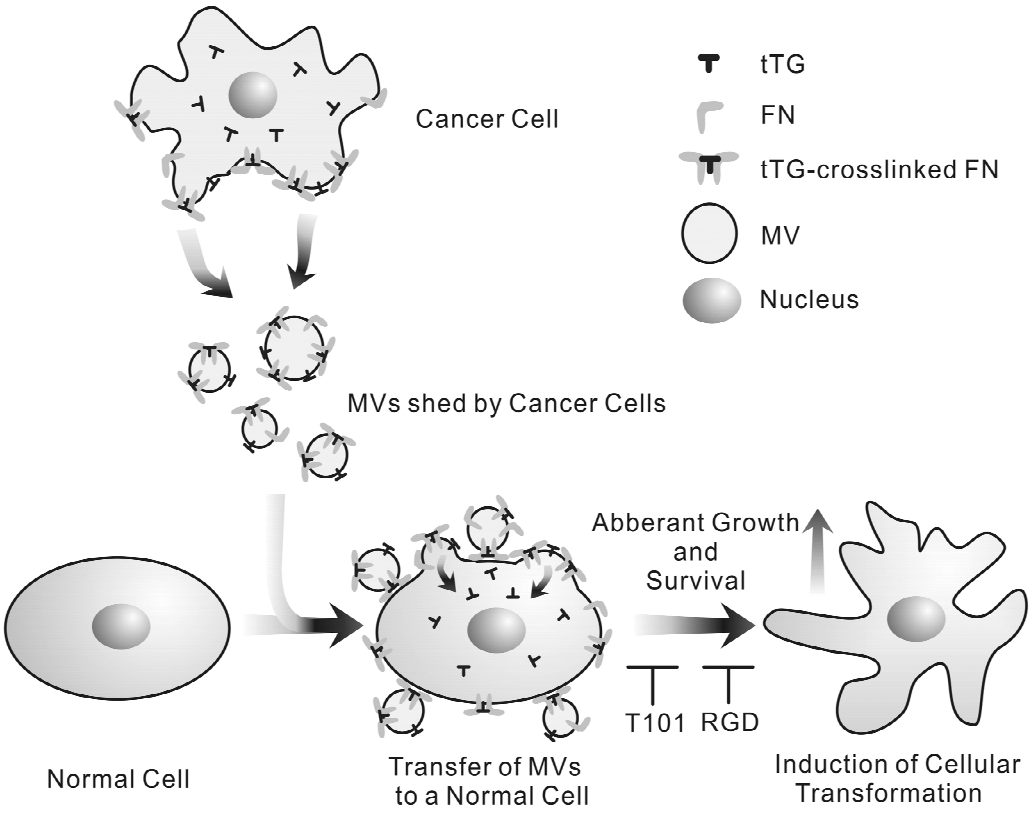

the tumor microenvironment to acquire the ability to form a tumor. To investigate this, I took advantage of the fact that exposing MDAMB231 cells to the mitotic arresting agent mitomycin-C, before injecting them into nude mice, inhibited their ability to form tumors under conditions where their control counterparts (untreated MDAMB231 cells) were quite effective at inducing tumor formation (Figure 3.6*H)*. However, when the mitomycin-C-treated MDAMB231 cells were co-injected with an equal number of normal (non-transformed) NIH3T3 fibroblasts into mice, 4 of 6 mice formed tumors, suggesting that the MVs shed by the mitotically arrested cancer cells were capable of causing the neighboring NIH3T3 fibroblasts to become transformed, inducing tumor growth. Interestingly, I then went on to show that knocking-down tTG expression in the mitotically-arrested MDAMB231 cells blocked the ability of the co-injected NIH3T3 fibroblasts to form tumors in mice. Thus, these results are consistent with the idea that cancer cells can generate MVs *in vivo*, and that their ability to cause normal cells in the tumor microenvironment to promote tumor formation is dependent on tTG.

These findings demonstrate that the MV-mediated transfer of tTG into recipient cells is necessary for the ability of MDAMB231 cell- and U87 cell-derived MVs to transform fibroblasts. However, is tTG alone sufficient to confer survival and transforming capabilities to the recipient cells? In fact, I found that while NIH3T3 fibroblasts stably overexpressing Myc-tagged tTG (Figure 3.7*A*) were indeed resistant to serum-deprivation-induced apoptosis, an effect that was ablated by treating the cells with MDC (Figure 3.7*B*), they were unable to form colonies in soft agar unlike the case when the vector-control expressing fibroblasts were incubated with MVs derived

from MDAMB231 cells (Figure 3.7*C*). This means that while overexpression/over-activation of tTG in normal cells is not sufficient to fully induce their transformation (i.e. NIH3T3 cells ectopically expressing tTG do not acquire the ability to form colonies when grown under anchorage-independent conditions), it does confer upon normal cells some characteristics of the transformed state, allowing them to grow in monolayer under low serum conditions, as well as to become less sensitive to serum-deprivation-induced cell death. However, these findings also indicate that in order for cancer cell-derived MVs to enable recipient cells to exhibit one of the major hallmarks of cellular transformation, namely anchorage-independent growth, another protein must be transferred along with tTG. The cytoskeletal component fibronectin (FN) was a particularly attractive candidate, as it is a known binding partner of tTG (16, 17, 19) and was identified in my proteomics screen of MDAMB231 cell- and U87 cell-derived MVs (Table 3.1). I confirmed that FN was expressed in the MVs collected from each of the cancer cell lines by immunoblot analysis (Figure 3.3*A*). I then assessed the potential role of the MV-associated FN in conferring upon fibroblasts the ability to exhibit anchorage-independent growth, by using the RGD-peptide as a means to interfere with the ability of FN to bind to and activate integrins on the surface of the recipient fibroblasts (20, 21). Anchorage-independent growth assays performed on fibroblasts co-treated with MVs derived from MDAMB231 or U87 cells, and either the RGD-peptide or the control RGE-peptide, showed that the RGD-peptide, like T101, blocked the MV-triggered induction of cellular transformation, whereas the control RGE-peptide did not (Figure 3.6*D* and 3.6*F*).

Since both tTG and FN are important for the ability of cancer cell-derived MVs to transform recipient cells, might they work together to elicit this cellular outcome? To address this I first examined whether tTG interacted with FN in MVs. Figure 3.7*D* shows that FN co-immunoprecipitates with tTG from MDAMB231 whole cell lysates as previously reported (16, 17, 19), as well as from lysates of MVs shed by these cells. In addition to binding the monomeric form of FN, tTG also associated with a larger form of FN with an apparent $M_r$ of ~440 kDa that likely represented cross-linked FN dimers and was detectable only in the MV lysate. Pre-treating intact MVs collected from MDAMB231 cells or U87 cells with the tTG inhibitor T101, prior to lysing the MVs and subjecting the extracts to immunoblot analysis, did not affect the ability of tTG to be co-immunoprecipitated with monomeric FN from the MV lysates (Figure 3.7*E*). However, pre-treating the MVs with the tTG inhibitor resulted in a marked reduction in the amount of the ~440 kDa FN species detected in the MV lysate samples (Figure 3.7*F*), suggesting that the higher molecular mass form of FN in the cancer cell-derived MVs is generated through the ability of tTG to interact with and cross-link FN.

The dimerization of FN strongly enhances its ability to bind and activate integrins on the surfaces of cells (22, 23). The ability of tTG to cross-link FN in MVs shed by cancer cells suggested that this covalently modified form of FN is capable of potentiating integrin activation. Indeed, I found that preparations of intact MVs isolated from the medium of serum-deprived MDAMB231 cells or U87 cells were capable of stimulating signaling activities that are well-known to be downstream from activated integrins including FAK and ERK (Figure 3.7*G*). Moreover, the activation of

these kinases by MVs was blocked either by using the tTG inhibitor T101 or the RGD peptide that interferes with integrin-signaling (Figure 3.7*G*), thus further demonstrating the importance of tTG and FN for the signaling functions of MVs.

**Discussion**

The findings described here shed important new light on an unconventional and poorly understood mechanism of cell-to-cell communication and how it may have significant consequences in human cancer progression. In particular, I have shown that exposing normal recipient cells to bio-active MVs that are constitutively shed by certain human cancer cells can cause them to acquire a transformed phenotype (Figure 3.7*H*). I have identified the protein cross-linking enzyme tTG and the extracellular matrix protein FN as components of cancer cell-derived MVs that functionally cooperate to mediate the transforming activities of the MVs. The fact that tTG and FN are aberrantly regulated in several types of human cancers (24-30), raises exciting possibilities regarding the broad roles played by MVs in cancer progression.

One aspect of my work to consider further involves the potential implications of MVs on tumor growth. There is a growing body of evidence demonstrating that cancer cells are capable of generating MVs *in vivo*, suggesting that the shedding of MVs by cancer cells is not merely an artifact of tissue culture, but rather represents a tumor-relevant process. A particularly good example comes from a recent study which showed that brain tumor cell-derived MVs could be routinely detected in blood samples taken from human patients afflicted with glioblastoma multiforme (4). Moreover, it was also shown that when MVs shed by cultures of several different

human primary tumor cells or established cancer cell lines were subsequently added back to the same cancer cells, the growth and the survival of these cells were significantly enhanced (4-7). When considering these findings in the context of a tumor setting, the increased proliferative capacity afforded by sharing MVs among cancer cells could be envisioned as a mechanism to augment tumor growth. However, my results now suggest that MVs may impact cancer progression in a new and unexpected way, specifically, by conferring upon normal cell lineages that are major constituents of the tumor microenvironment (i.e. fibroblasts and epithelial cells), the transformed characteristics of cancer cells. This would be consistent with the idea that the expansion of a tumor mass would not necessarily depend solely on the proliferation of the cancer cells, but rather could also include the aberrant growth exhibited by stromal cells (including fibroblasts) and normal epithelium in the tumor microenvironment that have been exposed to MVs shed by cancer cells. If this turns out to be true, then how we think about cancer progression *in vivo* needs to be adjusted to include the potential contribution of MVs.

However, it is important to note that the ability of the cancer cell-derived MVs to induce a transformed phenotype in normal (non-transformed) recipient cell types is not sustained. In order for MVs derived from either MDAMB231 breast cancer cells or U87 brain tumor cells to promote the growth of normal cells (i.e. NIH3T3 fibroblasts and MCF10A mammary epithelial cells) in low serum and to induce their ability to form colonies in soft agar, the recipient cells needed to be repeatedly treated with freshly prepared MVs throughout the duration of these growth assays. This implies that the proteins and RNA transcripts contained within MVs that are involved

in promoting their transforming activity, after being added to normal recipient cells, have a finite lifespan and need to be continuously replenished. When considering this in the context of a tumor setting, the chronic shedding of MVs by the cancer cells into their microenvironment might provide the continuous supply of MVs required by the nearby recipient stroma and normal epithelium to induce and maintain a transformed phenotype.

The MV field is still in its infancy and many of the advances made in our understanding of MV formation, as well as the identity of their contents and their mechanisms of action (i.e. transforming capability), have thus far been largely limited to tissue culture experiments. However, as our methods for isolating and characterizing cancer cell-derived MVs continue to advance, it will ultimately be important to extend these studies into animal models. Toward this end, I am currently focusing my efforts on understanding the signaling events that are coupled to the formation and shedding of MVs from the surface of human cancer cells, and on determining whether additional proteins (i.e. aside from tTG and FN) contribute to the abilities of cancer cell-derived MVs to transform recipient cells.

**Materials and Methods**

*Materials.* 4,6-diamidino-2-phenylindole (DAPI), brefelden A, mitomycin-C, and Exo1 were obtained from Calbiochem, while T101 was from Zedira. The rhodamine-conjugated phalloidin, EGF, Lipofectamine, Lipofectamine 2000, protein G beads, control and tTG siRNAs, and all cell culture reagents were from Invitrogen. The FN

antibody, MDC, and BPA were from Sigma. The tTG and actin antibodies were obtained from Lab Vision/Thermo. Flotillin-2 antibody was obtained from Santa Cruz, and HA and Myc antibodies were from Covance. The Steriflip PVDF-filters (0.45μm pore size) were from Millipore. The antibodies against IκBα, GFP, as well as antibodies that recognize ERK, AKT, FAK and the EGF receptor were from Cell Signaling.

*Cell Culture.* The MDAMB231, U87, MCF10A, and HeLa cell lines were grown in RPMI 1640 medium containing 10% fetal bovine serum, while the NIH3T3 cell line was grown in DMEM medium containing 10% calf serum. Expression constructs were transfected into cells using Lipofectamine, whereas the control and tTG siRNAs were introduced into cells with Lipofectamine 2000. As indicated, cells were incubated with serum-free medium containing combinations of 0.1 μg/ml EGF, 100 μM MDC, 10 μM T101, 10 μM BFA, and 10 μM Exo1. To mitotically arrest MDAMB231 cells, plates of cells were treated with 10 μg/ml mitomycin-C for 2 hours, before rinsing the solution away and allowing the cells to recover in growth medium (RPMI-1640 medium containing 10% FBS) for a day.

*Isolation of Microvesicles from Cancer Cells.* For each of the experiments that used MV preparations, the conditioned medium from 5.0 x $10^6$ serum-starved MDAMB231 cells or U87 cells (which is the equivalent of two nearly confluent 150 mm dishes of either of these cell lines) were collected and the MVs isolated from the medium as previously described (4, 5). Briefly, the conditioned medium was subjected to two

consecutive centrifugations; the first at 300 g for 10 minutes pelleted intact cells, while the second at 12,000 g for 20 minutes pelleted cell debris. To generate MV lysates, the conditioned medium was centrifuged a third time at 100,000 g for 2 hours and the resulting pellet was washed with PBS and then lysed in 250 µl cell lysis buffer (25 mM Tris, 100 mM NaCl, 1% Triton X-100, 1 mM EDTA, 1 mM DTT, 1 mM $NaVO_4$, 1 mM β-glycerol phosphate, and 1 µg/mL aprotinin). To generate intact MVs for the cell-based assays and other experiments as indicated, the partially purified conditioned medium (medium cleared of cells and cell debris) was then filtered using a Millipore Steriflip PVDF-filter with a 0.45 µm pore size. The microvesicles retained by the PVDF membrane were then resuspended in serum-free medium, with each preparation yielding enough MVs to treat 2-3 wells of a 6-well dish of recipient cells for a given experiment.

*Immunoblot Analysis and Immunoprecipitation.* The protein concentrations of the whole cell lysates (WCLs) were determined using the Bio-Rad DC protein assay, while the MV lysates were normalized for comparison by isolating them from the conditioned medium of 5.0 x $10^6$ serum-starved MDAMB231 cells or U87 cells for each of the experimental conditions assayed, and then lysing in 250 µl of cell lysis buffer. For immunoprecipitations, equal volumes of MV lysates, or 300 µg of WCLs, were incubated with a tTG antibody and protein G beads. The bead-antibody-protein complexes collected by centrifugation, as well as the WCLs (40 µg) and MV extracts (75 µl), were resolved by SDS-PAGE and the proteins transferred to polyvinylidene difluoride membranes. The filters were incubated with the indicated primary

antibodies diluted in TBST (20 mM Tris, 135 mM NaCl, and 0.02% Tween 20). The primary antibodies were detected with horseradish peroxidase-conjugated secondary antibodies (Amersham Biosciences) followed by exposure to ECL reagent.

*Immunofluorescence.* Cells were fixed with 3.7% paraformaldehyde and then some samples were permeabilized with phosphate-buffered saline (PBS) containing 0.1% Triton X-100. Permeabilized and non-permeabilized samples were incubated with a tTG antibody, and then incubated with Oregon green 488-conjugated secondary antibody. Rhodamine-conjugated phalloidin was used to stain actin and DAPI was used to stain nuclei. The cells were visualized by fluorescent microscopy and the images were captured and processed using IPLABS.

*Live Image Fluorescence Microscopy.* MDAMB231 cells transiently expressing GFP-PM, a GFP-tagged form of the plasma membrane targeting sequence in Lyn, were visualized by fluorescent microscopy. Images of the transfectants were captured in 30 second intervals over a span of 15 minutes.

*Transamidation Assay.* The transamidation activity in whole cell extracts was readout by the incorporation of BPA into lysate proteins as previously described (30), whereas the transamidation activity of recombinant tTG (0.1 μM) exposed to increasing concentrations of T101 was determined using a spectrophotometric assay (31). The transamidation activity associated with MVs was readout by incubating equal amounts (75 μl) of each MV sample in a buffer containing 40 mM N'N-dimethyl casein, 2 mM

BPA, 40 mM $CaCl_2$, and 40 mM dithiothreitol for 15 minutes. The reaction was stopped by the addition of Laemmli sample buffer followed by boiling. The reactions were then resolved by SDS-PAGE and the proteins transferred to polyvinylidene difluoride membranes. The filters were blocked with BBST (100 mM boric acid, 20 mM sodium borate, 0.01% SDS, 0.01% Tween 20, and 80 mM NaCl) containing 10% bovine serum albumin, and then incubated with horseradish peroxidase-conjugated streptavidin diluted in BBST containing 5% bovine serum albumin for 1 hour at room temperature, followed by extensive washing with BBST. The incorporation of BPA into N'N-dimethyl casein was visualized after exposing the membranes to ECL reagent.

*Scanning Electron Microscopy (SEM) and Immuno-SEM.* MDAMB231 cells grown on Lab-Tek chamber slides (Nunc) were fixed for 1 hour with 2% EM-grade glutaraldehyde diluted in a 0.05 M Cacodylic acid buffer solution (PH=7.4). For immuno-SEM, filter-isolated MDAMB231 cell-derived MVs were added to Lab-Tek chamber slides, allowed to attach, and then were fixed for 1 hour with 2% EM-grade glutaraldehyde in PBS. Following blocking for 15 minutes in 0.1M glycine, and for an additional 30 minutes in PBS containing 5% BSA, 0.1% gelatin and 5% goat serum, the MVs were incubated for 1 hour with the tTG antibody diluted in PBS (2 μg/mL). After washing with PBS, the MV samples were incubated for 1 hour with 6 nm gold particle-conjugated Goat-anti-Mouse IgG (Electron Microscopy Sciences) diluted in PBS. Both the cell and the immuno-labeled MV samples were post-fixed for 1 hour with 1% osmium tetroxide in PBS and dehydrated in graded ethanol solutions of 25%,

50%, 70%, 95%, and 100% ethanol, before being placed in a CPD-30 critical point drying machine (BAL-TEC SCD050). The cells were then sputter-coated with platinum, whereas the immuno-labeled MVs were sputter-coated with amorphous carbon, before being observed with a Leo 1550 Field-Emission Scanning Electron Microscope.

*Cell Growth Assays.* NIH3T3 cells were plated in each well of a 6-well dish at a density of $10\times10^4$ cells/well and were maintained in DMEM medium containing 2% CS supplemented without or with MVs derived from 5.0 X $10^6$ MDAMB231 cells or U87 cells. Once a day for three days, one set of cultures was collected and counted, while the remaining sets of cells had their culturing medium replenished (including the addition of freshly isolated MVs). The assays were performed three times and the results were averaged together and graphed.

*Anchorage-independent Growth Assays.* Parental NIH3T3 cells or MCF10A cells incubated without or with MVs derived from 5.0 X $10^6$ MDAMB231 cells or U87 cells, or NIH3T3 cells stably overexpressing the vector-control, wild-type tTG, or Cdc42 F28L, were plated at a density of $7\times10^3$ cells/ml in medium containing 0.3% agarose, without or with various inhibitors as indicated, onto underlays composed of growth medium containing 0.6% agarose in six-well dishes. The soft agar cultures were re-fed (including the addition of freshly prepared MVs and treatments with various inhibitors as indicated) every third day for 12 days, at which time the colonies

that formed were counted. Each of the assays was performed at least three times and the results were averaged together and graphed.

*Cell Death Assays.* NIH3T3 cells or MCF10A cells were plated in each well of a 6-well dish and then cultured in medium containing 2% CS or serum-free medium supplemented without or with MVs derived from 5.0 x $10^6$ MDAMB231 cells or U87 cells, and without or with MDC or T101, as indicated. Two days later the cultures were fixed and stained with DAPI for viewing by fluorescence microscopy. Cells undergoing apoptosis were identified by nuclear condensation or blebbing and the percentage of cell death was determined by calculating the ratio of apoptotic to total cells for each condition. These experiments were conducted at least three times and the results from each experiment were averaged together and graphed.

*Flow Cytometry.* Intact MVs were isolated from the conditioned medium of 5.0 x $10^6$ mock transfected MDAMB231 cells or MDAMB231 cells transiently expressing GFP using the filter method (described above) and re-suspended in PBS containing 0.1% BSA. The MV samples were evaluated using a BD LSR II flow cytometer by gating events that were between ~1-3 μm in size and determining whether they expressed GFP. At least 500 events were collected for each sample and then the data was analyzed using BD FACSDiva software. The experiments were performed at least three times, with similar results being obtained from each experiment.

*Proteomic Analyses.* Lysates of MDAMB231 cell- and U87 cell-derived MVs (~30 μg of each sample) were resolved by SDS-PAGE and then stained using the Colloidal Blue Staining Kit (Invitrogen) according to the manufacturer's protocol. The proteins were excised from the gel and then digested with trypsin. The resulting protein samples were analyzed at Cornell Proteomic Facility using a 4000 Q Trap (Triple quadrupole linear ion trap) On-line LC/MS/MS system (Applied Biosystems/MDS Sciex) or Synapt HDMS system (Waters). Protein identification was achieved by performing peptide alignment searches against the NCBI refseq protein database.

*Mouse Studies.* 5 x $10^5$ mitotically arrested (using mitomycin-C) MDAMB231 cells stably expressing control or tTG siRNAs were combined with 5 x $10^5$ NIH3T3 fibroblasts and growth factor-reduced Matrigel (BD Biosciences) to achieve 30% Matrigel in the final solution. The cell preparations were subcutaneously injected into the flanks of 6-8 weeks-old female NIH-III nude mice. As controls, parental MDAMB231 cells and NIH3T3 cells (5 x $10^5$ cells of each cell line) were singly combined with growth factor-reduced Matrigel (to a final concentration of 30% Matrigel) and then were injected into mice as well. After a month, the animals were sacrificed and the resulting tumors that formed for each experimental condition were excised and counted. The experiments involving mice were performed in accordance with the protocols approved by The Cornell Center for Animal Resources and Education (CARE).

## APPENDIX

The following table listed all the proteins identified from MDAMB231 cell- or U87 cell-derived microvesicles by proteomic analysis as described in the "materials and methods" section. As referred to each column, "Access No." presents the accession number of each identified protein in the NCBI Genebank. "Protein Name" and "MW/Da" are the name and molecular weight (as a unit of Dalton) of identified proteins. "Score" is the evaluation score of each protein hit given by Mass spectrometry, and "Matches" are the numbers of identified peptides for each protein. The order of protein list is arranged based on their evaluation score, and the item of "transglutaminase 2 isoform a" is highlighted in bold.

| Access No. | Protein Name | MW/Da | Score | Matches |
|---|---|---|---|---|
| | **[MDAMB231 cell-derived Microvesicles]** | | | |
| gi\|16933542 | fibronectin 1 isoform 3 preproprotein | 259063 | 3278 | 130 |
| gi\|4501887 | actin, gamma 1 propeptide | 41766 | 3152 | 121 |
| gi\|37138 | unnamed protein product | 129330 | 2990 | 126 |
| gi\|5031863 | galectin 3 binding protein | 65289 | 1891 | 74 |
| gi\|4501881 | actin, alpha 1, skeletal muscle | 42024 | 1765 | 83 |
| gi\|41872631 | fatty acid synthase | 273254 | 1527 | 83 |
| gi\|5174735 | tubulin, beta, 2 | 49799 | 1508 | 76 |
| gi\|340021 | alpha-tubulin | 50120 | 1372 | 53 |
| gi\|11602963 | heparan sulfate proteoglycan perlecan | 466304 | 1364 | 67 |
| gi\|14389309 | tubulin alpha 6 | 49863 | 1301 | 50 |
| gi\|33350932 | dynein, cytoplasmic, heavy polypeptide 1 | 532072 | 1285 | 99 |
| gi\|35505 | pyruvate kinase | 57841 | 1140 | 48 |
| gi\|32097 | unnamed protein product | 11260 | 1041 | 35 |
| gi\|88191913 | Chain A, Crystal Structure Of The Thrombospondin-1 N-Terminal Domain | 23554 | 1037 | 50 |
| gi\|223582 | histone H4 | 11230 | 957 | 28 |
| gi\|4758012 | clathrin heavy chain 1 | 191493 | 941 | 48 |
| gi\|18645167 | Annexin A2 | 38552 | 906 | 32 |
| gi\|31092 | unnamed protein product | 50095 | 851 | 46 |
| gi\|306891 | 90kDa heat shock protein | 83242 | 833 | 38 |
| gi\|31979 | histone H2A.2 | 13898 | 722 | 20 |
| gi\|1568551 | histone H2B | 13928 | 691 | 20 |
| gi\|6005942 | valosin-containing protein | 89266 | 594 | 41 |
| gi\|5729877 | heat shock 70kDa protein 8 isoform 1 | 70854 | 555 | 28 |
| gi\|21361181 | Na+/K+ -ATPase alpha 1 subunit isoform a proprotein | 112824 | 553 | 19 |

| | | | | |
|---|---|---|---|---|
| gi\|671527 | gamma subunit of CCT chaperonin | 60292 | 538 | 24 |
| gi\|31645 | glyceraldehyde-3-phosphate dehydrogenase | 36031 | 536 | 17 |
| gi\|4502101 | annexin I | 38690 | 534 | 14 |
| gi\|340062 | pro-ubiquitin | 17434 | 527 | 16 |
| gi\|4503483 | eukaryotic translation elongation factor 2 | 95277 | 517 | 33 |
| gi\|4503571 | enolase 1 | 47139 | 516 | 17 |
| gi\|2804273 | alpha actinin 4 | 102204 | 511 | 22 |
| gi\|32111 | unnamed protein product | 14164 | 509 | 16 |
| gi\|4503481 | eukaryotic translation elongation factor 1 gamma | 50087 | 498 | 21 |
| gi\|61656603 | Heat shock protein HSP 90-alpha 2 | 98052 | 488 | 25 |
| gi\|10800144 | histone cluster 1, H2aj | 13928 | 480 | 17 |
| gi\|35830 | ubiquitin activating enzyme E1 | 117715 | 479 | 16 |
| gi\|115206 | C-1-tetrahydrofolate synthase, cytoplasmic (C1-THF synthase) | 101495 | 452 | 18 |
| gi\|5174447 | guanine nucleotide binding protein (G protein), beta polypeptide 2-like 1 | 35055 | 448 | 14 |
| gi\|4092054 | GTP binding protein | 24440 | 440 | 15 |
| gi\|1136741 | KIAA0002 | 58465 | 440 | 17 |
| gi\|2988422 | agrin precursor | 212745 | 438 | 23 |
| gi\|4505763 | phosphoglycerate kinase 1 | 44586 | 433 | 13 |
| gi\|687239 | tumor necrosis factor type 1 receptor associated protein | 93863 | 412 | 18 |
| gi\|55770868 | tubulin, beta polypeptide 4, member Q | 48456 | 397 | 19 |
| gi\|1431788 | Chain A, Determination Of The Nmr Solution Structure Of The Cyclophilin A-Cyclosporin A Complex | 17981 | 395 | 11 |
| gi\|603074 | ATP:citrate lyase | 120748 | 386 | 19 |
| gi\|220141 | VLA-3 alpha subunit | 113433 | 385 | 25 |
| gi\|38455427 | chaperonin containing TCP1, subunit 4 (delta) | 57888 | 374 | 13 |
| gi\|6273399 | melanoma-associated antigen MG50 | 167105 | 371 | 15 |
| gi\|1346343 | Keratin, type II cytoskeletal 1 (Cytokeratin-1) (CK-1) (Keratin-1) (K1) (67 kDa cytokeratin) (Hair alpha protein) | 65978 | 368 | 17 |
| gi\|112911 | Alpha-2-macroglobulin precursor (Alpha-2-M) (C3 and PZP-like alpha-2-macroglobulin domain-containing protein 5) | 163175 | 364 | 20 |
| gi\|61744475 | solute carrier family 3 (activators of dibasic and neutral amino acid transport), member 2 isoform a | 71079 | 361 | 21 |
| gi\|28243 | unnamed protein product | 280586 | 358 | 17 |
| gi\|12667788 | myosin, heavy polypeptide 9, non-muscle | 226392 | 352 | 22 |
| gi\|21410823 | EGF-like repeats and discoidin I-like domains 3 | 53760 | 350 | 18 |
| gi\|356168 | histone H1b | 21721 | 347 | 14 |
| gi\|119625804 | moesin, isoform CRA_b | 66564 | 336 | 16 |
| gi\|31545 | valyl-tRNA synthetase | 140367 | 335 | 17 |
| gi\|19743813 | integrin beta 1 isoform 1A precursor | 88357 | 335 | 14 |

| | | | | |
|---|---|---|---|---|
| gi\|2506545 | 78 kDa glucose-regulated protein precursor (GRP 78) (Heat shock 70 kDa protein 5) (Immunoglobulin heavy chain-binding protein) (BiP) | 72377 | 329 | 17 |
| gi\|62089222 | heat shock 70kDa protein 1A variant | 77448 | 329 | 15 |
| gi\|4505467 | 5~ nucleotidase, ecto | 63327 | 327 | 12 |
| gi\|32358 | hnRNP U protein | 88890 | 316 | 8 |
| gi\|547754 | Keratin, type II cytoskeletal 2 epidermal (Cytokeratin-2e) (CK 2e) (K2e) (keratin-2) | 65825 | 313 | 13 |
| gi\|122920512 | Chain A, Human Serum Albumin Complexed With Myristate And Aspirin | 66412 | 310 | 15 |
| gi\|45439306 | aspartyl-tRNA synthetase | 57100 | 299 | 16 |
| gi\|122138 | HLA class I histocompatibility antigen, A-2 alpha chain precursor (MHC class I antigen A*2) | 40896 | 298 | 13 |
| gi\|4588526 | nuclear chloride channel | 26907 | 296 | 11 |
| gi\|20147503 | laminin alpha5 chain precursor | 399390 | 287 | 25 |
| gi\|2656092 | proteasome subunit p58 | 60968 | 286 | 15 |
| gi\|119606902 | phosphofructokinase, platelet, isoform CRA_b | 84001 | 284 | 15 |
| gi\|575249 | lymphocyte antigen | 40924 | 272 | 12 |
| gi\|34234 | laminin-binding protein | 31774 | 269 | 7 |
| gi\|13606056 | DNA dependent protein kinase catalytic subunit | 465266 | 266 | 22 |
| gi\|3282771 | actin-binding protein homolog ABP-278 | 278018 | 262 | 19 |
| gi\|93141047 | collagen, type XII, alpha 1 long isoform precursor | 332941 | 261 | 18 |
| gi\|809185 | Chain A, The Effect Of Metal Binding On The Structure Of Annexin V And Implications For Membrane Binding | 35783 | 256 | 14 |
| gi\|47775861 | MHC class I antigen | 34120 | 241 | 10 |
| gi\|179100 | asparagine synthetase | 64389 | 238 | 13 |
| gi\|4506607 | ribosomal protein L18 | 21621 | 237 | 7 |
| gi\|4503841 | ATP-dependent DNA helicase II, 70 kDa subunit | 69799 | 235 | 12 |
| gi\|11276938 | hypothetical protein DKFZp762H157.1 - human (fragment) | 73890 | 233 | 10 |
| gi\|5730023 | RuvB-like 2 | 51125 | 232 | 10 |
| gi\|4506667 | ribosomal protein P0 | 34252 | 227 | 6 |
| gi\|4506671 | ribosomal protein P2 | 11658 | 224 | 5 |
| gi\|126369 | Laminin subunit gamma-1 precursor (Laminin B2 chain) | 177492 | 222 | 10 |
| gi\|4503529 | eukaryotic translation initiation factor 4A isoform 1 | 46125 | 217 | 10 |
| gi\|1228049 | multifunctional protein CAD | 242762 | 214 | 14 |
| gi\|532313 | NF45 protein | 44669 | 214 | 6 |
| gi\|62088648 | tumor rejection antigen (gp96) 1 variant | 65912 | 213 | 8 |
| gi\|38638698 | KIAA1199 | 152900 | 207 | 15 |
| gi\|178277 | S-adenosylhomocysteine hydrolase | 47684 | 205 | 8 |
| gi\|2150046 | 26S proteasome subunit 9 | 47418 | 204 | 9 |
| **gi\|39777597** | **transglutaminase 2 isoform a** | **77280** | **198** | **15** |

| | | | | |
|---|---|---|---|---|
| gi\|1050527 | seryl-tRNA synthetase | 58713 | 197 | 11 |
| gi\|4506753 | RuvB-like 1 | 50196 | 193 | 8 |
| gi\|493066 | glycyl-tRNA synthetase | 77463 | 188 | 5 |
| gi\|306553 | ribosmal protein small subunit | 29980 | 187 | 7 |
| gi\|4504255 | H2A histone family, member Z | 13545 | 186 | 9 |
| gi\|30851181 | FER1L3 protein | 179438 | 185 | 9 |
| gi\|339880 | tripeptidyl peptidase II | 138362 | 185 | 9 |
| gi\|4826898 | profilin 1 | 15045 | 183 | 7 |
| gi\|183182 | guanine nucleotide-binding regulatory protein alpha-inhibitory subunit | 40437 | 183 | 5 |
| gi\|339834 | plasminogen activator | 62863 | 180 | 7 |
| gi\|2506380 | Lactadherin precursor (Milk fat globule-EGF factor 8) (MFG-E8) (HMFG) (Breast epithelial antigen BA46) (MFGM) | 43095 | 178 | 8 |
| gi\|5031857 | lactate dehydrogenase A | 36665 | 178 | 9 |
| gi\|7765076 | S3 ribosomal protein | 26699 | 177 | 9 |
| gi\|5032051 | ribosomal protein S14 | 16263 | 176 | 3 |
| gi\|7661914 | proteasome (prosome, macropain) 26S subunit, non-ATPase, 6 | 45502 | 172 | 8 |
| gi\|4504299 | histone cluster 3, H3 | 15499 | 170 | 14 |
| gi\|25777600 | proteasome 26S non-ATPase subunit 1 | 105769 | 170 | 13 |
| gi\|4506179 | proteasome alpha 1 subunit isoform 2 | 29537 | 168 | 5 |
| gi\|971270 | proteasome subunit p40 / Mov34 protein | 37037 | 166 | 4 |
| gi\|4506209 | proteasome 26S ATPase subunit 2 | 48603 | 165 | 10 |
| gi\|10863945 | ATP-dependent DNA helicase II | 82652 | 163 | 15 |
| gi\|4506743 | ribosomal protein S8 | 24190 | 161 | 4 |
| gi\|21361144 | proteasome 26S ATPase subunit 3 | 49172 | 161 | 9 |
| gi\|4505893 | proteolipid protein 2 (colonic epithelium-enriched) | 16680 | 161 | 3 |
| gi\|4502643 | chaperonin containing TCP1, subunit 6A isoform a | 57988 | 159 | 10 |
| gi\|1806048 | nuclear DNA helicase II | 140788 | 159 | 10 |
| gi\|4507467 | transforming growth factor, beta-induced, 68kDa precursor | 74634 | 158 | 4 |
| gi\|1526426 | proteasome subunit p42 | 44133 | 158 | 8 |
| gi\|1702932 | yeast methionyl-tRNA synthetase homolog | 101065 | 156 | 8 |
| gi\|4092058 | proteasome subunit HSPC | 27886 | 154 | 5 |
| gi\|6005882 | protease, serine, 23 precursor | 42974 | 154 | 10 |
| gi\|1705996 | Coatomer subunit alpha (Alpha-coat protein) (Alpha-COP) (HEP-COP) (HEPCOP) | 138244 | 153 | 13 |
| gi\|7705433 | eukaryotic translation initiation factor 3 subunit 6 interacting protein | 66684 | 153 | 5 |
| gi\|4504981 | beta-galactoside-binding lectin precursor | 14706 | 151 | 7 |
| gi\|31952 | unnamed protein product | 45623 | 150 | 5 |
| gi\|28317 | unnamed protein product | 59492 | 149 | 9 |
| gi\|4505011 | lysyl oxidase-like 2 precursor | 86668 | 147 | 9 |
| gi\|14591909 | ribosomal protein L5 | 34341 | 146 | 6 |
| gi\|976227 | 26S proteasome subunit p45 | 45624 | 145 | 5 |
| gi\|11559929 | coatomer protein complex, subunit gamma 1 | 97655 | 145 | 5 |

| | | | | |
|---|---|---|---|---|
| gi\|3493529 | histone macroH2A1.2 | 39576 | 144 | 5 |
| gi\|403456 | 26S protease (S4) regulatory subunit | 49155 | 139 | 5 |
| gi\|19070472 | p600 | 573536 | 138 | 9 |
| gi\|5106785 | HSPC027 | 42644 | 137 | 5 |
| gi\|190281 | protein phosphatase I alpha subunit (PPPIA) | 35103 | 136 | 6 |
| gi\|5453603 | chaperonin containing TCP1, subunit 2 | 57452 | 134 | 11 |
| gi\|15431301 | ribosomal protein L7 | 29207 | 133 | 9 |
| gi\|11545918 | tubulointerstitial nephritis antigen-like 1 | 52353 | 131 | 3 |
| gi\|4503519 | eukaryotic translation initiation factor 3, subunit 5 epsilon, 47kDa | 37540 | 131 | 4 |
| gi\|292059 | MTHSP75 | 73734 | 131 | 4 |
| gi\|37433 | unnamed protein product | 84848 | 130 | 6 |
| gi\|74709215 | Histone H2B type 2-C (H2.t) (H2B/t) | 21458 | 130 | 4 |
| gi\|6739602 | talin | 269486 | 129 | 11 |
| gi\|234746 | RAS-related protein MEL | 23582 | 129 | 4 |
| gi\|38014351 | EEF1D protein | 60845 | 128 | 4 |
| gi\|28614 | aldolase A | 39307 | 126 | 6 |
| gi\|33942 | integrin alpha6 subunit | 118824 | 125 | 4 |
| gi\|2736256 | aflatoxin aldehyde reductase AFAR | 36625 | 125 | 3 |
| gi\|999892 | Chain A, Crystal Structure Of Recombinant Human Triosephosphate Isomerase | 26522 | 124 | 4 |
| gi\|5031635 | cofilin 1 (non-muscle) | 18491 | 123 | 3 |
| gi\|4758648 | kinesin family member 5B | 109617 | 121 | 7 |
| gi\|460789 | transformation upregulated nuclear protein | 51040 | 120 | 4 |
| gi\|6424942 | ALG-2 interacting protein 1 | 96019 | 119 | 6 |
| gi\|124942 | Integrin alpha-2 precursor (Platelet membrane glycoprotein Ia) (GPIa) (Collagen receptor) (VLA-2 alpha chain) (CD49 antigen-like family member B) (CD49b antigen) | 129214 | 117 | 7 |
| gi\|440799 | isoleucyl-tRNA synthetase | 144388 | 116 | 13 |
| gi\|2529707 | Hpast | 60665 | 114 | 7 |
| gi\|1082300 | collagen alpha 1(XVIII) chain - human (fragment) | 70325 | 114 | 5 |
| gi\|13325075 | quiescin Q6 sulfhydryl oxidase 1 isoform a | 82526 | 114 | 7 |
| gi\|119616219 | adaptor-related protein complex 3, beta 1 subunit, isoform CRA_c | 68368 | 113 | 3 |
| gi\|126366 | Laminin subunit beta-1 precursor (Laminin B1 chain) | 197937 | 111 | 10 |
| gi\|7513316 | ribosomal protein L14 | 23788 | 108 | 4 |
| gi\|5031755 | heterogeneous nuclear ribonucleoprotein R isoform 2 | 70899 | 108 | 3 |
| gi\|36796 | t-complex polypeptide 1 | 60356 | 108 | 10 |
| gi\|4335941 | leucine aminopeptidase | 56014 | 108 | 6 |
| gi\|125333 | Ephrin type-A receptor 2 precursor (Tyrosine-protein kinase receptor ECK) (Epithelial cell kinase) | 108185 | 108 | 4 |
| gi\|8394076 | proteasome (prosome, macropain) subunit, alpha type 6 [Rattus norvegicus] | 27382 | 107 | 2 |
| gi\|182516 | ferritin light subunit | 16384 | 107 | 4 |

| | | | | |
|---|---|---|---|---|
| gi\|4506597 | ribosomal protein L12 | 17808 | 106 | 3 |
| gi\|951338 | CAS | 110244 | 106 | 11 |
| gi\|1174149 | small GTP binding protein Rab7 | 23447 | 106 | 4 |
| gi\|31958 | glutaminyl-tRNA synthetase | 162923 | 105 | 5 |
| gi\|662841 | heat shock protein 27 | 22313 | 105 | 4 |
| gi\|4507953 | tyrosine 3/tryptophan 5 -monooxygenase activation protein, zeta polypeptide | 27728 | 104 | 5 |
| gi\|33055 | unnamed protein product | 274133 | 104 | 5 |
| gi\|15341931 | Lysyl oxidase-like 4 | 84327 | 104 | 2 |
| gi\|1478281 | neutral amino acid transporter B | 56585 | 103 | 6 |
| gi\|4506017 | protein phosphatase 2, catalytic subunit, alpha isoform | 35571 | 103 | 3 |
| gi\|183303 | glucose transporter glycoprotein | 54083 | 102 | 8 |
| gi\|339992 | tumor necrosis factor | 41975 | 101 | 6 |
| gi\|2696613 | ATP-dependent RNA helicase #46 | 92770 | 101 | 4 |
| gi\|5031573 | ARP3 actin-related protein 3 homolog | 47341 | 101 | 5 |
| gi\|5453595 | adenylyl cyclase-associated protein | 51641 | 100 | 6 |
| gi\|42716297 | clusterin isoform 1 | 57796 | 100 | 7 |
| gi\|1778051 | Prt1 homolog | 98820 | 100 | 5 |
| gi\|4557032 | lactate dehydrogenase B | 36615 | 99 | 4 |
| gi\|38202255 | threonyl-tRNA synthetase | 83382 | 99 | 9 |
| gi\|4506631 | ribosomal protein L30 | 12776 | 99 | 2 |
| gi\|190074 | lysyl hydroxylase | 83527 | 98 | 5 |
| gi\|9802306 | DNA-binding protein TAXREB107 | 32871 | 97 | 5 |
| gi\|32449796 | EIF3A protein | 96804 | 97 | 11 |
| gi\|3088342 | ribosomal protein S23 | 6465 | 97 | 2 |
| gi\|4506141 | HtrA serine peptidase 1 precursor | 51255 | 97 | 5 |
| gi\|1040689 | Human Diff6,H5,CDC10 homologue | 46556 | 96 | 2 |
| gi\|28395033 | ras homolog gene family, member C precursor | 21992 | 95 | 2 |
| gi\|306875 | C protein | 31947 | 95 | 4 |
| gi\|183353 | glycogen phosphorylase | 97161 | 94 | 3 |
| gi\|4506691 | ribosomal protein S16 | 16435 | 94 | 5 |
| gi\|550021 | ribosomal protein S5 | 22763 | 93 | 2 |
| gi\|4758756 | nucleosome assembly protein 1-like 1 | 45346 | 93 | 2 |
| gi\|7243085 | KIAA1352 protein | 138273 | 92 | 10 |
| gi\|119611239 | ATPase, Na+/K+ transporting, beta 1 polypeptide, isoform CRA_b | 22414 | 91 | 3 |
| gi\|14495609 | CTP synthase | 66674 | 91 | 4 |
| gi\|119625894 | phosphoribosylaminoimidazole carboxylase, phosphoribosylaminoimidazole succinocarboxamide synthetase, isoform CRA_a | 49648 | 90 | 3 |
| gi\|6006515 | spliceosomal protein SAP 130 | 135507 | 89 | 4 |
| gi\|703093 | serine hydroxymethyltransferase | 52429 | 89 | 5 |
| gi\|23398 | 1-8U | 14581 | 88 | 1 |
| gi\|5257007 | beta-cop homolog | 107071 | 88 | 6 |
| gi\|3420181 | WDR1 protein | 57966 | 87 | 5 |
| gi\|5453607 | chaperonin containing TCP1, subunit 7 | 59329 | 87 | 10 |

| | | | | |
|---|---|---|---|---|
| | isoform a | | | |
| gi\|4506183 | proteasome alpha 3 subunit isoform 1 | 28415 | 87 | 4 |
| gi\|87196339 | collagen, type VI, alpha 1 precursor | 108462 | 87 | 5 |
| gi\|181914 | DNA-binding protein | 35801 | 86 | 5 |
| gi\|4506661 | ribosomal protein L7a | 29977 | 84 | 3 |
| gi\|4759160 | small nuclear ribonucleoprotein polypeptide D3 | 13907 | 84 | 4 |
| gi\|6042196 | cathepsin F | 53332 | 84 | 4 |
| gi\|37227 | tenascin | 240565 | 83 | 4 |
| gi\|6678271 | TAR DNA binding protein | 44711 | 83 | 2 |
| gi\|12804225 | Unknown (protein for IMAGE:3543711) | 59431 | 80 | 6 |
| gi\|5803225 | tyrosine 3/tryptophan 5 -monooxygenase activation protein, epsilon polypeptide | 29155 | 80 | 2 |
| gi\|181387 | cystatin C | 15819 | 77 | 2 |
| gi\|56203471 | histone cluster 2, H3, pseudogene 2 | 15421 | 77 | 10 |
| gi\|1477646 | plectin | 518173 | 77 | 14 |
| gi\|7023053 | unnamed protein product | 40297 | 77 | 4 |
| gi\|119618541 | hCG2016250, isoform CRA_j | 28191 | 76 | 6 |
| gi\|4759158 | small nuclear ribonucleoprotein polypeptide D2 | 13518 | 76 | 2 |
| gi\|37267 | transketolase | 67751 | 76 | 3 |
| gi\|32189394 | ATP synthase, H+ transporting, mitochondrial F1 complex, beta subunit precursor | 56525 | 75 | 6 |
| gi\|8886884 | platelet-derived growth factor C | 39019 | 75 | 1 |
| gi\|183008 | glucocerebrosidase precursor | 57399 | 75 | 1 |
| gi\|6808243 | hypothetical protein | 78295 | 75 | 3 |
| gi\|381964 | actin-related protein | 42545 | 75 | 6 |
| gi\|208115 | p21 protein | 21327 | 74 | 3 |
| gi\|4506221 | proteasome 26S non-ATPase subunit 12 | 52871 | 74 | 4 |
| gi\|307200 | brain glycogen phosphorylase | 98891 | 73 | 3 |
| gi\|219588 | DnaJ protein homolog | 44848 | 73 | 2 |
| gi\|11610605 | testis-specific poly(A)-binding protein | 70072 | 73 | 3 |
| gi\|4503523 | eukaryotic translation initiation factor 3 subunit D | 63932 | 73 | 4 |
| gi\|18379349 | vesicle amine transport protein 1 | 41893 | 72 | 8 |
| gi\|4680691 | CGI-26 protein | 36955 | 72 | 1 |
| gi\|1657268 | aminopeptidase | 98467 | 72 | 2 |
| gi\|5031977 | nicotinamide phosphoribosyltransferase precursor | 55487 | 71 | 2 |
| gi\|5453998 | importin 7 | 119440 | 71 | 3 |
| gi\|4503143 | cathepsin D preproprotein | 44524 | 70 | 9 |
| gi\|449441 | UDP-glucose pyrophosphorylase | 56914 | 70 | 1 |
| gi\|4506185 | proteasome alpha 4 subunit isoform 1 | 29465 | 70 | 2 |
| gi\|494066 | Chain A, Three-Dimensional Structure Of Class Pi Glutathione S- Transferase From Human Placenta In Complex With S-Hexylglutathione At 2.8 Angstroms Resolution | 23210 | 70 | 1 |
| gi\|10835165 | CD59 antigen preproprotein | 14168 | 70 | 3 |
| gi\|1419567 | dynactin | 139873 | 69 | 4 |

| | | | | |
|---|---|---|---|---|
| gi\|2624694 | Chain A, Human Mitochondrial Single-Stranded Dna Binding Protein | 15186 | 69 | 3 |
| gi\|4506613 | ribosomal protein L22 proprotein | 14778 | 69 | 1 |
| gi\|78070384 | CDC2 protein | 25923 | 69 | 5 |
| gi\|119599627 | hCG1646871 | 29121 | 69 | 4 |
| gi\|20146101 | EMMPRIN | 29134 | 69 | 3 |
| gi\|7212811 | EH domain containing 4 | 54530 | 68 | 1 |
| gi\|5107666 | Chain A, Structure Of Importin Beta Bound To The Ibb Domain Of Importin Alpha | 97172 | 68 | 5 |
| gi\|183709 | small G protein | 20214 | 68 | 3 |
| gi\|2209347 | p21-Arc | 20502 | 68 | 2 |
| gi\|21706696 | Calsyntenin 1 | 108601 | 68 | 2 |
| gi\|226021 | growth regulated nuclear 68 protein | 66881 | 68 | 3 |
| gi\|4504975 | low density lipoprotein receptor precursor | 95314 | 67 | 3 |
| gi\|4503981 | glucosamine-fructose-6-phosphate aminotransferase | 76698 | 67 | 3 |
| gi\|1346766 | 26S proteasome non-ATPase regulatory subunit 8 (26S proteasome regulatory subunit S14) (p31) | 29986 | 67 | 3 |
| gi\|462190 | Glypican-1 precursor [Contains: Secreted glypican-1] | 61611 | 67 | 2 |
| gi\|62511242 | 4-trimethylaminobutyraldehyde dehydrogenase (TMABADH) (Aldehyde dehydrogenase family 9 member A1) (Aldehyde dehydrogenase E3 isozyme) | 53767 | 67 | 3 |
| gi\|35218 | unnamed protein product | 75812 | 66 | 8 |
| gi\|4757944 | CD81 antigen | 25792 | 66 | 2 |
| gi\|2852617 | unknown | 12012 | 66 | 2 |
| gi\|4506787 | IQ motif containing GTPase activating protein 1 | 189134 | 66 | 4 |
| gi\|1931584 | eIF-3 p110 subunit | 105276 | 66 | 7 |
| gi\|5031931 | nascent polypeptide-associated complex alpha subunit isoform b | 23370 | 66 | 1 |
| gi\|6648067 | Malate dehydrogenase, mitochondrial precursor | 35509 | 66 | 2 |
| gi\|5031595 | actin related protein 2/3 complex subunit 4 isoform a | 19654 | 66 | 4 |
| gi\|9624998 | heterogeneous nuclear ribonucleoprotein H2 | 49232 | 65 | 2 |
| gi\|440177 | flightless-I homolog | 144528 | 65 | 2 |
| gi\|1217668 | arginyl-tRNA synthetase; ArgRS | 74930 | 65 | 4 |
| gi\|2791898 | CYR61 protein | 41997 | 65 | 7 |
| gi\|1699163 | ETX1 | 49901 | 64 | 2 |
| gi\|56203429 | copine I | 33831 | 64 | 3 |
| gi\|495126 | ribosomal protein L11 | 20103 | 64 | 1 |
| gi\|181486 | DNA-binding protein B | 39954 | 64 | 1 |
| gi\|550023 | ribosomal protein S9 | 22558 | 64 | 3 |
| gi\|45751608 | Myosin IC | 117876 | 64 | 6 |
| gi\|4505753 | phosphoglycerate mutase 1 (brain) | 28786 | 64 | 2 |
| gi\|306506 | antigen CD9 | 3227 | 64 | 1 |
| gi\|4506439 | retinoblastoma binding protein 7 | 47790 | 63 | 3 |

| | | | | |
|---|---|---|---|---|
| gi\|4261795 | eukaryotic initiation factor 5A | 16790 | 61 | 1 |
| gi\|12585547 | Tripartite motif-containing protein 25 (Zinc finger protein 147) (Estrogen-responsive finger protein) (Efp) (RING finger protein 147) | 70944 | 61 | 1 |
| gi\|4506605 | ribosomal protein L23 | 14856 | 60 | 1 |
| gi\|496902 | translation initiation factor | 46803 | 60 | 3 |
| gi\|3088338 | ribosomal protein S10 | 9429 | 60 | 2 |
| gi\|40789067 | KIAA0010 | 124156 | 60 | 3 |
| gi\|17986258 | myosin, light chain 6, alkali, smooth muscle and non-muscle isoform 1 | 16919 | 59 | 4 |
| gi\|23503239 | aldehyde dehydrogenase 16 family, member A1 | 85060 | 59 | 3 |
| gi\|1710248 | protein disulfide isomerase-related protein 5 | 46170 | 59 | 1 |
| gi\|119575878 | hCG37513, isoform CRA_a | 15044 | 58 | 2 |
| gi\|34412 | unnamed protein product | 78029 | 58 | 2 |
| gi\|119592221 | ribosomal protein S4, X-linked, isoform CRA_a | 43436 | 58 | 4 |
| gi\|31147 | PAI precursor polypeptide | 44973 | 58 | 6 |
| gi\|4506681 | ribosomal protein S11 | 18419 | 58 | 2 |
| gi\|4506181 | proteasome alpha 2 subunit | 25882 | 58 | 3 |
| gi\|40675522 | ARCN1 protein | 21840 | 58 | 4 |
| gi\|148225456 | hypothetical protein LOC644928 | 12969 | 57 | 2 |
| gi\|340368 | transfer RNA-Trp synthetase | 53054 | 57 | 1 |
| gi\|4758256 | eukaryotic translation initiation factor 2, subunit 1 alpha, 35kDa | 36089 | 56 | 1 |
| gi\|30173225 | Structural maintenance of chromosomes protein 2 (Chromosome-associated protein E) (hCAP-E) (XCAP-E homolog) | 135696 | 56 | 5 |
| gi\|577295 | KIAA0088 | 106702 | 56 | 3 |
| gi\|340219 | vimentin | 53681 | 56 | 4 |
| gi\|20521848 | KIAA0219 | 292956 | 56 | 6 |
| gi\|36142 | ribosomal protein homologous to yeast S24 | 14707 | 56 | 11 |
| gi\|2224677 | KIAA0368 | 159376 | 56 | 4 |
| gi\|307066 | inosine-5~-monophosphate dehydrogenase | 55885 | 56 | 3 |
| gi\|307110 | lysosomal membrane glycoprotein-2 | 44804 | 56 | 1 |
| gi\|19923903 | myeloid-associated differentiation marker | 35250 | 56 | 2 |
| gi\|14042058 | unnamed protein product | 100221 | 56 | 3 |
| gi\|62087228 | 3-mercaptopyruvate sulfurtransferase variant | 34730 | 56 | 2 |
| gi\|337514 | ribosomal protein S6 | 28614 | 55 | 4 |
| gi\|763130 | YPT3 | 24559 | 55 | 2 |
| gi\|4759300 | vesicle-associated membrane protein 3 | 11302 | 55 | 1 |
| gi\|4506697 | ribosomal protein S20 | 13364 | 55 | 2 |
| gi\|296734 | macropain subunit delta | 19362 | 55 | 2 |
| gi\|4506707 | ribosomal protein S25 | 13734 | 54 | 1 |
| gi\|4826878 | oxidative-stress responsive 1 | 57986 | 54 | 1 |
| gi\|263099 | Tat binding protein 7, TBP-7-transcriptional activator | 51519 | 53 | 3 |
| gi\|4503507 | eukaryotic translation initiation factor 2, subunit 3 gamma | 51077 | 53 | 3 |

| | | | | |
|---|---|---|---|---|
| gi\|119581148 | keratin 9 (epidermolytic palmoplantar keratoderma) | 57526 | 53 | 5 |
| gi\|1666075 | ubiquitin hydrolase | 289438 | 53 | 4 |
| gi\|4504897 | karyopherin alpha 2 | 57826 | 52 | 3 |
| gi\|531202 | spermidine synthase | 33790 | 52 | 1 |
| gi\|13172664 | hemidesmosomal tetraspanin CD151 | 28294 | 52 | 3 |
| gi\|7023260 | unnamed protein product | 48659 | 52 | 1 |
| gi\|438069 | thiol-specific antioxidant protein | 21843 | 52 | 2 |
| gi\|110171861 | decay-accelerating factor splicing variant 1 | 48482 | 51 | 2 |
| gi\|119609715 | integrin, beta 4, isoform CRA_d | 107154 | 51 | 3 |
| gi\|62897071 | oxygen regulated protein precursor variant | 111210 | 51 | 2 |
| gi\|4506625 | ribosomal protein L27a | 16551 | 51 | 2 |
| gi\|799177 | 100 kDa coactivator | 99628 | 50 | 3 |
| gi\|62897675 | ribosomal protein L4 variant | 47688 | 50 | 1 |
| gi\|119628884 | heat shock 105kDa/110kDa protein 1, isoform CRA_b | 97398 | 49 | 3 |
| gi\|542850 | heterogeneous nuclear ribonucleoprotein G - human | 47419 | 48 | 1 |
| gi\|31189 | unnamed protein product | 23182 | 48 | 1 |
| gi\|35068 | Nm23 protein | 20398 | 48 | 1 |
| gi\|118090 | Peptidyl-prolyl cis-trans isomerase B precursor (PPIase) (Rotamase) (Cyclophilin B) (S-cyclophilin) (SCYLP) (CYP-S1) | 22728 | 48 | 2 |
| gi\|4502171 | adenine phosphoribosyltransferase isoform a | 19595 | 48 | 2 |
| gi\|4758762 | asparaginyl-tRNA synthetase | 62903 | 47 | 2 |
| gi\|33985 | trypsin inhibitor | 106647 | 47 | 2 |
| gi\|458727 | RCK | 53183 | 47 | 1 |
| gi\|2323410 | Skb1Hs | 72740 | 47 | 3 |
| gi\|219510 | collagen alpha 1(V) chain precursor | 183505 | 47 | 2 |
| gi\|56417899 | ARF-binding protein 1 | 481605 | 47 | 2 |
| gi\|4506619 | ribosomal protein L24 | 17768 | 46 | 1 |
| gi\|32528284 | acyl-CoA thioesterase 7 isoform hBACHc | 38966 | 46 | 5 |
| gi\|22477159 | Sec23 homolog A (S. cerevisiae) | 86109 | 46 | 2 |
| gi\|1230564 | Gu protein | 89196 | 46 | 3 |
| gi\|508285 | Rab5c-like protein, similar to Canis familiaris Rab5c protein, PIR Accession Number S38625 | 23553 | 46 | 1 |
| gi\|29446 | unnamed protein product | 15956 | 46 | 1 |
| gi\|1403050 | phosphoenolpyruvate carboxykinase (GTP) | 70539 | 45 | 2 |
| gi\|473583 | DNA topoisomerase I | 90222 | 45 | 2 |
| gi\|83753119 | Chain A, Crystal Structure Of Human Full-Length Vinculin (Residues 1- 1066) | 115928 | 45 | 6 |
| gi\|6841182 | HSPC266 | 43276 | 43 | 2 |
| gi\|5454028 | related RAS viral (r-ras) oncogene homolog | 23466 | 43 | 1 |
| gi\|5803185 | synaptophysin-like 1 isoform a | 28547 | 43 | 1 |
| gi\|36038 | rho GDP dissociation inhibitor (GDI) | 23179 | 43 | 1 |
| gi\|114940 | Beta-galactosidase precursor (Acid beta-galactosidase) (Lactase) (Elastin receptor 1) | 76043 | 43 | 1 |
| gi\|2102696 | karyopherin beta 3 | 123512 | 42 | 3 |

| | | | | |
|---|---|---|---|---|
| gi\|4502281 | Na+/K+ -ATPase beta 3 subunit | 31492 | 41 | 1 |
| gi\|255317 | nuclear autoantigen RA33-A2 hnRNP homolog | 2371 | 41 | 1 |
| gi\|5031571 | actin-related protein 2 isoform b | 44732 | 41 | 7 |
| gi\|4689134 | 60S ribosomal protein L36 | 12227 | 40 | 2 |
| gi\|3288815 | citrate synthase | 51673 | 40 | 1 |
| gi\|4502875 | claudin 3 | 23303 | 40 | 1 |
| gi\|1942609 | Chain A, Human Rap1a, Residues 1-167, Double Mutant (E30d,K31e) Complexed With Gppnhp And The Ras-Binding-Domain Of Human C-Raf1, Residues 51-131 | 19011 | 40 | 2 |
| gi\|2224663 | KIAA0361 | 147958 | 39 | 1 |

**[U87 cell-derived Microvesicles]**

| | | | | |
|---|---|---|---|---|
| gi\|16933542 | fibronectin 1 isoform 3 preproprotein | 259063 | 3136 | 103 |
| gi\|55743098 | alpha 3 type VI collagen isoform 1 precursor | 343457 | 2823 | 118 |
| gi\|68533131 | TNC variant protein | 244248 | 2372 | 81 |
| gi\|1346343 | Keratin, type II cytoskeletal 1 (Cytokeratin-1) (CK-1) (Keratin-1) (K1) (Hair alpha protein) | 65978 | 2020 | 89 |
| gi\|28317 | unnamed protein product | 59492 | 1413 | 76 |
| gi\|55956899 | keratin 9 | 62027 | 1015 | 38 |
| gi\|112911 | Alpha-2-macroglobulin precursor (Alpha-2-M) (C3 and PZP-like alpha-2-macroglobulin domain-containing protein 5) | 163175 | 999 | 36 |
| gi\|4501885 | beta actin | 41710 | 983 | 29 |
| gi\|5031863 | galectin 3 binding protein | 65289 | 771 | 34 |
| gi\|122920512 | Chain A, Human Serum Albumin Complexed With Myristate And Aspirin | 66412 | 692 | 27 |
| gi\|4507467 | transforming growth factor, beta-induced, 68kDa precursor | 74634 | 660 | 22 |
| gi\|29799 | CD44R1 | 53366 | 631 | 20 |
| gi\|31645 | glyceraldehyde-3-phosphate dehydrogenase | 36031 | 586 | 13 |
| gi\|87196339 | collagen, type VI, alpha 1 precursor | 108462 | 578 | 20 |
| gi\|115298678 | complement component 3 precursor | 187030 | 559 | 25 |
| gi\|4501881 | actin, alpha 1, skeletal muscle | 42024 | 540 | 21 |
| gi\|22760207 | unnamed protein product | 96376 | 535 | 21 |
| gi\|7243270 | KIAA1436 protein | 102932 | 502 | 21 |
| gi\|547754 | Keratin, type II cytoskeletal 2 epidermal (Cytokeratin-2e) (CK 2e) (K2e) (keratin-2) | 65825 | 487 | 30 |
| gi\|5729877 | heat shock 70kDa protein 8 isoform 1 | 70854 | 456 | 15 |
| gi\|21361181 | Na+/K+ -ATPase alpha 1 subunit isoform a proprotein | 112824 | 454 | 17 |
| gi\|4503571 | enolase 1 | 47139 | 437 | 13 |
| gi\|4699714 | Chain A, Human Plasminogen Activator Inhibitor Type-1 In Complex With A Pentapeptide | 42800 | 435 | 21 |
| gi\|4505467 | 5~ nucleotidase, ecto | 63327 | 424 | 11 |

| | | | | |
|---|---|---|---|---|
| gi\|19743813 | integrin beta 1 isoform 1A precursor | 88357 | 407 | 18 |
| gi\|220141 | VLA-3 alpha subunit | 113433 | 399 | 19 |
| gi\|35825 | pregnancy zone protein | 163733 | 387 | 19 |
| gi\|1195531 | type I keratin 16; K16 | 51206 | 382 | 22 |
| gi\|12803709 | Keratin 14 (epidermolysis bullosa simplex, Dowling-Meara, Koebner) | 51619 | 373 | 24 |
| gi\|78101267 | Chain A, Human Complement Component C3 | 71146 | 369 | 15 |
| gi\|50080140 | MHC class I antigen | 31497 | 364 | 11 |
| gi\|122138 | HLA class I histocompatibility antigen, A-2 alpha chain precursor (MHC class I antigen A*2) | 40896 | 357 | 11 |
| gi\|4757756 | annexin A2 isoform 2 | 38580 | 335 | 12 |
| gi\|28614 | aldolase A | 39307 | 327 | 10 |
| gi\|180671 | collagenase type IV precursor | 72196 | 321 | 10 |
| gi\|339992 | tumor necrosis factor | 41975 | 316 | 8 |
| gi\|152148396 | MHC class I antigen | 34026 | 310 | 7 |
| gi\|33985 | trypsin inhibitor | 106647 | 300 | 7 |
| gi\|71680364 | Leucine rich repeat containing 15 | 64325 | 296 | 12 |
| gi\|4507265 | stanniocalcin 1 precursor | 27604 | 277 | 4 |
| gi\|5031857 | lactate dehydrogenase A | 36665 | 268 | 11 |
| gi\|126369 | Laminin subunit gamma-1 precursor (Laminin B2 chain) | 177492 | 262 | 8 |
| gi\|306891 | 90kDa heat shock protein | 83242 | 255 | 10 |
| gi\|258295 | C33 antigen | 29610 | 238 | 8 |
| gi\|50284497 | MHC class I antigen | 31623 | 233 | 6 |
| gi\|124942 | Integrin alpha-2 precursor (Platelet membrane glycoprotein Ia) (GPIa) (Collagen receptor) (VLA-2 alpha chain) (CD49 antigen-like family member B) (CD49b antigen) | 129214 | 232 | 9 |
| gi\|229532 | ubiquitin | 8446 | 231 | 9 |
| gi\|32488 | unnamed protein product | 84621 | 225 | 6 |
| gi\|4505763 | phosphoglycerate kinase 1 | 44586 | 220 | 5 |
| gi\|230867 | Chain R, Twinning In Crystals Of Human Skeletal Muscle D- Glyceraldehyde-3-Phosphate Dehydrogenase | 35853 | 215 | 6 |
| gi\|61744475 | solute carrier family 3 (activators of dibasic and neutral amino acid transport), member 2 isoform a | 71079 | 214 | 7 |
| gi\|6005942 | valosin-containing protein | 89266 | 205 | 12 |
| gi\|20146101 | EMMPRIN | 29134 | 204 | 8 |
| gi\|119617032 | keratin 6B, isoform CRA_a | 59874 | 201 | 15 |
| gi\|183182 | guanine nucleotide-binding regulatory protein alpha-inhibitory subunit | 40437 | 193 | 6 |
| gi\|50428530 | MHC class I antigen | 31698 | 192 | 6 |
| gi\|2506545 | 78 kDa glucose-regulated protein precursor (GRP 78) (Heat shock 70 kDa protein 5) (Immunoglobulin heavy chain-binding protein) (BiP) | 72377 | 189 | 9 |
| gi\|4557032 | lactate dehydrogenase B | 36615 | 189 | 5 |
| gi\|4505257 | moesin | 67778 | 185 | 13 |

| | | | | |
|---|---|---|---|---|
| gi\|4502101 | annexin I | 38690 | 170 | 4 |
| gi\|190074 | lysyl hydroxylase | 83527 | 170 | 5 |
| gi\|136066 | Triosephosphate isomerase (TIM) (Triose-phosphate isomerase) | 26609 | 165 | 3 |
| gi\|31438 | unnamed protein product | 114437 | 165 | 7 |
| gi\|16445029 | immunoglobulin superfamily, member 8 | 64994 | 155 | 4 |
| gi\|5031977 | nicotinamide phosphoribosyltransferase precursor | 55487 | 139 | 6 |
| gi\|12274842 | laminin, alpha 5 | 398951 | 139 | 12 |
| gi\|46016221 | MHC class I antigen | 21098 | 137 | 4 |
| gi\|998626 | 85 kda glioma membrane protein/CD44 homolog | 1336 | 135 | 3 |
| gi\|4506141 | HtrA serine peptidase 1 precursor | 51255 | 132 | 7 |
| gi\|183531 | platelet glycoprotein IIIa | 84277 | 130 | 3 |
| gi\|13603394 | type VI collagen alpha 2 chain precursor | 108506 | 127 | 8 |
| gi\|112910 | Alpha-2-HS-glycoprotein precursor (Ba-alpha-2-glycoprotein) (Alpha-2-Z-globulin) (Fetuin-A) | 39300 | 125 | 4 |
| gi\|312137 | fructose bisphosphate aldolase | 39417 | 122 | 3 |
| gi\|553734 | putative | 2212 | 121 | 18 |
| gi\|34412 | unnamed protein product | 78029 | 120 | 4 |
| gi\|4758012 | clathrin heavy chain 1 | 191493 | 108 | 3 |
| gi\|286005 | KIAA0006 | 51586 | 108 | 4 |
| gi\|187387 | myristoylated alanine-rich C-kinase substrate | 31857 | 106 | 3 |
| gi\|5729850 | guanine nucleotide binding protein (G protein), alpha inhibiting activity polypeptide 3 | 40506 | 104 | 2 |
| gi\|4502719 | cadherin 13 preproprotein | 78238 | 102 | 2 |
| gi\|2804273 | alpha actinin 4 | 102204 | 101 | 5 |
| gi\|31189 | unnamed protein product | 23182 | 97 | 2 |
| **gi\|39777597** | **transglutaminase 2 isoform a** | **77280** | **96** | **4** |
| gi\|93141049 | collagen, type XII, alpha 1 short isoform precursor | 205363 | 94 | 5 |
| gi\|908801 | keratin type II | 60163 | 93 | 10 |
| gi\|4504763 | integrin alpha-V precursor | 115978 | 92 | 3 |
| gi\|35505 | pyruvate kinase | 57841 | 91 | 3 |
| gi\|4502049 | aldo-keto reductase family 1, member B1 | 35830 | 89 | 2 |
| gi\|31092 | unnamed protein product | 50095 | 84 | 3 |
| gi\|4502281 | Na+/K+ -ATPase beta 3 subunit | 31492 | 83 | 3 |
| gi\|28334 | unnamed protein product | 102910 | 83 | 4 |
| gi\|4506803 | stem cell growth factor precursor | 35672 | 82 | 4 |
| gi\|31952 | unnamed protein product | 45623 | 82 | 2 |
| gi\|1136741 | KIAA0002 | 58465 | 82 | 2 |
| gi\|30795231 | brain abundant, membrane attached signal protein 1 | 22680 | 81 | 5 |
| gi\|4502107 | annexin 5 | 35914 | 79 | 3 |
| gi\|296736 | macropain subunit iota | 24564 | 74 | 1 |
| gi\|1708865 | Prolow-density lipoprotein receptor-related protein 1 precursor (LRP) (Alpha-2-macroglobulin receptor) (A2MR) | 504245 | 71 | 3 |

| | | | | |
|---|---|---|---|---|
| | (Apolipoprotein E receptor) (APOER) (CD91 antigen) | | | |
| gi\|4507953 | tyrosine 3/tryptophan 5 -monooxygenase activation protein, zeta polypeptide | 27728 | 71 | 2 |
| gi\|126366 | Laminin subunit beta-1 precursor (Laminin B1 chain) | 197937 | 70 | 4 |
| gi\|558526 | proteasome subunit X | 22882 | 70 | 2 |
| gi\|404722 | guanine nucleotide regulatory protein | 44036 | 70 | 2 |
| gi\|21754275 | unnamed protein product | 76396 | 70 | 2 |
| gi\|178855 | apolipoprotein J precursor | 48772 | 69 | 2 |
| gi\|4506183 | proteasome alpha 3 subunit isoform 1 | 28415 | 68 | 1 |
| gi\|4218955 | gamma-filamin | 288721 | 68 | 5 |
| gi\|558528 | proteasome subunit Y | 25299 | 67 | 2 |
| gi\|119593150 | filamin A, alpha (actin binding protein 280), isoform CRA_a | 248350 | 67 | 4 |
| gi\|21739753 | hypothetical protein | 90929 | 66 | 3 |
| gi\|6980496 | Chain C, Hemochromatosis Protein Hfe Complexed With Transferrin Receptor | 71681 | 65 | 3 |
| gi\|7671639 | dJ34F7.1.1 (tenascin XB (isoform 1)) | 463945 | 65 | 4 |
| gi\|5821140 | ASY | 40308 | 64 | 2 |
| gi\|189868 | phosphoglycerate mutase | 28832 | 63 | 2 |
| gi\|18999435 | Keratin 5 (epidermolysis bullosa simplex, Dowling-Meara/Kobner/Weber-Cockayne types) | 62340 | 62 | 7 |
| gi\|2344812 | Drg1 | 42796 | 61 | 1 |
| gi\|2407641 | neuropilin | 103056 | 61 | 1 |
| gi\|4503481 | eukaryotic translation elongation factor 1 gamma | 50087 | 59 | 2 |
| gi\|5453914 | phospholipid transfer protein isoform a precursor | 54705 | 59 | 1 |
| gi\|4503483 | eukaryotic translation elongation factor 2 | 95277 | 58 | 1 |
| gi\|30102 | type I collagen | 41496 | 58 | 1 |
| gi\|178277 | S-adenosylhomocysteine hydrolase | 47684 | 57 | 2 |
| gi\|577295 | KIAA0088 | 106702 | 57 | 1 |
| gi\|463907 | syntaxin | 34173 | 56 | 1 |
| gi\|5851638 | major vault protein | 19256 | 54 | 4 |
| gi\|4505011 | lysyl oxidase-like 2 precursor | 86668 | 53 | 1 |
| gi\|4505891 | procollagen-lysine, 2-oxoglutarate 5-dioxygenase 3 precursor | 84731 | 53 | 1 |
| gi\|5803225 | tyrosine 3/tryptophan 5 -monooxygenase activation protein, epsilon polypeptide | 29155 | 52 | 2 |
| gi\|135691 | Latent-transforming growth factor beta-binding protein, isoform 1S precursor (LTBP-1) (Transforming growth factor beta-1-binding protein 1) (TGF-beta1-BP-1) | 152689 | 51 | 1 |
| gi\|11545873 | secreted modular calcium-binding protein 1 isoform 2 | 48132 | 48 | 1 |
| gi\|21739834 | hypothetical protein | 55126 | 47 | 6 |
| gi\|21265101 | transmembrane 4 superfamily member 1 | 21617 | 46 | 1 |

| | | | | |
|---|---|---|---|---|
| gi\|1916850 | scaffold protein Pbp1 | 32397 | 45 | 1 |
| gi\|190447 | prosomal protein P30-33K | 30208 | 45 | 1 |
| gi\|31979 | histone H2A.2 | 13898 | 45 | 2 |
| gi\|4691726 | ARF GTPase-activating protein GIT1 | 84279 | 44 | 1 |
| gi\|6424942 | ALG-2 interacting protein 1 | 96019 | 43 | 2 |
| gi\|340219 | vimentin | 53681 | 43 | 3 |
| gi\|119599578 | hCG2040552 | 8864 | 43 | 1 |
| gi\|1000702 | p54/58N | 49699 | 42 | 1 |
| gi\|34234 | laminin-binding protein | 31774 | 40 | 1 |
| gi\|4235275 | talin | 269661 | 40 | 2 |
| gi\|2988400 | Unknown gene product | 61410 | 40 | 1 |
| gi\|87901 | Ig lambda chain V-IV region | 15451 | 39 | 1 |
| gi\|188619 | matrix metalloproteinase-3 | 53944 | 39 | 1 |
| gi\|48425723 | Chain E, Structure Of Human Transferrin Receptor-Transferrin Complex | 38222 | 39 | 1 |
| gi\|13537204 | MAST205 | 189320 | 39 | 1 |

## REFERENCES


1. Al-Nedawi K, Meehan B, Rak J (2009) Microvesicles: messengers and mediators of tumor progression. *Cell Cycle* 8:2014-2018.

2. Cocucci E, Racchetti G, Meldolesi J (2009) Shedding microvesicles: artefacts no more. *Trends Cell Biol* 19:43-51.

3. Ratajczak J, Wysoczynski M, Hayek F, Janowska-Wieczorek A, Ratajczak MZ (2006) Membrane-derived microvesicles: important and underappreciated mediators of cell-to-cell communication. *Leukemia* 20:1487-1495.

4. Skog J, et al. (2008) Glioblastoma microvesicles transport RNA and proteins that promote tumour growth and provide diagnostic biomarkers. *Nat Cell Biol* 10:1470-1476.

5. Al-Nedawi K, et al. (2008) Intercellular transfer of the oncogenic receptor EGFRvIII by microvesicles derived from tumour cells. *Nat Cell Biol* 10:619-624.

6. Graner MW, et al. (2009) Proteomic and immunologic analyses of brain tumor exosomes. *Faseb J* 23:1541-1557.

7. Di Vizio D, et al. (2009) Oncosome formation in prostate cancer: association with a region of frequent chromosomal deletion in metastatic disease. *Cancer Res* 69:5601-5609.

8. Mathivanan S, Simpson RJ (2009) ExoCarta: A compendium of exosomal proteins and RNA. *Proteomics* 9:4997-5000.

9. Al-Nedawi K, Meehan B, Kerbel RS, Allison AC, Rak J (2009) Endothelial expression of autocrine VEGF upon the uptake of tumor-derived microvesicles containing oncogenic EGFR. *Proc Natl Acad Sci U S A* 106:3794-3799.

10. Li B, et al. (2010) EGF potentiated oncogenesis requires a tissue transglutaminase-dependent signaling pathway leading to Src activation. *Proc Natl Acad Sci U S A* 107:1408-1413.

11. Yamaguchi H, Wang HG (2006) Tissue transglutaminase serves as an inhibitor of apoptosis by cross-linking caspase 3 in thapsigargin-treated cells. *Mol Cell Biol* 26:569-579.

12. Hwang JY, et al. (2008) Clinical and biological significance of tissue transglutaminase in ovarian carcinoma. *Cancer Res* 68:5849-5858.

13. Mann AP, et al. (2006) Overexpression of tissue transglutaminase leads to constitutive activation of nuclear factor-kappaB in cancer cells: delineation of a novel pathway. *Cancer Res* 66:8788-8795.

14. Mangala LS, Fok JY, Zorrilla-Calancha IR, Verma A, Mehta K (2006) Tissue transglutaminase expression promotes cell attachment, invasion and survival in breast cancer cells. *Oncogene* 26:2459-2470.

15. Yuan L, et al. (2007) Transglutaminase 2 inhibitor, KCC009, disrupts fibronectin assembly in the extracellular matrix and sensitizes orthotopic glioblastomas to chemotherapy. *Oncogene* 26:2563-2573.

16. Balklava Z, et al. (2002) Analysis of tissue transglutaminase function in the migration of Swiss 3T3 fibroblasts: the active-state conformation of the enzyme does not affect cell motility but is important for its secretion. *J Biol Chem* 277:16567-16575.

17. Akimov SS, Krylov D, Fleischman LF, Belkin AM (2000) Tissue transglutaminase is an integrin-binding adhesion coreceptor for fibronectin. *J Cell Biol* 148:825-838.

18. Feng Y, et al. (2003) Exo1: a new chemical inhibitor of the exocytic pathway. *Proc Natl Acad Sci U S A* 100:6469-6474.

19. Gaudry CA, et al. (1999) Cell surface localization of tissue transglutaminase is dependent on a fibronectin-binding site in its N-terminal beta-sandwich domain. *J Biol Chem* 274:30707-30714.

20. Yang W, Lin Q, Guan JL, Cerione RA (1999) Activation of the Cdc42-associated tyrosine kinase-2 (ACK-2) by cell adhesion via integrin beta1. *J Biol Chem* 274:8524-8530.

21. Ruoslahti E, Pierschbacher MD (1987) New perspectives in cell adhesion: RGD and integrins. *Science* 238:491-497.

22. Wierzbicka-Patynowski I, Schwarzbauer JE (2003) The ins and outs of fibronectin matrix assembly. *J Cell Sci* 116:3269-3276.

23. Leiss M, Beckmann K, Giros A, Costell M, Fassler R (2008) The role of integrin binding sites in fibronectin matrix assembly in vivo. *Curr Opin Cell Biol* 20:502-507.

24. Shao M, et al. (2009) Epithelial-to-mesenchymal transition and ovarian tumor progression induced by tissue transglutaminase. *Cancer Res* 69:9192-9201.

25. Hettasch JM, et al. (1996) Tissue transglutaminase expression in human breast cancer. *Lab Invest* 75:637-645.

26. Singer CF, et al. (2006) Tissue array-based expression of transglutaminase-2 in human breast and ovarian cancer. *Clin Exp Metastasis* 23:33-39.

27. Williams CM, Engler AJ, Slone RD, Galante LL, Schwarzbauer JE (2008) Fibronectin expression modulates mammary epithelial cell proliferation during acinar differentiation. *Cancer Res* 68:3185-3192.

28. Barkan D, et al. (2008) Inhibition of metastatic outgrowth from single dormant tumor cells by targeting the cytoskeleton. *Cancer Res* 68:6241-6250.

29. Clark EA, Golub TR, Lander ES, Hynes RO (2000) Genomic analysis of metastasis reveals an essential role for RhoC. *Nature* 406:532-535.

30. Antonyak MA, et al. (2004) Augmentation of tissue transglutaminase expression and activation by epidermal growth factor inhibit doxorubicin-induced apoptosis in human breast cancer cells. *J Biol Chem* 279:41461-41467.

# CHAPTER 4

## RhoA-ROCK-Lim kinase signaling triggers the biogenesis of cancer cell-derived microvesicles

### Introduction

Classical cell-cell communication involves the secretion of hormones or cytokines that stimulate signaling activities within cells in either an autocrine or paracrine fashion upon binding to their cell-surface receptors (1, 2). Although these secretory events have been commonly assumed to serve as the predominant mode of cell-cell communication, a novel type of vesicle secretion, referred to as microvesicles (MVs) or oncosomes (when shed from cancer cells), has begun to receive a great deal of attention (3-7). MVs are an unconventional form of cellular secretory structures that are directly shed from the plasma membranes of cells. They contain a variety of types of cargo including cell surface receptors and other signaling proteins, as well as mRNA transcripts, with their specific composition being primarily determined by their cellular origins (8-15). MVs have sometimes been mis-identified as exosomes, which are conventional secretory vesicles generated through the classical endosome - multivesicular body (MVB) trafficking pathway (16). However, MVs are distinct from exosomes with regard to how they are generated, as well as their size, lipid composition, and cargo (17).

Once shed from donor cells, MVs are able to either alter the microenvironment through their cargo, or fuse to recipient cells where certain signaling activities can be

triggered upon the transfer of their cargo. For example, MVs secreted from endothelial cells, platelets, or monocytes were shown to contain phosphatidylserine and tissue factor, which can bind and facilitate the actions of coagulation factor at the vascular site of injury (18), whereas MVs generated from microglial cells were able to transfer interleukin-1β into recipient cells that do not express this cytokine, thereby regulating their inflammatory response (19). Moreover, it was recently shown that murine embryonic stem cell-derived MVs are capable of prolonging the expansion of hematopoietic progenitor cells (HPCs) by transferring mRNAs encoding several pluripotent transcription factors into recipient HPCs (20).

In addition to the biological functions described above, there has been a rapidly growing appreciation that MVs play important roles in different aspects of cancer progression. It was recently discovered that several malignant cancer cell lines exhibit significantly enhanced MV production, including glioblastoma, melanoma, prostate, colorectal and breast cancer cells (3, 4, 6, 21-25). Cancer cell-derived MVs were shown to play critical roles by influencing the tumor microenvironment as well as stimulating angiogenesis and metastasis, and promoting tumor growth (13-15, 26, 27). Moreover, MVs shed from cancer cells have been shown to help to generate a more "tumor-friendly" niche through the actions of some of their cargo such as metallo-proteases, or by directly stimulating signaling activities within recipient cells following the transfer of their cargo (28, 29). For example, it was recently shown that the overexpression of the constitutively-active truncated form of the EGF receptor, EGFR vIII, in glioblastomas stimulates MV formation in these cancer cells. EGFR vIII was also found to be part of the cargo of the released MVs, which upon engaging

neighboring glioblastoma cells, induced enhanced EGFR-signaling and oncogenic transformation (3).

Remarkably, recent studies have shown that MV-mediated intercellular communication not only occurs between cancer cells, but also between cancer cells and adjacent normal cells, including stromal fibroblasts and endothelial cells (29, 30). Indeed, we recently demonstrated that MVs derived from breast cancer or glioblastoma cells are capable of conferring onto normal fibroblasts, as well as normal epithelial cells, the characteristics of transformed cells. This required the MV-mediated transfer of an essential protein cargo, tissue transglutaminase (tTG), together with its transamidation substrate, fibronectin (6). When taken together, these results highlight a previously unappreciated role of MVs in cancer progression, suggesting that tumor formation not only depends on cancer cell proliferation, but also involves the MV-mediated exchange of cargo among cancer cells, normal cells, and their microenvironment.

Given the important roles played by MVs in cancer progression, it is of great interest to understand how these vesicles are generated in cancer cells. Studies performed in colorectal cancer cells suggested that MV production may be an outcome of mutated K-Ras or the result of the deletion of p53 (23), while studies in glioblastoma and prostate cancer cells have suggested that MV formation is stimulated by EGFR activation (3, 22). However, thus far the mechanisms underlying the biogenesis of these vesicles have remained largely undetermined. In the present study, I set out to delineate the signals responsible for MV biogenesis in two different types of cancer cells, MDAMB231 breast cancer cells and HeLa cervical carcinoma cells. I

**Figure 4.1 Various human cancer cells generate tTG- and actin-containing MVs that are capable of transforming NIH3T3 fibroblasts.** (**A**) A MDAMB231 cell shedding MVs from its surface was visualized by scanning electron microscope (SEM). (**B**) Shown are immunofluorescence pictures of MDAMB231 cells, U87 cells or HeLa cells treated without or with EGF. The cells were stained using tTG antibody, rhodamine-conjugated phalloidin and DAPI to visualize tTG, actin filaments and cell nuclei respectively. Some of the pronounced MVs associated with cell membranes were denoted by arrows. (**C**) Quantification of the experiments performed in (B). Cells showing membrane-bound MVs were counted over the total cells in the field. The histogram represents the mean ± standard deviation from three independent experiments. (**D**) MDAMB231cells or U87 cells were lysed, and the MVs shed into the medium were isolated and lysed as well. The whole cell lysates (WCLs) and the MV lysates were then immunoblotted with antibodies against tTG, actin, the MV marker flotillin-2, and the cytosolic-specific marker IκBα. (**E**) Serum-starved HeLa cells treated without or with EGF, as well as the secreted MVs were lysed and subjected to Western blot analysis using tTG, flotillin-2 and IκBα antibodies. (**F**) MDAMB231cells overexpressing empty vector or the dominant-negative truncation of V5-tagged CHMP3 protein were lysed, and the secreted MVs were also isolated and lysed. The whole cell lysates (WCLs) and the MV lysates were then immunoblotted with antibodies against tTG, V5, the MV marker flotillin-2, and the cytosolic marker IκBα. (**G**) NIH3T3 fibroblasts incubated without or with MVs derived from MDAMB231 cells, U87 cells or HeLa cells treated without or with EGF were subjected to anchorage-independent growth assay. The soft agar cultures were re-fed every fourth day for 12 days, when the colony numbers were scored. The histogram represents the mean ± standard deviation from three independent experiments. (**H**) Representative images of the resulting colonies that formed in (G). (**I**) Mitotically-arrested MDAMB231 cells were mixed without or with NIH3T3 cells, or the same number of parental MDAMB231 or NIH3T3 cells were injected into nude mice as described in the materials and methods. A month later the formed tumors were counted and presented.

*The experiments described in (B), (C) and (I) were performed by Marc A. Antonyak and Bo Li.

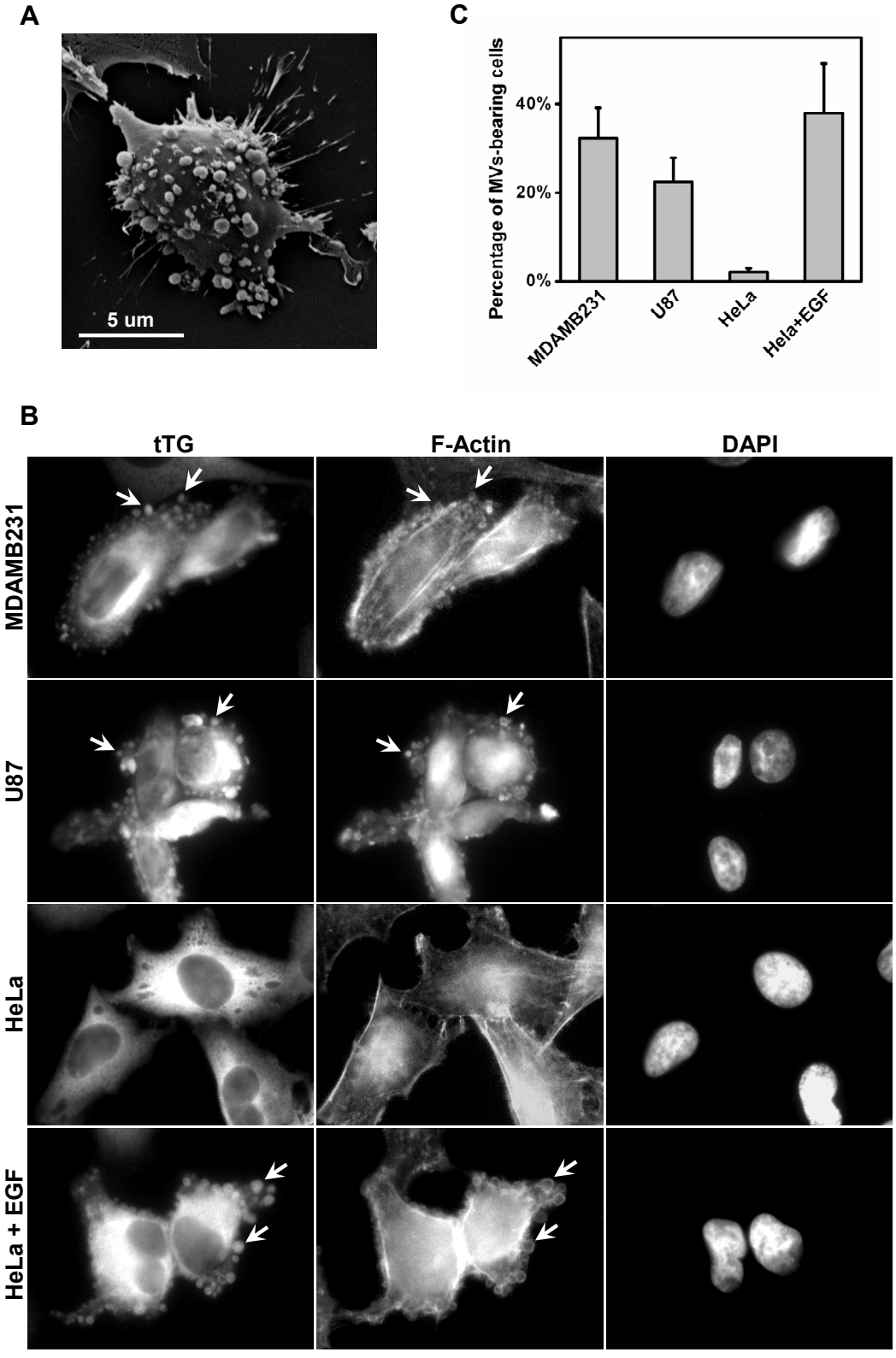
A
5 um
C
Percentage of MVs-bearing cells
40%
20%
0%
MDAMB231
U87
HeLa
Hela+EGF
B
tTG
F-Actin
DAPI
MDAMB231
U87
HeLa
HeLa + EGF

Figure 4.1 (Continued)

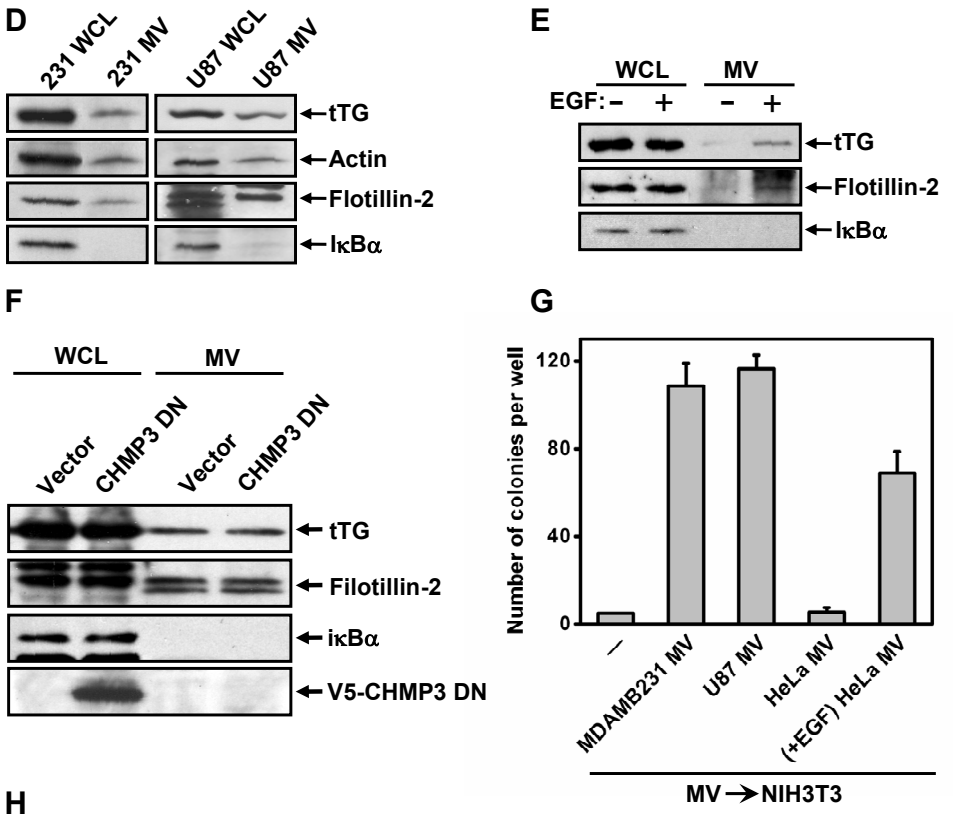


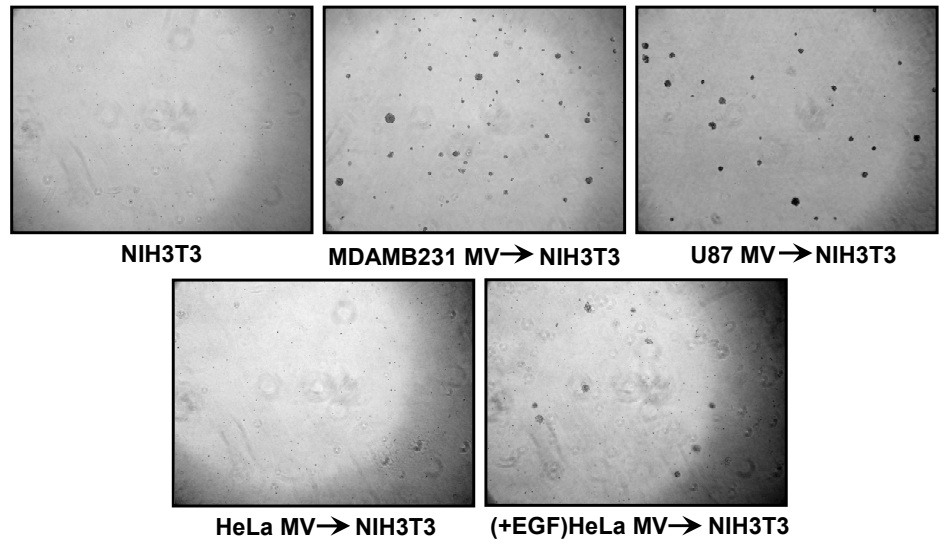


I

| Cells Injected | Tumors/Injection | Cells Injected | Tumors/Injection |
|---|---|---|---|
| MDAMB231 | 4/4 | Mito-C-MDAMB231 | 0/6 |
| NIH3T3 | 0/6 | Mito-C-MDAMB231(siCont) + NIH3T3 | 4/6 |

show that the formation of MVs is an outcome of a specific Rho GTPase-dependent signaling pathway that is activated in HeLa cells by EGF and is constitutively activated in MDAMB231 cells. This pathway triggers the activation of Rho kinase (ROCK), and subsequently Lim kinase (LIMK), culminating in the phosphorylation of cofilin. I further demonstrate that the hyper-activation of this signaling pathway and the resultant generation of MVs have a significant impact on tumor formation in mice. In light of the roles suggested for Rho GTPases and ROCK in cancer cell migration, invasion, and the development of the metastatic state (31), these findings carry exciting implications regarding how these signaling proteins might contribute to malignant transformation.

**Results**

*Several malignant cancer cell lines exhibit membrane-bound MVs*

The generation of MVs has been observed in different malignant human cancer cell lines. An example is shown in Figure 4.1*A*, in which MVs are visualized on the surface of a MDAMB231 breast cancer cell by scanning electron microscopy. MVs can also be visualized by immunofluorescence, as demonstrated for MDAMB231 cells, U87 glioblastoma cells, and HeLa cervical carcinoma cells stimulated by EGF (Figure 4.1*B*). In each case, the cells were co-stained using rhodamine-conjugated phalloidin to label actin filaments which form the base of the MVs, and with an antibody against tTG, a protein cross-linking enzyme that is overexpressed in a number of cancer types including brain, pancreatic, ovarian and breast cancers (32-35), and is a component of MV cargo (6). Increased tTG expression in cancer cells has been suggested to

contribute to multiple aspects of cancer progression, with recent studies showing that this may be the result of tTG's ability to cross-link fibronectin in MVs, thereby generating a potent activator of integrin-signaling in acceptor cells (36). As shown in Figure 4.1*B*, the anti-tTG antibody labeled the membrane-bound MVs with higher contrast compared to phalloidin, and therefore I have used tTG staining to visualize MVs, and to quantify the percentage of cells bearing these vesicles (Figure 4.1*C*). Approximately 35% of MDAMB231 cells, 25% of U87 cells, and 40% of EGF-stimulated HeLa cells exhibited membrane-associated MVs (Figure 4.1*C*), whereas HeLa cells that were not treated with EGF showed little or no MV production.

*MVs shed from cancer cells are capable of inducing malignant transformation*

As an initial step toward demonstrating that MVs formed on the surfaces of cancer cells can be shed and influence their surrounding environment, I collected MVs from the conditioned medium of MDAMB231 and U87 cells. Figure 4.1*D* shows that the isolated MVs contained the cargo proteins tTG and actin, as well as flotillin-2, which has been used as a general MV-marker (3). The cytosolic protein IκBα served as a negative control and was absent from these MV preparations, verifying the lack of cytosolic contamination. Moreover, in the case of HeLa cells, I was only able to collect MVs when these cancer cells were stimulated by EGF, and not in the absence of growth factor treatment (Figure 4.1*E*), which are consistent with my immunofluorescence studies (Figures 4.1*B* and 4.1*C*). To confirm that the MV preparations from these different cancer cell lines did not contain exosomes, I ectopically expressed the dominant-negative form of the CHMP3 protein (CHMP3

DN), which is the mammalian homolog of the yeast VPS24 protein that is essential for the secretion of exosomes (37), in MDAMB231 cells. The levels of MVs were unaffected by the presence of CHMP3 DN (Figure 4.1*F*), indicating that MVs and exosomes are distinct species.

Recently, we reported that MVs isolated from cancer cells were biologically active and capable of inducing the transformation of normal cells (6). Indeed, an example of their transforming capability can be demonstrated through the following type of experiment. MVs generated in a constitutive manner from MDAMB231 or U87 cells, as well as MVs produced in an EGF-dependent manner in HeLa cells, were collected and added to NIH3T3 cells. The ability of the MV-treated cells to exhibit anchorage-independent growth, which is often considered a hallmark for malignant transformation, was then examined. As shown in Figures 4.1*G* and 4.1*H*, while normal NIH3T3 cells were unable to form colonies in soft agar, those fibroblasts that were incubated with the cancer cell-derived MVs were capable of forming colonies. The numbers and sizes of these colonies correlated well with the amount of MVs secreted from the different cancer cells. Perhaps even more significant is our finding that the ability of cancer cell-derived MVs to induce transformation in cell culture, carries-over to tumor formation *in vivo*. This was demonstrated by treating MDAMB231 cells with the mitosis-arresting reagent mitomycin-C and then injecting the treated cells into nude mice, alone or together with an equivalent number of NIH3T3 fibroblasts. Incubation with mitomycin-C completely abolished the ability of MDAMB231 cells to form tumors, whereas their control counterparts (i.e. MDAMB231 cells that were untreated) were quite effective at inducing tumor formation under the same

**Figure 4.2 RhoA signaling pathway is specific for controlling the generation of MVs in cancer cells.** (**A**) HeLa cells overexpressing the HA-tagged activated forms of Rac (Rac F28L), Cdc42 (Cdc42 F28L), Ras (Ras G12V) or RhoA (RhoA F30L) were immunostained with tTG and HA antibodies. Noted were MVs specifically generated from RhoA F30L-overexpressing HeLa cells, some of which were denoted by arrows. (**B**) Quantification of the immunofluorescence experiments performed in (A). Shown percentage is the ratio of MVs-bearing cells over the pool of HeLa cells overexpressing various constructs. The histogram represents the mean ± standard deviation from three independent experiments. (**C**) HeLa cells overexpressing Vector or RhoA F30L were lysed and the secreted MVs were also collected from the conditioned medium. Both WCLs and MV lysates were then immunoblotted using tTG, flotillin-2, HA and IκBα antibodies. HeLa cells treated without or with EGF (**D**) or MDAMB231 cells (**E**) transfected with control siRNA or RhoA specific siRNAs were lysed, and the secreted MVs were also lysed. Immunoblotting on collected lysates were performed by using tTG, flotillin-2, IκBα and RhoA antibodies. (**F**) The RBD binding assay was performed on lysates collected from MDAMB231 cells, or HeLa cells treated without or with EGF as described in the materials and methods. The amount of active or total RhoA protein was detected by using anti-RhoA antibody, and actin antibody was also applied on the same membrane to conform equal input. (**G**) Quantification of the MVs-bearing HeLa Cells respectively overexpressing vector, RhoA F30L, RhoC F30L, Src Y527F or the oncogenic form of Dbl protein (Onco-Dbl). The histogram represents the mean ± standard deviation from three independent experiments.

*The experiments described in (A), (B) and (G) were performed by Marc A. Antonyak and Bo Li.

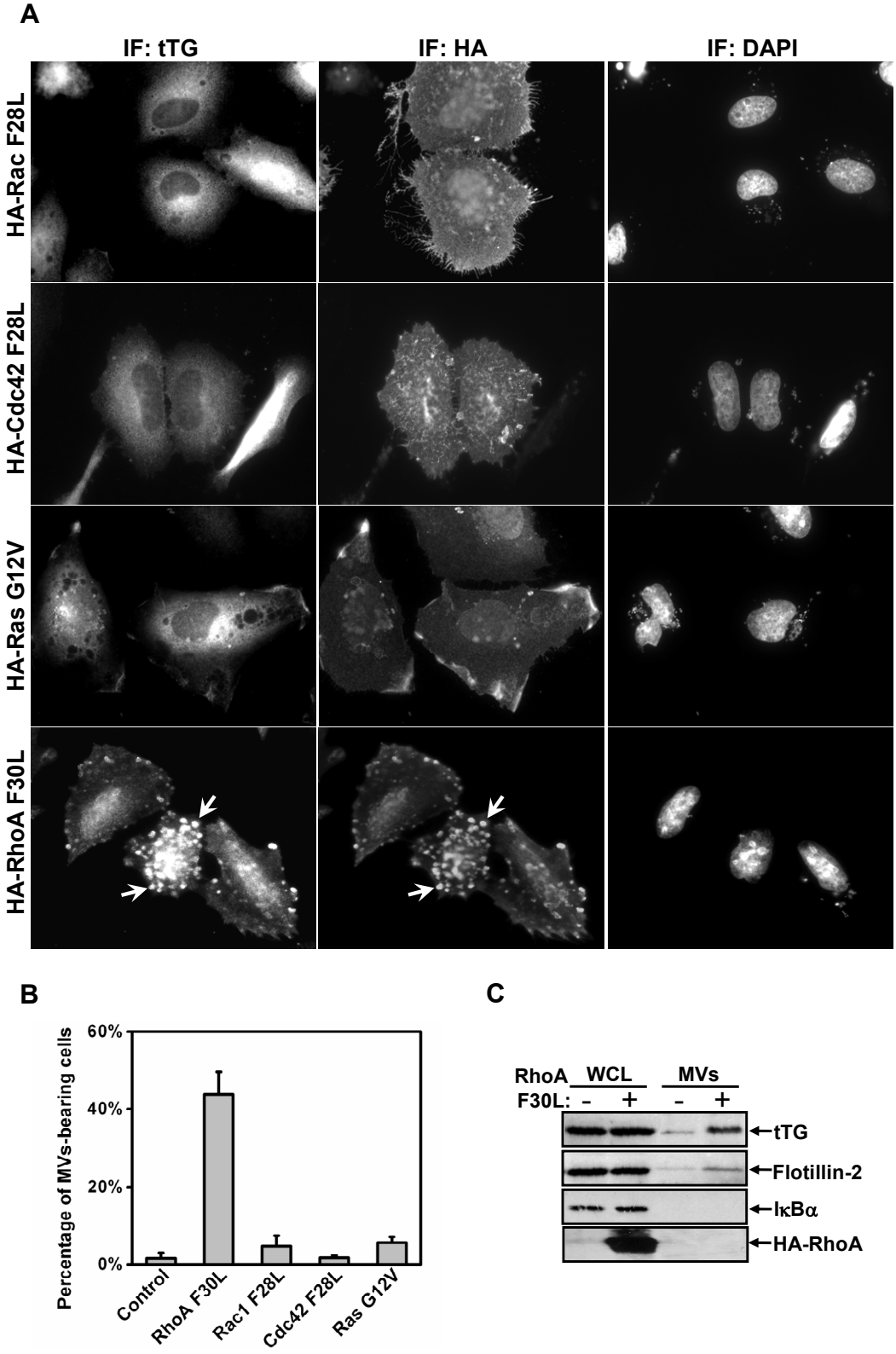
A
IF: tTG
IF: HA
IF: DAPI
HA-Rac F28L
HA-Cdc42 F28L
HA-Ras G12V
HA-RhoA F30L
B
Percentage of MVs-bearing cells
60%
40%
20%
0%
Control
RhoA F30L
Rac1 F28L
Cdc42 F28L
Ras G12V
C
RhoA
WCL
MVs
F30L: - + - +
tTG
Flotillin-2
IκBα
HA-RhoA

Figure 4.2 (Continued)

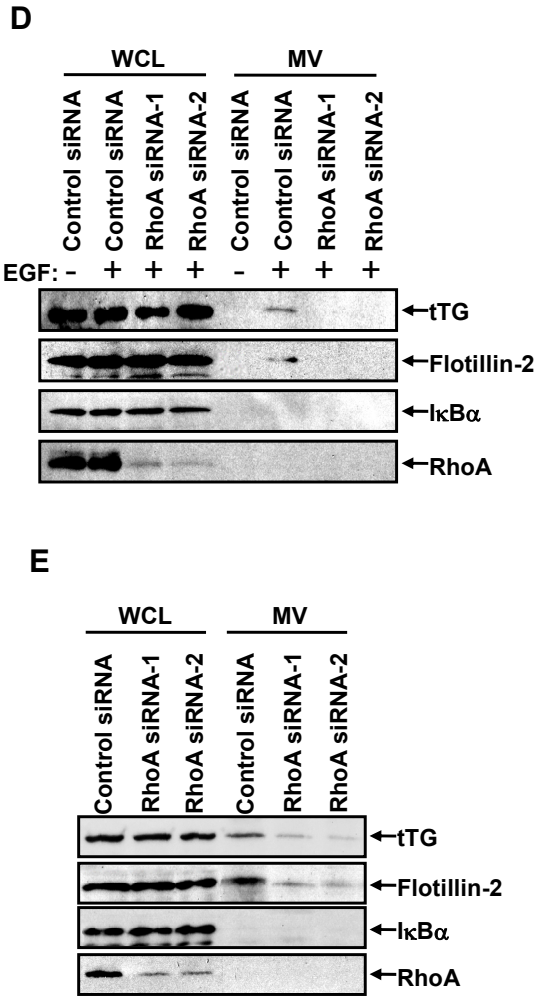

experimental conditions (Figure 4.1*I*). However, when the mitotically-arrested MDAMB231 cells were co-injected with NIH3T3 fibroblasts into nude mice, 4 tumors were formed following 6 injections (Figure 4.1*I*). Thus, MVs shed by the mitotically-arrested cancer cells were capable of causing the co-injected fibroblasts to become transformed *in vivo*, as indicted by the observed tumor formation.

*Activated RhoA is both necessary and sufficient for inducing the biogenesis of MVs in cancer cells*

Given the indications that cancer cell-derived MVs play critically important roles in malignant transformation, a key question then becomes the underlying mechanistic basis for their biogenesis. In various cancer cell lines, including HeLa cervical carcinoma cells, U373 glioblastoma cells, and DU145 prostate cancer cells, MV production appears to be stimulated by EGF treatment (3, 6, 22). Thus, I used HeLa cells as the model system to determine the signaling proteins downstream of EGFR that are responsible for controlling the formation of MVs. The fact that MVs are characterized by "actin-ring" structures (Figure 4.1*B*) suggested the possible involvement of the cytoskeletal machinery, which prompted me to consider the potential roles of small GTPases in MV biogenesis. Among the different classes of GTPases, the Ras, Rac, Rho and Cdc42 proteins are best known for their ability to reorganize actin cytoskeletal structures in cells upon EGF stimulation (38-40). To determine whether any of these GTPases are linked to MV formation, I first individually overexpressed the HA-tagged dominant-active forms of Rac (Rac F28L), Cdc42 (Cdc42 F28L), Ras (Ras G12V), or RhoA (RhoA F30L) in HeLa cells, and

then visualized MVs along the cell surface by immunostaining transfected cells with tTG and HA antibodies. As shown in Figure 4.2*A*, neither activated Rac, Cdc42, nor Ras, was able to induce the generation of MVs in HeLa cells. However, cells expressing the constitutively-active form of RhoA exhibited significant MV formation (Figure 4.2*A*, bottom row). Quantification of the immunofluorescence results showed that approximately 40% of HeLa cells-expressing RhoA F30L produced MVs, compared to ~5% of the HeLa cells ectopically expressing the other constitutively active small GTPases (Figure 4.2*B*). Likewise, cells expressing activated RhoA showed increased amounts of MVs in the conditioned medium (Figure 4.2*C*).

Since RhoA-dependent signaling is sufficient to induce MV formation, I then asked whether RhoA is essential for the ability of EGF to trigger MV production in HeLa cells. By using two siRNAs specifically targeting RhoA, I found that knocking-down RhoA expression from HeLa cells completely abolished EGF-stimulated MV formation (Figure 4.2*D*). Similar results were obtained in MDAMB231 cells, where the levels of endogenous MVs were greatly reduced upon the introduction of siRNAs targeting RhoA (Figure 4.2*E*).

The ability of MDAMB231 cells to constitutively generate MVs, whereas HeLa cells required EGF treatment to produce these vesicles, exactly matched the activation status of RhoA in these cancer cells. Specifically, RhoA was constitutively activated in MDAMB231 cells, while its activation required EGF treatment in HeLa cells (Figure 4.2*F*). Interestingly, RhoC was ineffective in generating MVs despite sharing a high degree of sequence similarity with RhoA. The over-expression of oncogenic Src or onco-Dbl was also unable to mimic the actions of RhoA in HeLa

**Figure 4.3 Activation of ROCK signaling is both necessary and sufficient to induce the MV formation in HeLa cells.** (**A**) Serum-starved HeLa cells, MDAMB231 cells and U87 were left untreated or were incubated with ROCK specific inhibitor Y-27632. The HeLa cells were further treated with EGF as indicated and then all of the cells were stained for tTG to identify MVs. (**B**) Quantification of the experiments performed in (A). Shown is the percentage of MVs-bearing cells over the total cells in the field. The error bars represent the standard deviation from three independent experiments. (**C**) The WCLs and MV lysates were collected from MDAMB231 cells and U87 cells treated without or with Y-27632 and then subjected to immunoblotting analysis using tTG, flotillin-2 and IκBα antibodies. (**D**) HeLa cells overexpressing Myc-tagged wild-type ROCK-2 (ROCK WT) were fixed and then immunostained with tTG and Myc antibodies. DAPI stain was also applied to show the nuclei. (**E**) Quantification of the MV generation in HeLa cells transfected with vector, RhoA F30L and ROCK WT. The data shown was the average of three experiments and errors bars represent standard deviation. (**F**) HeLa cells transfected with vector, ROCK WT or RhoA F30L were lysed and the MVs secreted into the medium were also collected and lysed. Both WCLs and MV lysates were then subjected to Western blot analysis using indicated antibodies. (**G**) Picture illustrating the downstream signaling pathway of ROCK. Briefly, active ROCK can phosphorylate LIMK, which turns on its kinase activity and then phosphorylates cofilin, therefore prevents cofilin's actin-severing activity. On the other hand, active ROCK can also phosphorylate MYLP, which inhibits its phosphatase activity, therefore increases the phosphorylation and activity of myosin. Please note that the cellular outcome of suppressing MYLP activity by ROCK can also be achieved by enhancing MYLK activity. (**H**) Serum-starved HeLa cells stimulated by EGF for indicated period of time treated without or with ROCK inhibitor Y-27632 were lysed and blotted with various antibodies.

*The experiments described in (A), (B), (D) and (E) were performed by Marc A. Antonyak and Bo Li.

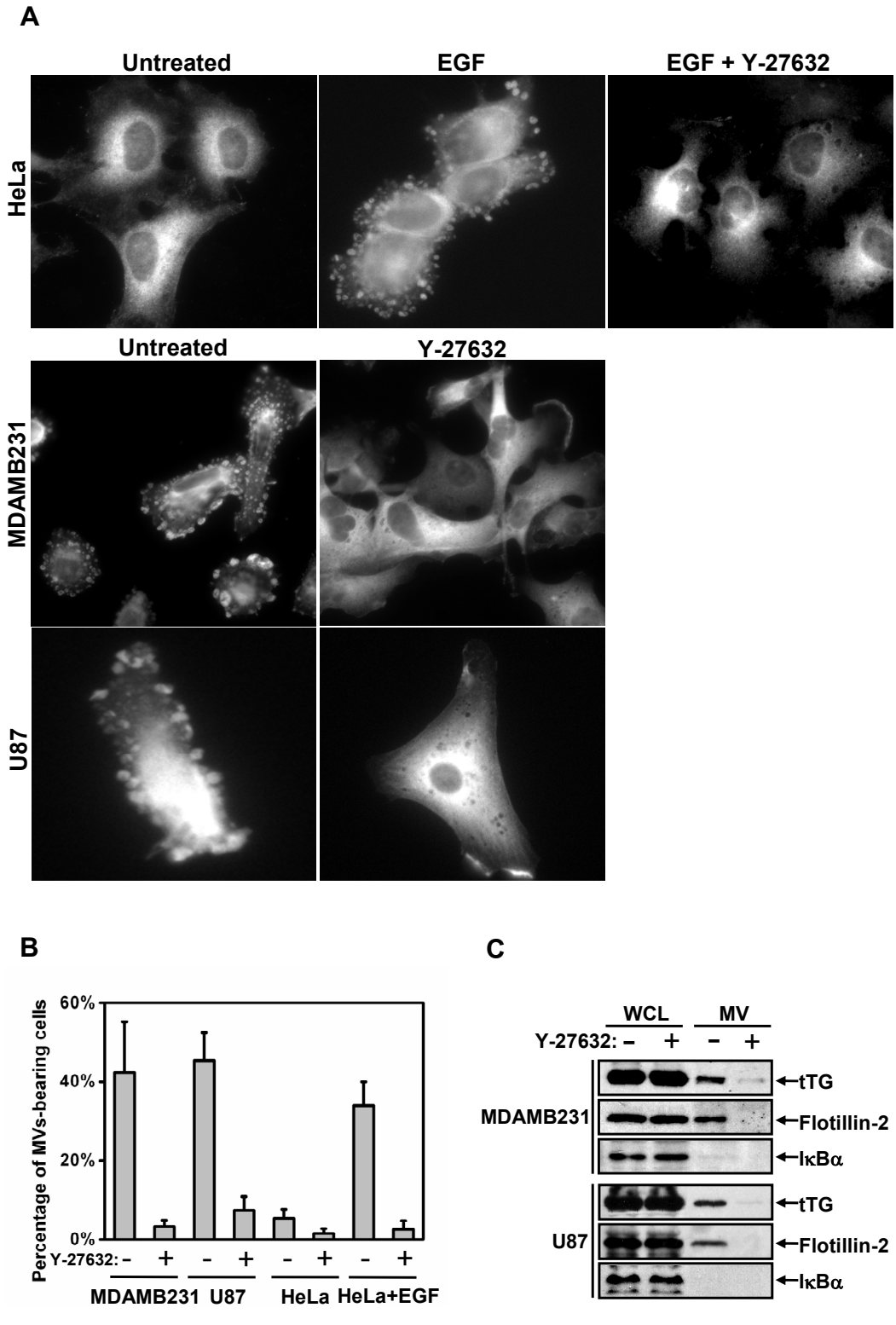
A
Untreated
EGF
EGF + Y-27632
HeLa
Untreated
Y-27632
MDAMB231
U87
B
Percentage of MVs-bearing cells
60%
40%
20%
0%
Y-27632: - + - + - + - +
MDAMB231 U87 HeLa HeLa+EGF
C
WCL
MV
Y-27632: - + - +
MDAMB231
tTG
Flotillin-2
IκBα
U87
tTG
Flotillin-2
IκBα

Figure 4.3 (Continued)

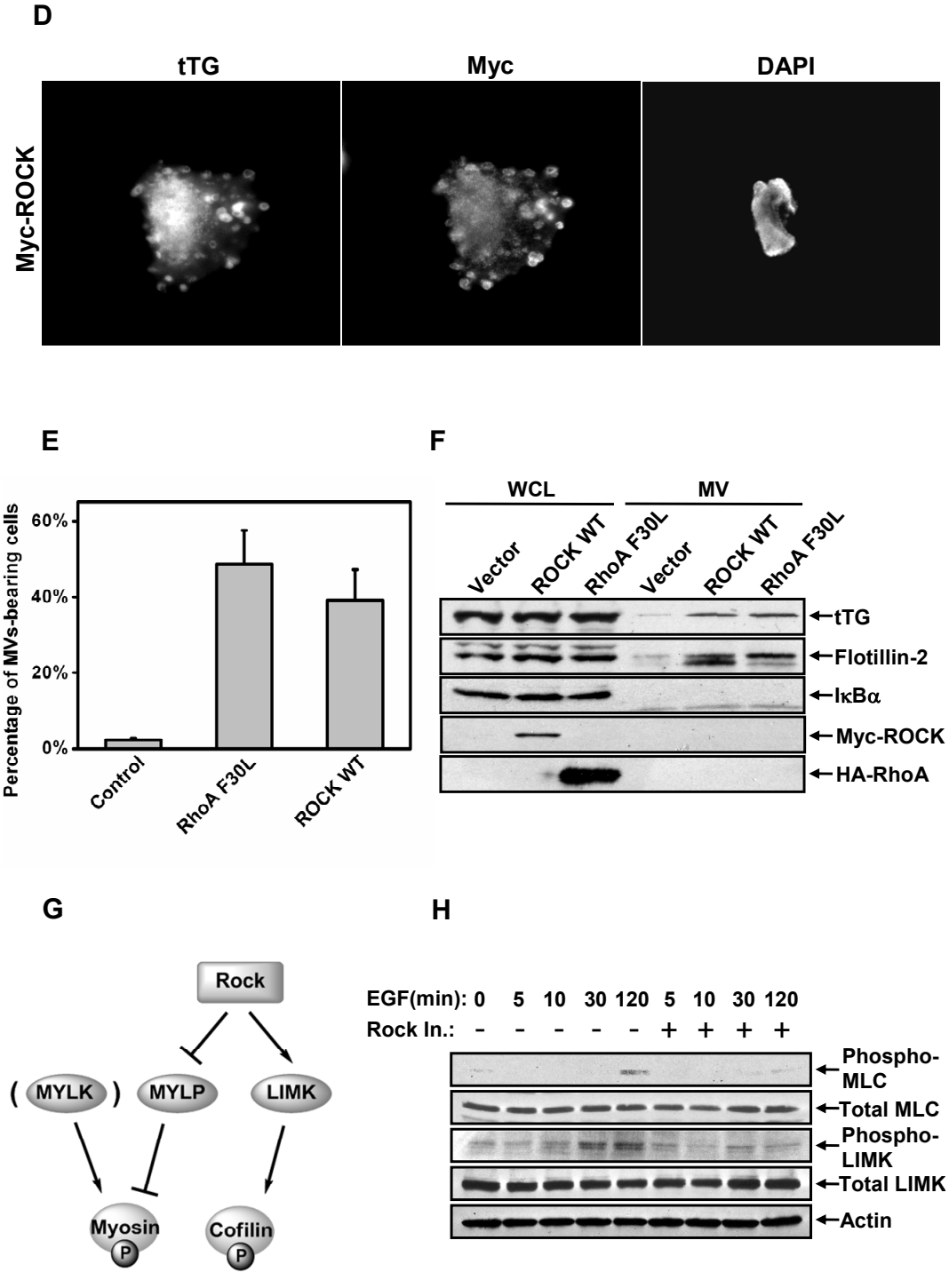

cells (Figure 4.2*G*). The ineffectiveness of onco-Dbl was particularly interesting as it serves as a guanine exchange factor (GEF) that activates RhoA and Cdc42 (41). Thus, the inability of onco-Dbl to induce MV formation suggests that active Cdc42 may counteract RhoA in this process.

*ROCK is a specific signaling target downstream from RhoA in the pathway leading to MV generation*

The essential role of RhoA in regulating MV formation prompted me to search for its downstream signaling partners that are involved in this process. There are several known protein targets for activated RhoA, with the serine/threonine protein kinases ROCK-1 and ROCK-2 (for Rho kinases 1 and 2), collectively referred to as ROCK, being especially attractive candidates because of their roles in actin cytoskeletal remodeling and actomyosin contraction (31, 42). As a first step in examining the roles of these Rho effector proteins in MV formation, I took advantage of the small molecule Y-27632, which is a specific ATP-competitive inhibitor of both ROCK-1 and ROCK-2 (43). Figures 4.3*A* and 4.3*B* show that treatment of MDAMB231 cells, U87 cells, or EGF-stimulated HeLa cells, with Y-27632 completely eliminated the appearance of MVs along the cell surface. Similarly, the amount of MVs collected from MDAMB231 cells or U87 cells was significantly reduced upon Y-27632 treatment (Figure 4.3*C*).

Thus far, attempts to determine whether ROCK-1, ROCK-2 or both protein kinases can mediate the signaling actions of RhoA in MV formation, based on RNAi knock-down experiments have failed. Therefore, I set out to complement these efforts

by seeing whether the overexpression of ROCK was sufficient to drive the MV formation in cancer cells. While I have not obtained significant ectopic expression of ROCK-1 in HeLa cells, I have achieved measurable overexpression of Myc-tagged ROCK-2. Figure 4.3*D* shows that I observed a clear increase in the amount of membrane-bound MVs in HeLa cells overexpressing ROCK-2, with the extent of MV formation in cells overexpressing ROCK-2 being comparable to that obtained when ectopically expressing the constitutively active RhoA (Figure 4.3*E*). Consistent with this finding, the overexpression of ROCK-2 also promoted the secretion of MVs from HeLa cells that could be isolated using the standard MV preparation (Figure 4.3*F*). Collectively, these results indicated that the RhoA-ROCK-signaling pathway is essential for generating MVs in cancer cells.

*The generation of MVs in cancer cells is dependent on a Lim kinase-cofilin signaling pathway activated by ROCK*

There are two well-studied signaling targets thought to be immediately downstream from ROCK, namely Lim kinase (LIMK) and myosin light chain phosphatase (MYLP), both of which can regulate actin cytoskeletal dynamics (44-46) (Figure 4.3*G*). Activated ROCK phosphorylates the kinase domain of LIMK, thereby stimulating its kinase activity. Upon activation by ROCK, LIMK phosphorylates Ser3 on cofilin, which prevents cofilin from severing actin filaments and thereby prolongs the extension of actin fibers *in situ* (45). ROCK is also able to inhibit MLCP activity through the direct phosphorylation of the myosin phosphatase-targeting subunit (MYPT), a critical regulatory component of MLCP, which results in a significant

**Figure 4.4 LIMK and cofilin, but not MYLK or Myosin, are the critical effectors downstream of ROCK to regulate MV formation in HeLa cells.** (**A**) HeLa cells overexpressing either HA-tagged wild-type LIMK (LIMK WT) or Myc-tagged wild-type MYLK (MYLK WT) were fixed and then immunostained with tTG and HA or Myc antibodies. DAPI staining was also performed. The experiments in (A) were quantified by counting MVs-associated cells over cells transfected with LIMK WT (**B**) or MYLK WT (**D**) as compared to vector- and RhoA F30L-overexpressing cells. The error bars represent the standard deviation from three experiments. (**C&E)** The same sets of transfected HeLa cells as in (B) or (D) were collected together with their secreted MVs in the medium, and then probed by tTG, HA, Myc, flotillin-2 and IκBα antibodies in the subsequent Western blot experiments. (**F**) HeLa cells transfected without or with RhoA F30L were co-transfected with mock, dominant-negative LIMK (LIMK D460N) or dominant-negative MYLK (MYLK ATPDEL) as indicated and immunostained for MVs. The percentage of MVs-bearing cells was calculated from three parallel experiments and errors bars represent standard deviation. (**G**) HeLa cells treated with EGF, or MDAMB231 cells were transfected with V5-tagged cofilin S3A. The cells were then fixed and stained with tTG and V5 antibodies. Noted that cells overexpressing V5-tagged cofilin S3A were deprived of membrane-bound MVs. The MVs on HeLa cells stimulated without or with EGF (**H**), or MDAMB231 cells (**I**) overexpressing various constructs were visualized and quantified. Experiments were repeated three times and errors bars represent standard deviation.

*The experiments described in (A), (B), (D), (F), (G), (H) and (I) were performed by Marc A. Antonyak and Bo Li.

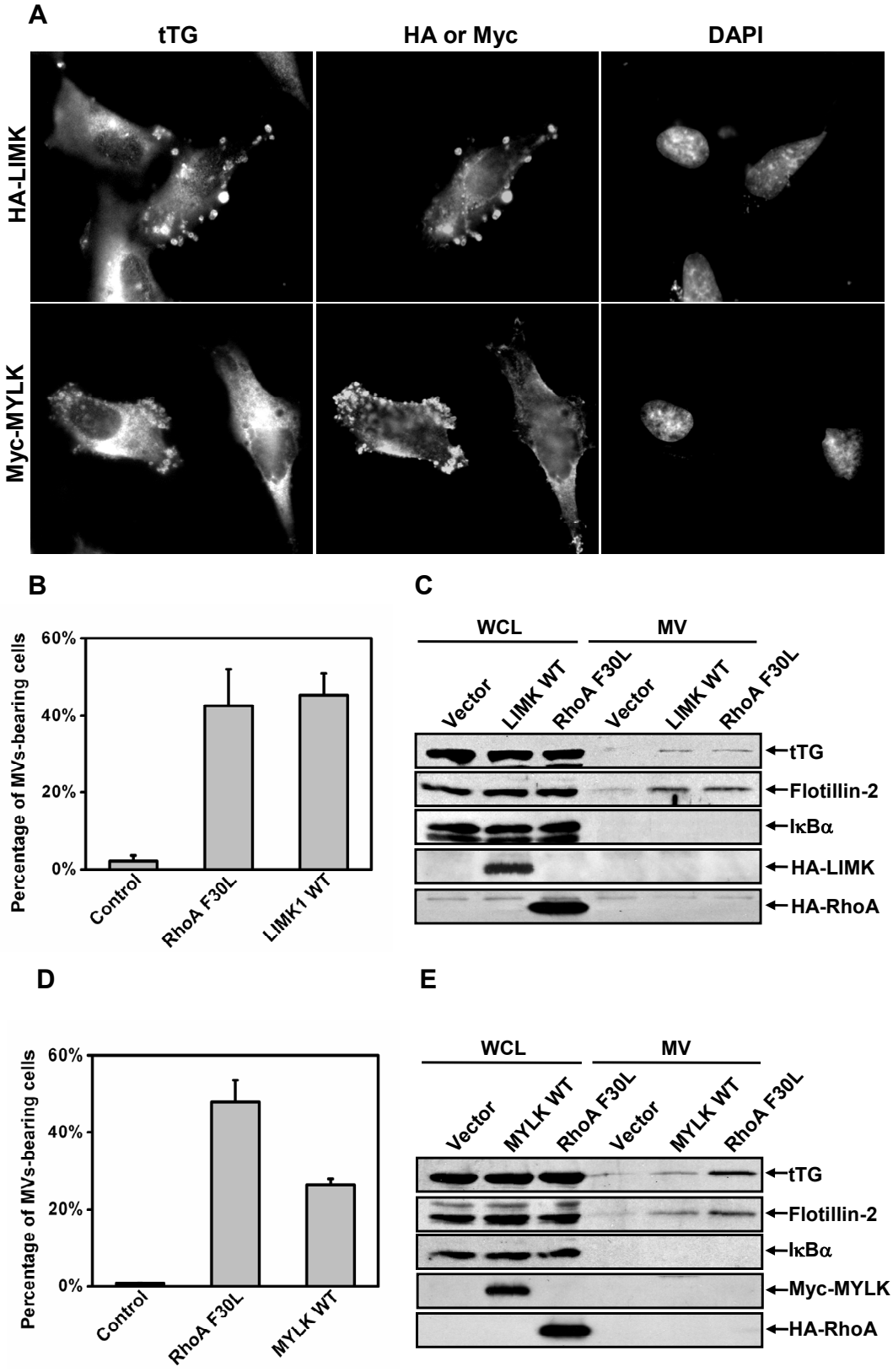
A
tTG
HA or Myc
DAPI
HA-LIMK
Myc-MYLK
B
Percentage of MVs-bearing cells
60%
40%
20%
0%
Control
RhoA F30L
LIMK1 WT
C
WCL
MV
Vector
LIMK WT
RhoA F30L
Vector
LIMK WT
RhoA F30L
tTG
Flotillin-2
IκBα
HA-LIMK
HA-RhoA
D
Percentage of MVs-bearing cells
60%
40%
20%
0%
Control
RhoA F30L
MYLK WT
E
WCL
MV
Vector
MYLK WT
RhoA F30L
Vector
MYLK WT
RhoA F30L
tTG
Flotillin-2
IκBα
Myc-MYLK
HA-RhoA

Figure 4.4 (Continued)

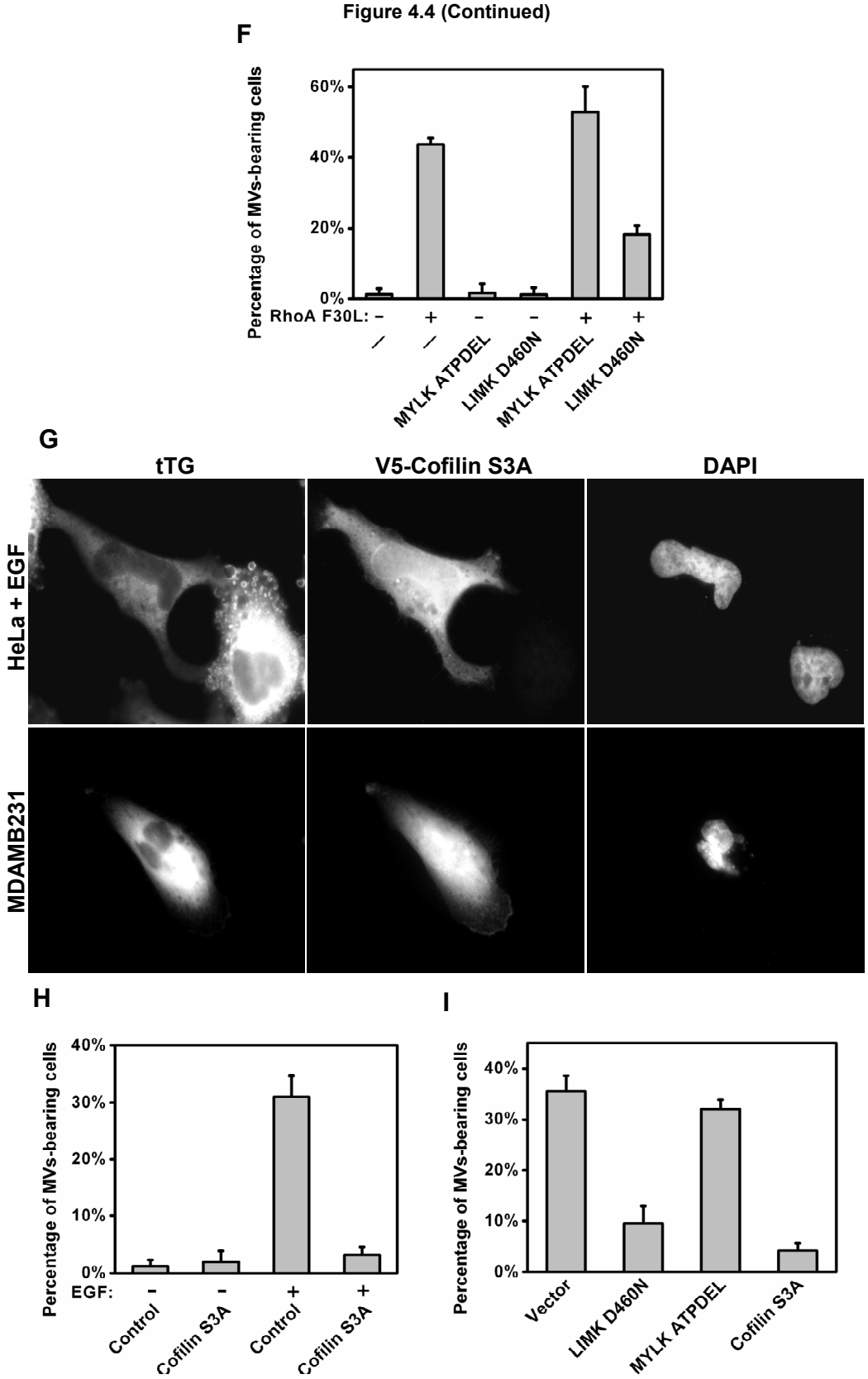

enhancement of myosin phosphorylation and actomyosin contraction (46). Figure 4.3*H* shows that the treatment of HeLa cells with EGF significantly increased the phosphorylation of LIMK and myosin, with each of these phosphorylation events being antagonized by the specific ROCK inhibitor Y-27632. I then examined whether the overexpression of LIMK in HeLa cells, or the increased phosphorylation of myosin that occurs when overexpressing myosin light chain kinase (MYLK), mimicked the ability of ROCK to stimulate MV formation. Interestingly, I found that while the overexpression of MYLK gave rise to only a modest increase in MV formation (Figure 4.4*A*, bottom row and Figure 4.4*D*), the ectopic expression of wild-type LIMK (LIMK WT) in HeLa cells was sufficient to generate MVs to an extent comparable to RhoA F30L (Figure 4.4*A*, top row, and Figure 4.4*B*) or ROCK (Figure 4.3*E*). The overexpression of LIMK, but not the overexpression of MYLK, also gave rise to MVs that were shed and subsequently isolated from EGF-treated HeLa cells in much the same way as occurred when ectopically expressing the constitutively active RhoA (Figure 4.4*C* and 4.4*E*).

I then examined whether disabling LIMK had adverse effects on the ability of RhoA to induce MV formation in cancer cells. In particular, I first wanted to see whether the LIMK D460N mutant, that is defective for protein kinase activity (45), might act as a dominant-negative inhibitor of MV formation. Figure 4.4*F* shows that while the overexpression of LIMK D460N alone in HeLa cells had no effect on the generation of MVs, the co-expression of LIMK D460N together with the constitutively active RhoA F30L mutant in HeLa cells significantly suppressed the ability of RhoA to induce MV formation (compare the last column with the second

column). For the sake of comparison, I also examined the MYLK ATPDEL mutant, which is kinase-defective because of an internal deletion that prevents the binding of ATP to MYLK (47), as a potential dominant-negative inhibitor of RhoA-dependent MV formation. However, overexpressing MYLK ATPDEL together with RhoA F30L exhibited little, if any inhibitory effect (Figure 4.4*F*, compare the second column to the fifth column).

I then investigated the role of cofilin, the major downstream effector of LIMK, in MV formation. I generated a dominant-active form of cofilin (cofilin S3A), which prevented it from being phosphorylated by LIMK, and then transfected this mutant into HeLa cells treated with or without EGF. Immunofluorescence experiments suggested that over-expression of cofilin S3A severely impaired the generation of MVs in HeLa cells stimulated by EGF (Figure 4.4*G*, top row), and this was further supported by quantifying the percentage of MVs-bearing cells in these samples (Figure 4.4*H*). The same was true when ectopically expressing the cofilin S3A mutant in MDAMB231 cells, as it strongly blocked the constitutive shedding of MVs from these breast cancer cells in a manner similar to the kinase-defective LIMK D460N mutant (Figure 4.4*G*, bottom row, and Figure 4.4*I*).

*RhoA signaling to LIMK and cofilin is essential for MV-mediated transformation*

To further confirm the significance of LIMK, I collected MVs from MDAMB231 cells that stably expressed a control siRNA, or two siRNAs that specifically targeted LIMK. As expected, the effectiveness of the LIMK knock-down (Figure 4.5*A*) was inversely correlated with the amount of MVs secreted from

**Figure 4.5 Suppressing LIMK expression inhibits the biogenesis of MVs in cancer cells and blocks MV-mediated transformation of recipient fibroblasts.** (**A**) Control siRNA and two specific LIMK siRNAs were transfected into HeLa cells. The cells were lysed and immunoblotted by LIMK and actin antibodies. Three sets of MDAMB231 cells were stably transfected with the referred control siRNA and LIMK siRNAs. One set of MDAMB231 cells were lysed together with the MVs secreted from these cells and subjected to Western blot analysis (**B**), using tTG, flotillin-2 and IκBα antibodies. MVs collected from the second set of MDAMB231 cells were mixed with the parental NIH3T3 fibroblasts, which were used to perform the anchorage-independent growth assay (**C**). The histogram presents the average number of formed colonies obtained from three independent experiments. Errors bars represent standard deviation. (**D**) The third set of mitotically-arrested MDAMB231 cells stably expressing control siRNA or two specific LIMK siRNAs were mixed with the same number of NIH3T3 cells and then respectively injected into nude mice. The shown box plot described the mass distribution of formed tumors derived from 6 independent injections of each cell samples. The box range indicates the standard deviation, and the black dots on the left side of each box represent the original data of measured tumor mass. (**E**) Schematic representation of the signaling pathways that control the generation of MVs in human cancer cells.

*The experiments described in (D) were performed by Marc A. Antonyak and Bo Li.

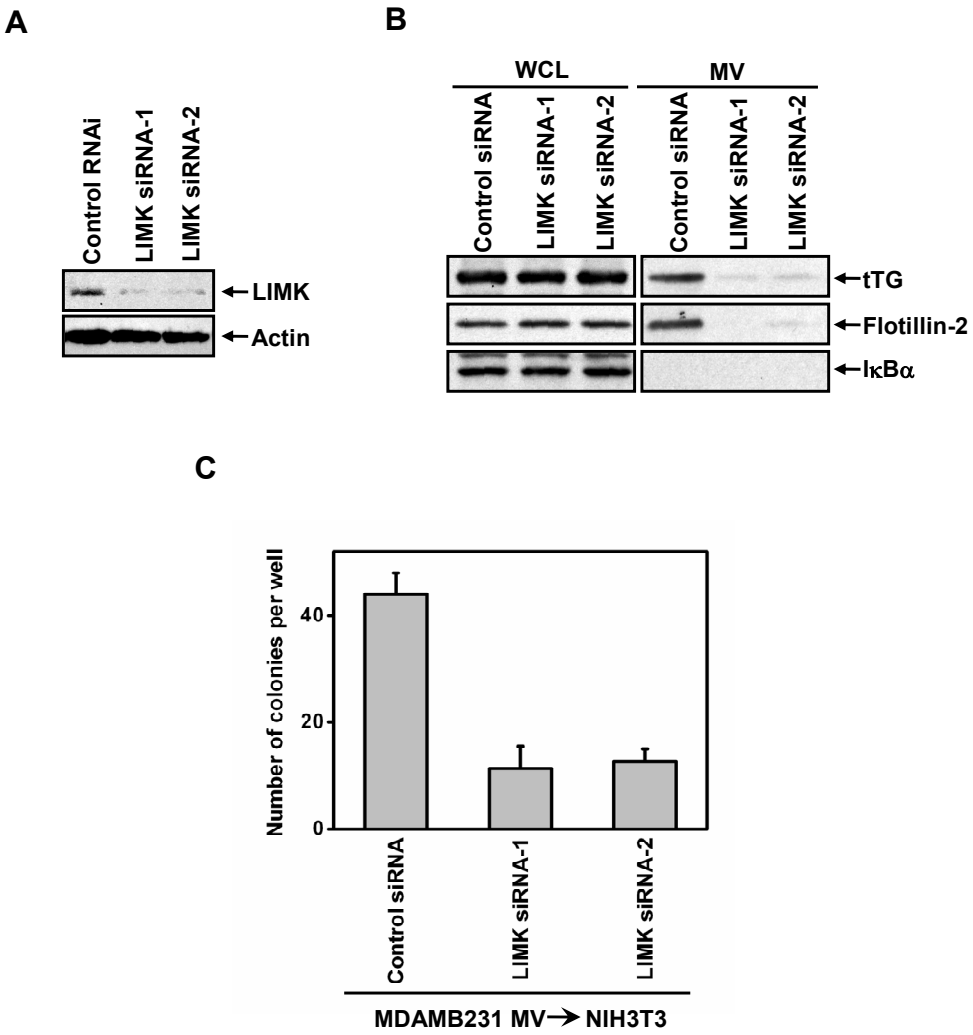
A
Control RNAi
LIMK siRNA-1
LIMK siRNA-2
LIMK
Actin
B
WCL
MV
Control siRNA
LIMK siRNA-1
LIMK siRNA-2
Control siRNA
LIMK siRNA-1
LIMK siRNA-2
tTG
Flotillin-2
IκBα
C
Number of colonies per well
40
20
0
Control siRNA
LIMK siRNA-1
LIMK siRNA-2
MDAMB231 MV→ NIH3T3
D
Weight of Tumors (g)
2
1
0
Control
LIMK KD-1
LIMK KD-2

**Figure 4.5 (Continued)**

**E**

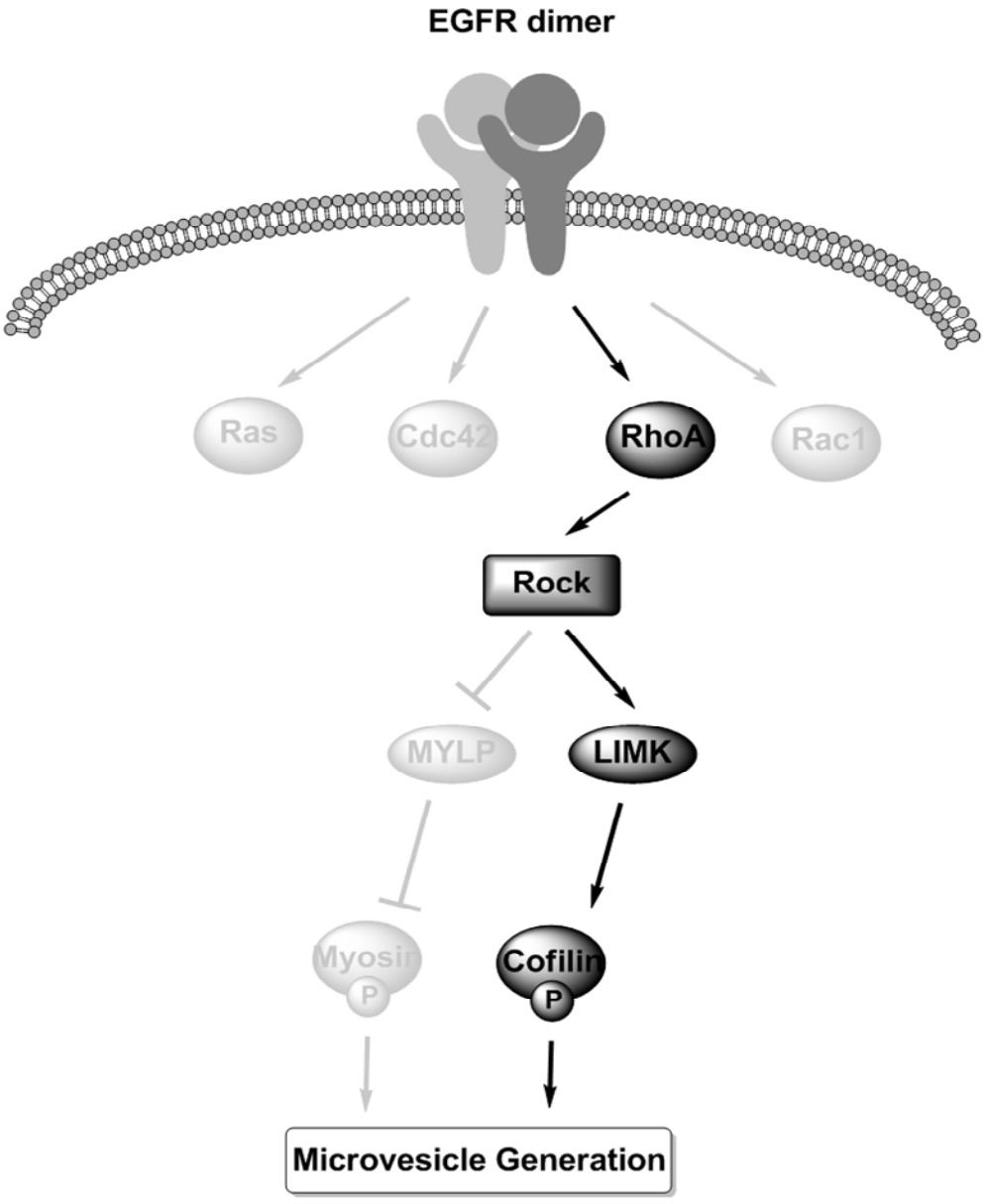

MDAMB231 cells (Figure 4.5*B*) and, in a corresponding manner, with the extent of anchorage-independent growth that these MVs were able to induce in the recipient NIH3T3 cells (Figure 4.5*C*). I then set out to establish the importance of LIMK activity for MV-mediated tumor formation *in vivo* by using a similar experimental strategy that was initially utilized to establish the role of MVs in this process. Figure 4.5*D* shows that the stable knock-down of LIMK expression in mitotically-arrested MDAMB231 cells markedly suppressed the ability of co-injected NIH3T3 fibroblasts to form tumors in mice. Thus, when taken together, these findings are consistent with the depiction in Figure 4.5*E,* which shows that the biogenesis of MVs as a result of a hyper-activated RhoA-ROCK-LIMK pathway in cancer cells can have a profound effect on the ability of recipient normal cells to show transformed properties in cultures, and also to give rise to tumors in mice.

**Discussion**

Tumor development involves the interaction and communication of cancer cells with the tumor microenvironment, including the surrounding tumor cells, normal stromal cells, blood vessels, macrophages, as well as the extracellular matrix (48). To facilitate tumor growth, invasion and metastasis, cancer cells exchange information with the tumor microenvironment, as predominantly occurs through secretory events. One such secretory mechanism that has been receiving a great deal of attention involves the generation and shedding of large, 2 micron-diameter vesicles (MVs) from cancer cells. These vesicles appear to play multiple roles in promoting cancer progression, including extracellular matrix remodeling, stimulation of blood vessel

formation, recruitment of tumor-associated microphages, activation of surrounding tumor cells, and the induction of transformed phenotypes within neighboring normal cells (13-15). This in turn has led to the thinking that the development and growth of a tumor not only involves the proliferation of compartmentalized tumor cells, but also requires the tight cooperation of adjacent tumor cells, stromal cells, and other components in the tumor "niche", through their communication via MVs. Given the increasingly important roles that MVs play in cancer progression, a great deal of attention has been directed toward understanding how these vesicles are generated from cancer cells. Although there have been suggestions that EGFR-signaling plays an important part in regulating MV formation, the details of this signaling pathway have remained elusive. Here my findings shed new light on this question by demonstrating that a RhoA-ROCK signaling pathway, which can be activated downstream from EGFR, works through LIMK and cofilin to generate MVs in cancer cells.

Interestingly, RhoA-ROCK signaling has also been implicated in the formation and regulation of another type of membrane structure, commonly referred to as plasma membrane blebs (PM blebs). PM blebs are initiated by the local disruption of the membrane-actomyosin connection, which results in a rapid protrusion of the plasma membrane due to intracellular hydrostatic pressure (49). The subsequent steps in forming PM blebs involves the recruitment of the actomyosin machinery beneath the detached membrane, the *in situ* build-up of new actin cortex, as well as the final retraction of the mature blebs (50). Although PM blebs were initially thought to only form in apoptotic cells, later studies indicated that PM blebs were also frequently generated in non-apoptotic cells, where they participated in several important cellular

activities including cytokinesis and cell migration (51). Surprisingly, studies focused on non-apoptotic PM blebs highlight some common features shared between these structures and membrane-associated MVs, i.e. an identical "actin-ring" phenotype as visualized by phalloidin staining, and a similar biogenesis as initiated by activated RhoA-ROCK signaling (50). This raises the question of how similar these two membrane vesicular structures are to each other. In fact, I am unaware of a study that specifically addresses this issue, and no specific markers have been proposed to distinguish blebs from MVs, which leads me to hypothesize that PM blebs and MVs may arise through a common mechanism from initiation to maturation. Their divergence might occur at a later point, such that those membrane structures undergoing inward contraction represent PM blebs, whereas those that are shed outward from the cell surface become secreted MVs. This raises the interesting possibility that there might be some signaling/regulatory proteins that influence the ratio of MV shedding to bleb retraction, in which case, understanding how cells maintain the balance between these two structures is important and deserves further research attention.

The actions of ROCK in reorganizing the actin cytoskeleton are generally mediated by two sets of downstream signaling activities, one resulting in the phosphorylation of cofilin by LIMK and the other being the phosphorylation of myosin through the regulation of MYLP. I have shown that LIMK activity induced by ROCK is not only necessary but also sufficient for the biogenesis of MVs from cancer cells. This is achieved through the ability of LIMK to phosphorylate its substrate cofilin, thereby inhibiting its actin-severing activity. The resultant elongation of actin

filaments along the plasma membranes is thought to precede the formation of an "actin-ring" structure, which is an established hallmark and also an essential step for the maturation of MVs. In contrast to LIMK, the ROCK target MYLP is phosphorylated and consequently inhibited by activated ROCK. As a result, the phosphorylation of myosin is significantly enhanced. Interestingly, I found that overexpression of MYLK, which mimics the cellular effects of inhibiting MYLP by ROCK, can also cause a modest stimulation of MV formation. This is consistent with an earlier finding in melanoma cells, where the activation of Arf6, a small GTPase involved in membrane trafficking, leads to a MYLK-dependent stimulation of MV production (21). Although my work suggests that myosin phosphorylation is not necessary for the formation of RhoA-induced MVs in HeLa cells, or for the constitutive formation of MVs in MDAMB231 cells, it is still possible that in some cellular contexts, MVs can be induced by signals that feed into the regulation of myosin, as apparently can occur downstream from activated Arf6 in the case of melanoma cells.

It has been shown that tumor-derived MVs are able to not only alter the surrounding environment to facilitate tumor progression, but also contain protein cargo and RNA transcripts that reflect the oncogenic features of the tumor cells from which they originate. A good deal of effort including work from our own laboratory has been focused on characterizing the components of MVs derived from cancer cells or tumors, which has provided insight into the molecular mechanisms of how these vesicles contribute to different aspects of oncogenesis, as well as raised the intriguing possibility of using MVs as novel tumor biomarkers. My discovery that RhoA-ROCK-

signaling controls the biogenesis of MVs provides further support to the idea that targeting RhoA-signaling may offer important strategies for interfering with tumor progression. What I find to be truly remarkable is that RhoA, and not the highly similar family member RhoC, is specifically responsible for signaling through ROCK to drive MV formation in cancer cells. This raises some interesting questions regarding where RhoC, which has also been often implicated in cancer progression and particularly with the development of metastasis (52), fits in relative to the actions of RhoA. Presumably, RhoC might be involved in the sorting of the MV cargo that is responsible for mediating the transforming capability of MVs, especially given the expectation that there is a tight coordination between MV biogenesis and vesicle cargo trafficking.

**Materials and Methods**

*Materials.* Cell culture reagents, EGF, oregon green or texas red–conjugated secondary IgG, rhodamine-conjugated phalloidin, Lipofectamine, Lipofectamine 2000, RhoA, LIMK and ROCK siRNAs were purchased from Invitrogen. Y-27632 and 4,6-diamidino-2-phenylindole (DAPI) were from Calbiochem. The tTG and actin antibodies were from Lab Vision/Thermo, Flotillin-2 and ROCK antibody were obtained from Santa Cruz, and HA and Myc antibodies were from Covance. The antibodies against IκBα, RhoA, LIMK, phospho-LIMK, MLC and phospho-MLC were from Cell Signaling.

*Cell Culture.* HeLa, MDAMB231 and U87 cell lines were grown in RPMI 1640 medium containing 10% fetal bovine serum, and NIH3T3 cells were maintained in DMEM medium containing 10% calf serum. RhoA (NM_001664), Rac (NM_006908), Ras (NM_005343), Cdc42 (NM_001791), Src (XM_001232484) and onco-Dbl (J03639) were cloned into PKH3 vector, while ROCK-1 (NM_005406.2), ROCK-2 (NM_004850), LIMK (NM_002314), MYLK (NM_053025), Cofilin (NM_005507), CHMP3 (NM_016079) and RhoC (NM_175744) were cloned into PCDNA3 plasmid. Different point mutations or truncations were generated as indicated in the paper. All of the expression constructs were transfected into cells using Lipofectamine, while the control, ROCK, LIMK and RhoA siRNAs were introduced into cells using Lipofectamine 2000. Where indicated, cells were treated with 0.1 μg/ml EGF or 10 μM Y-27632. To mitotically arrest MDAMB231 cells, plates of cells were treated with 10 μg/ml mitomycin-C for 2 hours, before rinsing the solution away and allowing the cells to recover in the complete growth medium for a day.

*Isolation of MVs from Cancer Cells.* For preparing MVs subjected to Western blot analysis, the conditioned medium from 5.0 x $10^6$ serum-starved MDAMB231 cells, U87 or HeLa cells stimulated without or with EGF were collected and the MVs were isolated from the medium as previously described. Briefly, the conditioned medium was subjected to two consecutive centrifugations; the first at 300 g for 10 minutes to pellet down floating cells, while the second at 12,000 g for 20 minutes to pellet down cell debris. The supernatant was then subjected to the third centrifugation at 100,000 g for 1.5 hours and the resulting pellet was washed with PBS and then lysed in cell lysis

buffer. To generate intact MVs for anchorage-independent growth assay, the supernatant after the first two spins (medium cleared of cells and cell debris) was then filtered though a Millipore Steriflip PVDF-filter with a 0.22 μm pore size. The MVs trapped on top of the PVDF membrane were resuspended in serum-free medium, and then mixed with NIH3T3 cell suspension supplemented with serum and agarose as indicated below.

*Immunoblot Analysis.* Cells were lysed with lysis buffer (25 mM Tris, 100 mM NaCl, 1% Triton X-100, 1 mM EDTA, 1 mM DTT, 1 mM $NaVO_4$, 1 mM β-glycerol phosphate, and 1 μg/mL aprotinin), and the lysate proteins were resolved by SDS-PAGE and then transferred to PDVF membranes. The membranes were first incubated with various primary antibodies diluted in TBST (20 mM Tris, 135 mM NaCl, and 0.05% Tween 20), and then with horseradish peroxidase-conjugated secondary antibodies followed by exposure to ECL reagent.

*RBD Binding Assay.* Equal amount of whole cell lysates collected from MDAMB231 cells or HeLa cells stimulated without or with EGF for 24 hours were incubated with agarose beads conjugated with the Rho-binding domain of Rhotekin. After an hour incubation, the beads were pelleted down and washed for three times. The precipitates were then subjected to Western blot analysis by using anti-RhoA antibody, to detect the amount of activated RhoA that interacted with the Rho-binding domain of Rhotekin.

*Immunofluorescence.* Cells overexpressing various constructs or treated with different reagents as indicated were fixed using 3.7% formaldehyde in PBS for 20 min, permeabilized by 0.2% Triton X-100 for 20 min, and then blocked by 10% BSA in PBS for half an hour. Following that cells were incubated with either tTG, HA, Myc or V5 antibodies as indicated for 1.5 hours, washed by PBS for 3 times and then incubated with fluorophore-conjugated secondary antibody for a hour. Sometimes in this step rhodamine-conjugated phalloidin was applied to stain actin filaments and DAPI was used to stain the cell nuclei. The samples were visualized by Zeiss fluorescent microscope and the images were captured using IPlab software.

*Anchorage-independent Growth Assays.* Parental NIH3T3 cells incubated without or with MVs derived from 5.0 x $10^6$ MDAMB231 cells, U87 cells, or HeLa cells simulated without or with EGF were plated in a density of 7,000 cells/mL in the medium containing 0.3% agarose and 10% calf serum, onto underlays composed of 10% calf serum and 0.6% agarose in six-well dishes. The soft agar cultures were re-fed (including the addition of freshly prepared MVs and calf serum) every fourth day for 12 days, at which time the colonies that formed were counted. Each of the assays was performed three times and the results were averaged.

*Scanning Electron Microscopy (SEM).* MDAMB231 cells grown on Lab-Tek chamber slides (Nunc/Lab Vision) were preliminarily fixed for 1 hour with 2% EM-grade glutaraldehyde diluted in 0.05 M cacodylic acid buffer solution (PH=7.4). The samples were then deeply fixed for 1 hour by 1% osmium tetroxide in PBS and

dehydrated in gradient solutions of 25%, 50%, 70%, 95%, and 100% ethanol. After that, the slides were further dehydrated in a CPD-30 critical point drying machine (BAL-TEC SCD050). The samples were then sputter-coated by thin-layered platinum, before being observed under a Leica 440 Scanning Electron Microscope.

*Mouse Studies.* 1 x $10^6$ mitotically arrested (using mitomycin-C) MDAMB231 cells stably expressing control or LIMK siRNAs were combined with 1 x $10^6$ NIH3T3 fibroblasts and growth factor-reduced Matrigel (BD Biosciences) to achieve 30% Matrigel in the final solution. The cell preparations were subcutaneously injected into the flanks of 6-8 weeks-old female NIH-III nude mice. As controls, parental MDAMB231 cells and NIH3T3 cells (1 x $10^6$ cells of each cell line) were singly combined with growth factor-reduced Matrigel (to a final concentration of 30% Matrigel) and then were injected into mice as well. After a month, the animals were sacrificed and the resulting tumors that formed for each experimental condition were excised and weighed. The experiments involving mice were performed in accordance with the protocols approved by The Cornell Center for Animal Resources and Education (CARE).

## REFERENCES


1. Sherer NM, Mothes W (2008) Cytonemes and tunneling nanotubules in cell-cell communication and viral pathogenesis. *Trends Cell Biol* 18:414-420.

2. Ratajczak J, Wysoczynski M, Hayek F, Janowska-Wieczorek A, Ratajczak MZ (2006) Membrane-derived microvesicles: important and underappreciated mediators of cell-to-cell communication. *Leukemia* 20:1487-1495.

3. Al-Nedawi K, et al. (2008) Intercellular transfer of the oncogenic receptor EGFRvIII by microvesicles derived from tumour cells. *Nat Cell Biol* 10:619-624.

4. Skog J, et al. (2008) Glioblastoma microvesicles transport RNA and proteins that promote tumour growth and provide diagnostic biomarkers. *Nat Cell Biol* 10:1470-1476.

5. Al-Nedawi K, Meehan B, Kerbel RS, Allison AC, Rak J (2009) Endothelial expression of autocrine VEGF upon the uptake of tumor-derived microvesicles containing oncogenic EGFR. *Proc Natl Acad Sci U S A* 106:3794-3799.

6. Antonyak MA, et al. (2011) Cancer cell-derived microvesicles induce transformation by transferring tissue transglutaminase and fibronectin to recipient cells. *Proc Natl Acad Sci U S A* 108:4852-4857.

7. Balaj L, et al. (2011) Tumour microvesicles contain retrotransposon elements and amplified oncogene sequences. *Nat Commun* 2:180.

8. George JN, Thoi LL, McManus LM, Reimann TA (1982) Isolation of human platelet membrane microparticles from plasma and serum. *Blood* 60:834-840.

9. Hess C, Sadallah S, Hefti A, Landmann R, Schifferli JA (1999) Ectosomes released by human neutrophils are specialized functional units. *J Immunol* 163:4564-4573.

10. Greco V, Hannus M, Eaton S (2001) Argosomes: a potential vehicle for the spread of morphogens through epithelia. *Cell* 106:633-645.

11. Martinez MC, Tesse A, Zobairi F, Andriantsitohaina R (2005) Shed membrane microparticles from circulating and vascular cells in regulating vascular function. *Am J Physiol Heart Circ Physiol* 288:H1004-1009.

12. Iero M, et al. (2008) Tumour-released exosomes and their implications in cancer immunity. *Cell Death Differ* 15:80-88.

13. Al-Nedawi K, Meehan B, Rak J (2009) Microvesicles: messengers and mediators of tumor progression. *Cell Cycle* 8:2014-2018.

14. Rak J (2010) Microparticles in cancer. *Semin Thromb Hemost* 36:888-906.

15. Lee TH, et al. (2011) Microvesicles as mediators of intercellular communication in cancer-the emerging science of cellular 'debris'. *Semin Immunopathol*.

16. Keller S, Sanderson MP, Stoeck A, Altevogt P (2006) Exosomes: from biogenesis and secretion to biological function. *Immunol Lett* 107:102-108.

17. Cocucci E, Racchetti G, Meldolesi J (2009) Shedding microvesicles: artefacts no more. *Trends Cell Biol* 19:43-51.

18. Del Conde I, Shrimpton CN, Thiagarajan P, Lopez JA (2005) Tissue-factor-bearing microvesicles arise from lipid rafts and fuse with activated platelets to initiate coagulation. *Blood* 106:1604-1611.

19. Bianco F, et al. (2009) Acid sphingomyelinase activity triggers microparticle release from glial cells. *EMBO J* 28:1043-1054.

20. Ratajczak J, et al. (2006) Embryonic stem cell-derived microvesicles reprogram hematopoietic progenitors: evidence for horizontal transfer of mRNA and protein delivery. *Leukemia* 20:847-856.

21. Muralidharan-Chari V, et al. (2009) ARF6-regulated shedding of tumor cell-derived plasma membrane microvesicles. *Curr Biol* 19:1875-1885.

22. Di Vizio D, et al. (2009) Oncosome formation in prostate cancer: association with a region of frequent chromosomal deletion in metastatic disease. *Cancer Res* 69:5601-5609.

23. Yu X, Harris SL, Levine AJ (2006) The regulation of exosome secretion: a novel function of the p53 protein. *Cancer Res* 66:4795-4801.

24. Janowska-Wieczorek A, et al. (2005) Microvesicles derived from activated platelets induce metastasis and angiogenesis in lung cancer. *Int J Cancer* 113:752-760.

25. Hong BS, et al. (2009) Colorectal cancer cell-derived microvesicles are enriched in cell cycle-related mRNAs that promote proliferation of endothelial cells. *BMC Genomics* 10:556.

26. Hao S, et al. (2006) Epigenetic transfer of metastatic activity by uptake of highly metastatic B16 melanoma cell-released exosomes. *Exp Oncol* 28:126-131.

27. Lima LG, Chammas R, Monteiro RQ, Moreira ME, Barcinski MA (2009) Tumor-derived microvesicles modulate the establishment of metastatic melanoma in a phosphatidylserine-dependent manner. *Cancer Lett* 283:168-175.

28. Jung T, et al. (2009) CD44v6 dependence of premetastatic niche preparation by exosomes. *Neoplasia* 11:1093-1105.

29. Castellana D, et al. (2009) Membrane microvesicles as actors in the establishment of a favorable prostatic tumoral niche: a role for activated fibroblasts and CX3CL1-CX3CR1 axis. *Cancer Res* 69:785-793.

30. Wysoczynski M, Ratajczak MZ (2009) Lung cancer secreted microvesicles: underappreciated modulators of microenvironment in expanding tumors. *Int J Cancer* 125:1595-1603.

31. Narumiya S, Tanji M, Ishizaki T (2009) Rho signaling, ROCK and mDia1, in transformation, metastasis and invasion. *Cancer Metastasis Rev* 28:65-76.

32. Li B, et al. (2010) EGF potentiated oncogenesis requires a tissue transglutaminase-dependent signaling pathway leading to Src activation. *Proc Natl Acad Sci U S A* 107:1408-1413.

33. Mangala LS, Fok JY, Zorrilla-Calancha IR, Verma A, Mehta K (2006) Tissue transglutaminase expression promotes cell attachment, invasion and survival in breast cancer cells. *Oncogene* 26:2459-2470.

34. Mann AP, et al. (2006) Overexpression of tissue transglutaminase leads to constitutive activation of nuclear factor-kappaB in cancer cells: delineation of a novel pathway. *Cancer Res* 66:8788-8795.

35. Yuan L, et al. (2007) Transglutaminase 2 inhibitor, KCC009, disrupts fibronectin assembly in the extracellular matrix and sensitizes orthotopic glioblastomas to chemotherapy. *Oncogene* 26:2563-2573.

36. Akimov SS, Krylov D, Fleischman LF, Belkin AM (2000) Tissue transglutaminase is an integrin-binding adhesion coreceptor for fibronectin. *J Cell Biol* 148:825-838.

37. Teis D, Saksena S, Emr SD (2009) SnapShot: the ESCRT machinery. *Cell* 137:182-182 e181.

38. Heasman SJ, Ridley AJ (2008) Mammalian Rho GTPases: new insights into their functions from in vivo studies. *Nat Rev Mol Cell Biol* 9:690-701.

39. Karlsson R, Pedersen ED, Wang Z, Brakebusch C (2009) Rho GTPase function in tumorigenesis. *Biochim Biophys Acta* 1796:91-98.

40. Roberts PJ, Der CJ (2007) Targeting the Raf-MEK-ERK mitogen-activated protein kinase cascade for the treatment of cancer. *Oncogene* 26:3291-3310.

41. Cerione RA, Zheng Y (1996) The Dbl family of oncogenes. *Current opinion in cell biology.* 8:216-222.

42. Loirand G, Guerin P, Pacaud P (2006) Rho kinases in cardiovascular physiology and pathophysiology. *Circ Res* 98:322-334.

43. Narumiya S, Ishizaki T, Uehata M (2000) Use and properties of ROCK-specific inhibitor Y-27632. *Methods Enzymol* 325:273-284.

44. Maekawa M, et al. (1999) Signaling from Rho to the actin cytoskeleton through protein kinases ROCK and LIM-kinase. *Science* 285:895-898.

45. Yang N, et al. (1998) Cofilin phosphorylation by LIM-kinase 1 and its role in Rac-mediated actin reorganization. *Nature* 393:809-812.

46. Kawano Y, et al. (1999) Phosphorylation of myosin-binding subunit (MBS) of myosin phosphatase by Rho-kinase in vivo. *J Cell Biol* 147:1023-1038.

47. Petrache I, et al. (2003) Caspase-dependent cleavage of myosin light chain kinase (MLCK) is involved in TNF-alpha-mediated bovine pulmonary endothelial cell apoptosis. *FASEB J* 17:407-416.

48. Mbeunkui F, Johann DJ, Jr. (2009) Cancer and the tumor microenvironment: a review of an essential relationship. *Cancer Chemother Pharmacol* 63:571-582.

49. Fackler OT, Grosse R (2008) Cell motility through plasma membrane blebbing. *J Cell Biol* 181:879-884.

50. Charras GT, Hu CK, Coughlin M, Mitchison TJ (2006) Reassembly of contractile actin cortex in cell blebs. *J Cell Biol* 175:477-490.

51. Charras G, Paluch E (2008) Blebs lead the way: how to migrate without lamellipodia. *Nat Rev Mol Cell Biol* 9:730-736.

52. Clark EA, Golub TR, Lander ES, Hynes RO (2000) Genomic analysis of metastasis reveals an essential role for RhoC. *Nature* 406:532-535.

# CHAPTER 5

## Conclusions

*The regulation and function of tTG in EGF-promoted oncogenesis*

The critical role of tTG in EGF-stimulated cancer cell survival and migration, which was demonstrated in a number of cancer cell lines (1-5), prompted me to consider the possibility that tTG might also be essential for EGF-stimulated cancer cell growth. To investigate this issue, I took advantage of the fact that exposing SKBR3 breast cancer cells to EGF not only augmented their proliferative capacity and ability to form colonies in soft agar, but also resulted in the induction of tTG expression and activation. I found that suppressing tTG expression using tTG-specific siRNAs, or blocking its transamidation activity using the competitive inhibitor MDC, potently inhibited the growth-promoting effects afforded to SKBR3 cells by EGF stimulation. Moreover, overexpressing tTG in SKBR3 cells was sufficient to mimic the actions of EGF and strongly stimulate the growth of these cells in monolayer and under anchorage-independent conditions.

These results prompted two follow-up questions: How is tTG expression up-regulated by EGF stimulation and how does it enhance cell proliferation? To answer the first question, I continued using the SKBR3 cell line as my model system and delineated the EGF-mediated signaling pathways that were responsible for inducing tTG expression. I found that individually activating signaling pathways known to be coupled to EGF stimulation by ectopically expressing activated forms of a variety of

signaling proteins including Ras, Rac, RhoA and Cdc42 (6) in SKBR3 cells did not result in the induction of tTG expression. Surprisingly, co-expression of activated forms of Ras and Cdc42 in these cells was able to successfully induce tTG expression. The fact that the up-regulation of tTG was caused by a combination of Ras and Cdc42 led to the conclusion that common effector(s) acting downstream of these two GTPases might be involved. PI3K (7) turned out to be one such effector protein. Interestingly, I found that expressing a constitutively active form of PI3K alone in SKBR3 cells did not lead to increases in tTG expression. This finding argued that while PI3K functioned as an essential signaling component in the induction of tTG expression by the co-activation of Ras and Cdc42, additional Ras- and/or Cdc42-dependent signaling events were also needed. In fact, another downstream participant that contributed to the up-regulation of tTG expression was NFκB (8). Blocking NFκB activity in SKBR3 cells using the small molecule inhibitor BAY 11-7082 completely abolished the up-regulation of tTG expression by EGF treatment. Taken together, co-signaling events from multiple small GTPases, such as Ras and Cdc42, leading to the activation of PI3K and NFκB, provide a mechanism by which EGF up-regulates tTG in breast cancer cells.

The fact that tTG up-regulation is crucial for EGF-mediated cell growth enhancement suggests that the signaling pathway(s) activated by tTG to promote SKBR3 cell growth very likely overlaps EGF-coupled signaling cascades. While I checked the tyrosine phosphorylation profile for lysates collected from SKBR3 cells overexpressing tTG or vector, a unique 60 kD protein exhibited a two-fold increase in its tyrosine phosphorylation, which led me to consider whether tTG promoted the

phosphorylation and subsequent activation of Src (9), a well-established non-receptor tyrosine kinase of $M_r$ ~60 kDa. Indeed, I was able to show that SKBR3 cells overexpressing wild-type tTG exhibited a significant increase in Src activity compared to cells overexpressing vector or the transamidation-deficient tTG (C277V) mutant, which further raised the question of how tTG activates Src in breast cancer cells. The classical model for Src activation starts with the recruitment of a phosphatase upon receiving upstream signals, which dephosphorylates a C-terminal tyrosine residue of Src (Tyr527) that normally forms an auto-inhibitory loop with the SH2 domain of Src (10). However, this classical model is unable to provide a straightforward explanation of how tTG activates Src because tTG neither exhibits phosphatase activity, nor has it been reported to activate a phosphatase.

Several groups recently provided an unconventional mechanism for activating Src, namely through Src-binding proteins that displace the inhibitory loop away from the catalytic domain of Src, thereby driving it to assume its active conformation (10, 11). I suspect that tTG activates Src though this type of mechanism because the association of tTG with Src was observed in multiple breast cancer cell lines. However, this association seems likely to be indirect due to the fact that recombinant tTG did not exhibit any binding affinity toward GST-tagged Src, as demonstrated by *in vitro* GST-pull-down assays. Given that wild-type tTG, but not the transamidation-deficient mutant (C277V), is capable of activating Src, the formation of a proposed Src-activating complex seems to require the transamidation-competent tTG. Efforts to search for candidate transamidation substrates of tTG led me to the intermediate filament protein K19. As a component of cytoskeleton-building blocks, the main

functions of the keratins are believed to provide the mechanical support to maintain the desired cell shape (12, 13). However, recent studies revealed that keratins were also able to bind and regulate the activities of signaling effectors, thereby functioning as scaffold proteins to modulate a number of cellular events including metabolic responses, cell migration and cell growth (12-15). These findings prompted me to consider the possibility of K19 as the mediator for tTG-Src interactions in breast cancer cells. This in fact turned out to be the case, as shown by the result that knocking-down K19 expression seriously impaired the interaction between tTG and Src in SKBR3 cells. Furthermore, suppressing K19 expression greatly compromised the ability of tTG to activate Src and its ability to promote the anchorage-independent growth of SKBR3 cells. Thus, my findings showing that K19 bridges the interaction between tTG and Src, depict a novel signaling pathway that is used by cancer cells to obtain a growth advantage.

However, many of the molecular details about how K19 mediates the interaction between tTG and Src remain to be determined. For instance, which part of K19 interacts with tTG and Src respectively? How does the catalytic site of tTG contribute to the activation of Src? Are there any additional components involved in this signaling complex? If so, what are their specific functions? Future works and efforts are needed to answer these follow-up questions.

*Cancer cell-derived microvesicles require tTG and fibronectin to induce the transformation of normal cells*

Microvesicles (MVs) are one type of unconventional cellular secretion structures that directly bud off from the plasma membrane (16, 17). It was frequently observed that several malignant cancer cell lines exhibited the phenotype of membrane-bound MVs (18-23), however, the cellular function associated with these cancer cell-derived MVs are poorly understood. In a recent report by Al-Nedawi, K *et al.*, the authors showed that human glioblastoma cell line U373 transfected by EGFR VIII, an in-frame truncation of the EGFR that is constitutively active, shed MVs that contained this specific variant type of the EGFR (18). Interestingly, the secreted MVs, when collected from the conditioned medium, were capable of fusing to the recipient U373 cells that did not express EGFR VIII, thus conferring upon the recipient cells EGFR VIII-signaling capability. Building upon this finding, I hypothesized that cancer cell-derived MVs are not only able to dock to the same type of cancer cells from which they originated, thereby enhancing their oncogenic potential, but MVs are also able to interact and stimulate the oncogenic signaling in recipient normal (non-transformed) cells, such as those that exist in the tumor microenvironment.

To test this idea, MVs were collected from the conditioned medium of MDAMB231 breast cancer cells or U87 glioblastoma cells, the two human cancer cell lines that constitutively generate and shed MVs, and then added to normal NIH3T3 fibroblasts. Surprisingly, it appeared that MDAMB231 and U87 cell-derived MVs were able to cause the recipient fibroblasts to acquire transformed phenotypes, as indicated by their enhanced survival rate under serum starvation and their abilities to form colonies in anchorage-independent culturing conditions. The fact that cancer cell-derived MVs are capable of inducing the transformation of normal fibroblasts

highlights the necessity to identify the critical protein cargo that is responsible for this effect.

Efforts to address this issue led me to perform the proteomic screening on the collected MV preps, with approximately 40 proteins being eventually identified as the common protein cargo shared by MDAMB231 and U87 cell-derived MVs. Interestingly, tTG was highlighted as one such cargo. My earlier findings showing that overexpression and activation of tTG is sufficient to promote the oncogenesis of human breast cancer cells raised the possibility that tTG might be one of the critical cargo used by MVs to confer the transforming properties onto NIH3T3 fibroblasts. To test this hypothesis, I took advantage of a commercially-available tTG inhibitor T101, a small-molecule that covalently modifies the active site of tTG. The fact that T101 covalently modifies tTG allowed me to treat tTG-containing MVs during the purification steps, with MV-associated tTG remaining inactivated even after MVs were transferred to recipient cells, which provided me a great tool to examine the importance of tTG for MVs. Interestingly, the abilities of both types of MVs to induce cellular transformation were found to be severely inhibited after incubation with T101, suggesting that tTG is in fact a critical component for the transforming capabilities of cancer cell-derived MVs. At the same time, tTG expression was knocked down from MDAMB231 cells using two specific siRNAs, and the tTG-depleted MVs collected from these cells exhibited much less potency at inducing the transformation of NIH3T3 fibroblasts, which was consistent with the results obtained by using T101 inhibitor.

Although tTG is essential for the ability of cancer cell-derived MVs to transform normal cells, the ectopic expression of tTG in normal cells is not sufficient to trigger their cellular transformation. Efforts to identify additional MV cargo that cooperate with tTG to fully transform normal cells led me to fibronectin, another protein cargo contained in both MDAMB231 and U87-derived MVs. As one of the best-studied tTG substrates, fibronectin can be cross-linked into oligomers by tTG on the cell surface (24, 25), resulting in the recruitment and assembly of fibronectin-bound β1-integrins whose clustering events would lead to the activation of Focal Adhesion Kinase (FAK) (26, 27).

As one of the most-studied signaling "hubs" in cancer cells, activated FAK has been shown to be able to stimulate cell proliferation, migration and survival (28, 29), all of which are associated with a more transformed phenotype. To examine the possibility that tTG may cross-link fibronectin in MVs, Western blot analyses of fibronectin were performed on lysates collected from MDAMB231 cells and MDAMB231 cell-derived MVs. Surprisingly, the fibronectin dimer was only found to be present in MV lysates. Moreover, I was able to show that the amount of fibronectin dimer was sensitive to T101 treatment, suggesting that tTG is the particular enzyme that catalyzes the formation of fibronectin dimer in MVs. In line with this finding, FAK signaling is significantly enhanced within MV-treated NIH3T3 cells, while such a signaling increase can be potently inhibited by pre-treating MVs with the tTG inhibitor T101. This signaling profile was successfully mimicked by pre-treating MVs with RGD, a small peptide inhibitor that specifically disrupts the fibronectin-integrin interaction. All of these results suggested that tTG was functioning through the

fibronectin-integrin-FAK-signaling pathway to help MVs confer the transforming properties onto normal cells.

Although tTG and fibronectin were suggested to be the critical cargo involved in MV-mediated transformation, additional MV components may also contribute to this effect. For example, pyruvate kinase M2, one of the mitochondrial enzymes that participate in the metabolic reprogramming of cancer cells, is also present in MVs collected from MDAMB231 cells and U87 cells. In addition, MVs not only contain protein cargo but also carry mRNA transcripts, which may add another dimension to the cellular functions of MVs. Future studies focused on these issues will shed more light on the molecular mechanisms underlying the various biological outcomes triggered by MVs.

*RhoA-ROCK-LIMK signaling controls the biogenesis of MVs in cancer cells*

The newly-discovered importance of MVs in cancer progression underscores the demand to understand how they are generated from cancer cells. However, thus far, the molecular mechanism underlying this process is poorly understood. It was found that activated EGFR signaling is capable of inducing MV formation in several cancer cell lines including U373 glioblastoma cells, DU145 prostate cancer cells and HeLa cervical carcinoma cells (18, 19, 21). Although how the EGFR stimulates MV formation was unclear, several lines of evidence seemed to implicate signaling pathways that influence the cytoskeletal reorganization or actomyosin regulation (19, 21). Among the many downstream effectors of the EGFR, the group of small GTPases including Ras, Rho, Rac and Cdc42 (30, 31), are best known for their ability to

reorganize cytoskeletal structure. In order to determine whether any of these GTPases were linked to MV formation, I individually overexpressed the dominant-active forms of Rac, Cdc42, Ras or RhoA in HeLa cells and examined their ability to induce MV formation. Interestingly, overexpression of the dominant-active form of RhoA, but not Rac, Cdc42 or Ras, dramatically stimulated the formation and secretion of MVs. Since active RhoA is sufficient to induce MV formation, I then asked whether RhoA is also essential for the ability of EGF to trigger the MV production. By using two siRNAs specifically targeting RhoA, I found that knocking-down RhoA expression from HeLa cells completely abolished EGF-stimulated MV formation, suggesting that RhoA is both necessary and sufficient for controlling the biogenesis of MVs in cancer cells.

The essential role of RhoA in regulating MV formation prompted me to search for its critical downstream effector(s) that is involved in this process. It was known that several protein targets can be activated by RhoA, including Rhotekin, Rhophilin, mDia, ROCK and PKN (32, 33). Among them, ROCK represents a highly attractive candidate because of its established function in cytoskeletal remodeling and actomyosin contraction (34). To examine the possible role of ROCK in MV formation, I took advantage of the ROCK-specific inhibitor Y-27632. Interestingly, treatment of MDAMB231 cells, U87 cells, or EGF-stimulated HeLa cells, with Y-27632 completely eliminated the formation of MVs. Although attempts to knock-down ROCK expression had failed, overexpression of wild-type ROCK in HeLa cells, which is sufficient to activate ROCK signaling, dramatically stimulated MV formation.

As the next step, I tried to further delineate the downstream pathways of ROCK that linked to MV production. There are two well-studied signaling targets of

ROCK, namely Lim kinase (LIMK) and Myosin light chain phosphatase (MYLP) (33), both of which are able to regulate the cytoskeleton dynamics. Activated ROCK phosphorylates LIMK and MYLP, which respectively stimulates LIMK and inhibits MYLP activity (34, 35). Surprisingly, I found that either activating the LIMK pathway by overexpressing wild-type LIMK, or attenuating the effect of MYLP by overexpressing wild-type Myosin light chain kinase (MYLK), is sufficient to induce MV formation in HeLa cells. The fact that cancer cells have two signaling pathways that are capable of generating microvesicles then raised the question of whether cells prefer to use one pathway over the other, or a combination of both. To answer this question, I introduced the dominant-negative form of LIMK or MYLK into HeLa cells overexpressing the activated form of RhoA. While dominant-negative MYLK did not interfere the ability of RhoA to generate MVs, overexpression of dominant-negative LIMK significantly reduced the number of MV-producing cells triggered by activated RhoA. I went on to show that the preference of using LIMK as a MV-inducing pathway is not restricted to HeLa cells, because introducing the dominant-negative LIMK mutant also compromised the formation of 231 cell-derived MVs, while the MYLK mutant again exhibited little effect. To further confirm the importance of LIMK pathway to MV formation, LIMK expression was knocked down in MDAMB231 cells using two specific LIMK siRNAs, and I was able to show that the amount of MVs secreted from MDAMB231 cells dramatically decreased while LIMK expression was suppressed. As a conclusion, RhoA-ROCK signaling, one of the signature downstream pathways of EGFR that leads to LIMK activation, appears to be predominantly responsible for the biogenesis of MVs in cancer cells.

Although the major driving force for MV formation has been attributed to RhoA-ROCK-LIMK signaling pathway, little is known about the cargo-sorting mechanism that accompanies with this process. Our proteomic screenings as well as studies from other groups (19, 21) suggest that MVs prefer to enrich specific types of cargo. Two follow-up questions are truly prompted by these findings: How is MV cargo selectively grouped and transported to the budding site? What signaling pathways are responsible to direct and package MV cargo? Understanding the molecular details of these processes will not only shed more light on the mechanism of MV formation, but should also provide potentially new targets for chemical intervention to block the biogenesis of MVs in cancer cells.

## REFERENCES


1. Li B, et al. (2010) EGF potentiated oncogenesis requires a tissue transglutaminase-dependent signaling pathway leading to Src activation. *Proc Natl Acad Sci U S A* 107:1408-1413.

2. Hwang JY, et al. (2008) Clinical and biological significance of tissue transglutaminase in ovarian carcinoma. *Cancer Res* 68:5849-5858.

3. Mann AP, et al. (2006) Overexpression of tissue transglutaminase leads to constitutive activation of nuclear factor-kappaB in cancer cells: delineation of a novel pathway. *Cancer Res* 66:8788-8795.

4. Mangala LS, Fok JY, Zorrilla-Calancha IR, Verma A, Mehta K (2006) Tissue transglutaminase expression promotes cell attachment, invasion and survival in breast cancer cells. *Oncogene* 26:2459-2470.

5. Yuan L, et al. (2007) Transglutaminase 2 inhibitor, KCC009, disrupts fibronectin assembly in the extracellular matrix and sensitizes orthotopic glioblastomas to chemotherapy. *Oncogene* 26:2563-2573.

6. Yarden Y, Shilo BZ (2007) SnapShot: EGFR signaling pathway. *Cell* 131:1018.

7. Liu W, Bagaitkar J, Watabe K (2007) Roles of AKT signal in breast cancer. *Front Biosci* 12:4011-4019.

8. Hayden MS, Ghosh S (2008) Shared principles in NF-kappaB signaling. *Cell* 132:344-362.

9. Parsons SJ, Parsons JT (2004) Src family kinases, key regulators of signal transduction. *Oncogene* 23:7906-7909.

10. Moarefi I, et al. (1997) Activation of the Src-family tyrosine kinase Hck by SH3 domain displacement. *Nature* 385:650-653.

11. Arias-Salgado EG, et al. (2003) Src kinase activation by direct interaction with the integrin beta cytoplasmic domain. *Proc Natl Acad Sci U S A* 100:13298-13302.

12. Stewart M (1990) Intermediate filaments: structure, assembly and molecular interactions. *Curr Opin Cell Biol* 2:91-100.

13. Herrmann H, Aebi U (2004) Intermediate filaments: molecular structure, assembly mechanism, and integration into functionally distinct intracellular Scaffolds. *Annu Rev Biochem* 73:749-789.

14. Coulombe PA, Wong P (2004) Cytoplasmic intermediate filaments revealed as dynamic and multipurpose scaffolds. *Nat Cell Biol* 6:699-706.

15. Pallari HM, Eriksson JE (2006) Intermediate filaments as signaling platforms. *Sci STKE* 2006:pe53.

16. Al-Nedawi K, Meehan B, Rak J (2009) Microvesicles: messengers and mediators of tumor progression. *Cell Cycle* 8:2014-2018.

17. Cocucci E, Racchetti G, Meldolesi J (2009) Shedding microvesicles: artefacts no more. *Trends Cell Biol* 19:43-51.

18. Al-Nedawi K, et al. (2008) Intercellular transfer of the oncogenic receptor EGFRvIII by microvesicles derived from tumour cells. *Nat Cell Biol* 10:619-624.

19. Antonyak MA, et al. (2011) Cancer cell-derived microvesicles induce transformation by transferring tissue transglutaminase and fibronectin to recipient cells. *Proc Natl Acad Sci U S A* 108:4852-4857.

20. Muralidharan-Chari V, et al. (2009) ARF6-regulated shedding of tumor cell-derived plasma membrane microvesicles. *Curr Biol* 19:1875-1885.

21. Di Vizio D, et al. (2009) Oncosome formation in prostate cancer: association with a region of frequent chromosomal deletion in metastatic disease. *Cancer Res* 69:5601-5609.

22. Yu X, Harris SL, Levine AJ (2006) The regulation of exosome secretion: a novel function of the p53 protein. *Cancer Res* 66:4795-4801.

23. Janowska-Wieczorek A, et al. (2005) Microvesicles derived from activated platelets induce metastasis and angiogenesis in lung cancer. *Int J Cancer* 113:752-760.

24. Akimov SS, Krylov D, Fleischman LF, Belkin AM (2000) Tissue transglutaminase is an integrin-binding adhesion coreceptor for fibronectin. *J Cell Biol* 148:825-838.

25. Gaudry CA, et al. (1999) Cell surface localization of tissue transglutaminase is dependent on a fibronectin-binding site in its N-terminal beta-sandwich domain. *J Biol Chem* 274:30707-30714.

26. Wierzbicka-Patynowski I, Schwarzbauer JE (2003) The ins and outs of fibronectin matrix assembly. *J Cell Sci* 116:3269-3276.

27. Leiss M, Beckmann K, Giros A, Costell M, Fassler R (2008) The role of integrin binding sites in fibronectin matrix assembly in vivo. *Curr Opin Cell Biol* 20:502-507.

28. Golubovskaya VM, Kweh FA, Cance WG (2009) Focal adhesion kinase and cancer. *Histol Histopathol* 24:503-510.

29. Zhao J, Guan JL (2009) Signal transduction by focal adhesion kinase in cancer. *Cancer Metastasis Rev* 28:35-49.

30. Karlsson R, Pedersen ED, Wang Z, Brakebusch C (2009) Rho GTPase function in tumorigenesis. *Biochim Biophys Acta* 1796:91-98.

31. Roberts PJ, Der CJ (2007) Targeting the Raf-MEK-ERK mitogen-activated protein kinase cascade for the treatment of cancer. *Oncogene* 26:3291-3310.

32. Narumiya S, Tanji M, Ishizaki T (2009) Rho signaling, ROCK and mDia1, in transformation, metastasis and invasion. *Cancer Metastasis Rev* 28:65-76.

33. Loirand G, Guerin P, Pacaud P (2006) Rho kinases in cardiovascular physiology and pathophysiology. *Circ Res* 98:322-334.

34. Maekawa M, et al. (1999) Signaling from Rho to the actin cytoskeleton through protein kinases ROCK and LIM-kinase. *Science* 285:895-898.

35. Kawano Y, et al. (1999) Phosphorylation of myosin-binding subunit (MBS) of myosin phosphatase by Rho-kinase in vivo. *J Cell Biol* 147:1023-1038.